2023-09-20

Investigating the effect of dynamic culture and lactate on colony formation of human induced pluripotent stem cells (hiPSCs)

Malinovska, Julia

UNIVERSITY OF CALGARY

Investigating the effect of dynamic culture and lactate on colony formation of human induced pluripotent stem cells (hiPSCs)

by

Julia Malinovska

A THESIS

SUBMITTED TO THE FACULTY OF GRADUATE STUDIES

IN PARTIAL FULFILMENT OF THE REQUIREMENTS FOR THE

DEGREE OF MASTER OF SCIENCE

GRADUATE PROGRAM IN BIOMEDICAL ENGINEERING

CALGARY, ALBERTA

SEPTEMBER, 2023

Abstract

Research into stem cell treatments has led to the ability to reprogram somatic cells in the body, like skin cells and bloods cells, to behave like stem cells, and have pluripotent characteristics, ability to self-renew and develop into almost any cell type or tissue. These reprogrammed cells, referred to as human induced pluripotent stem cells (hiPSCs), have broad applications in cell therapy, drug screening, and disease modelling. Unlike traditional pluripotent cells, these cells are more accessible, avoid ethical concerns, and can be used for autologous therapies.

Various methods of reprogramming somatic cells are available but come with challenges of virus integration into the genome, low reprogramming efficiency, and long transition from cultivation to large-scale manufacturing. The proposed research addresses this by combining two innovative approaches for improved somatic cell reprogramming: 1. transient exposure to lactate, and 2. dynamic culture environment. The generation of hiPSCs is highly dependent on a metabolic shift from oxidative phosphorylation (OXPHOS) to glycolysis and lactate has shown to facilitate this metabolic shift thereby potentially increasing reprogramming efficiency. The dynamic environment also plays a role in reprogramming and the subsequent physiology which allows for great cell expansion, heterogeneity and scale-up.

This study first outlines the isolated effects of a dynamic system and transient lactate exposure on the reprogramming process as well as the optimization of these conditions. The two approaches were then integrated with findings suggesting that the independent conditions outperformed the tandem. Further phenotype and functional testing post reprogramming is required, however the examined conditions show promise in increasing reprogramming efficiency, reducing time of reprogramming process and improving translation to a bioprocess.

Preface

This thesis is original, unpublished, independent work by the author, Julia Malinovska. It was supported by research funding to Dr. Michael Kallos from the Canadian Institutes of Health Research (CIHR).

Acknowledgements

I am grateful to Dr. Michael Kallos for taking me on as a summer student and keeping me around for my master's program. I am extremely thankful for this opportunity and all the exciting things I got to learn.

I would like to express many thanks to my collaborators, Dr. Dean Betts, Dr. Robert Cumming and Alexandra Kozlov for all of their input and suggestions on this project.

I would also like to acknowledge the assistance and support of Dr.Pina Colarusso and Dr. Lucy Swift at the Live Cell Imaging Lab and Ranjan Maity and Yiping Liu at the Flow Cytometry Facility. I have learned a lot from these individuals and greatly appreciate the help they have given me.

Thank you to everyone at PPRF for providing a fun outlet during all the stressful times. An especially big thank you to Tiffany Dang for teaching me the ways of cell culture and being my friend and mentor from Day 1. Her continuous support, patience and encouragement has meant a lot to me. Special thank you to my desk neighbour, Heather Booth, for listening to my cell "drama" and teaching me to "not fret, fritter".

The completion of this thesis would not have been possible without the support of those closest to me. I am thankful for my parents who sacrificed many things for me to have the opportunity to be here and perform this research. I am forever grateful to them. Thank you to my sister Nadine, for setting the bar high and being an incredible role model. I am inspired by her hard work and ethic every day and I am lucky to have her support in all that I do. And finally, thank you to all my friends and those who surrounded me during this time, for the continued love and support.

Table of Contents

Abstract i
Preface ii
Acknowledgements iii
Table of Contents iv
List of Figures viii
List of Tables xv
List of Abbreviations xvi
Nomenclature xviii
Chapter 1 Introduction 2
1.1 Motivation 2
1.2 Scope of Thesis 3
1.3 Thesis Outline 4
Chapter 2 Literature Review 5
2.1 Overview 5
2.2 Pluripotent Stem Cells (PSCs) 5
2.3 Induced Pluripotent Stem Cells (iPSCs) 6
2.4 Human Induced Pluripotent Stem Cells (hiPSCs) 7
2.4.1 Current Challenges 8
2.4.2 Bioprocess Development 9
2.5 Dynamic Culture 10
2.6 Microcarriers 11
2.7 Types of Bioreactors 13
2.8 iPSC Characterization 16
2.9 Methods of Reprogramming 17
2.9.1 Retroviral / Lentiviral Reprogramming 18
2.9.2 Adenovirus 18
2.9.3 mRNA Reprogramming 18
2.9.4 Protein Transduction 19
2.9.5 Episomal Vector Reprogramming 19
2.9.6 Sendai Virus Reprogramming 19
2.9.7 Comparison of Reprogramming Approaches 20
2.10 Role of Metabolism in Reprogramming 21
2.11 Metabolism of Cancer Cells 23

2.12 Addition of Lactate to Reprogramming Process 24
Chapter 3 Methodology 27
3.1 Cell Source 27
3.1.1 CRL 2522 27
3.1.2 PGPC3 27
3.2 Culture Media 27
3.2.1 Fibroblast Media 27
3.2.2 hiPSC Media 27
3.3 Static Culture Procedure for CRL 2522 28
3.3.1 Thawing 29
3.3.2 Passaging 29
3.3.3 Cryopreservation 30
3.4 Static Culture Procedure for PGPC3 30
3.4.1 Matrigel Preparation 31
3.4.2 Thawing 32
3.4.3 Passaging 33
3.5 Glassware Preparation for Microcarrier Culture 34
3.6 Microcarrier Preparation 34
3.6.1 Autoclaving Procedure 35
3.7 Microcarrier Screening 36
3.7.1 Experiment Set-up 36
3.8 Reprogramming Timeline Overview 37
3.9 Static Reprogramming Protocol 38
3.10 Dynamic Reprogramming 41
3.10.1 Reprogramming on Microcarriers 42
3.10.2 Media change in Suspension 42
3.11 Addition of Lactate to Reprogramming Process 42
3.11.1 Lactate Medium 43
3.11.2 Glucose Medium 44
3.11.3 Lactate Reprogramming Protocol 44
3.12 Counting Techniques 44
3.12.1 Crystal Violet Assay 45
3.12.2 NucleoCounter 46
3.13 Validation of Pluripotency 47
3.13.1 Alkaline phosphatase live stain 47
3.13.2 Immunocytochemistry 48

3.13.3 Flow Cytometry 48
3.14 Flow Cytometry Procedure 49
3.15 Reprogramming Efficiency 51
3.16 Lactate and Glucose Assay 52
3.16.1 Sample Preparation 52
3.17 Brightfield Imaging 52
3.18 Confocal Imaging 53
3.18.1 Protocol for iPSC immunocytochemistry 53
3.19 CellCyte X Imaging 55
3.19.1 Stitching images 55
3.19.2 Manual Colony Selection 59
3.19.3 Automated Colony Selection 60
Chapter 4 Aim 1- Small-Scale Dynamic Culture Reprogramming 62
4.1 Overview 62
4.2 Introduction 62
4.3 Results and Discussion 63
4.3.1 Microcarrier Screening 63
4.3.2 Reprogramming on microcarriers 71
4.3.3 Effect of shaking at different Stages of Reprogramming process 74
4.3.4 Shaking at different Stages of Reprogramming process at 60,000 cells/well 77
4.3.5 Reprogramming on an orbital shaker plate with Low Attachment plate 83
4.3.6 Potential for reprogramming in 10mL stirred suspension bioreactor 87
4.4 Conclusion 88
Chapter 5 Aim 2 - Addition of Lactate to Static Culture Reprogramming 89
5.1 Overview 89
5.2 Introduction 89
5.3 Results and Discussion 90
5.3.1 Brightfield Images 92
5.4 Conclusion 93
Chapter 6 Aim 3 - Small-Scale Dynamic Culture Reprogramming with Addition of Lactate 94
6.1 Overview 94
6.2 Introduction 94
6.3 Results and Discussion 95
6.3.1 Day 7 and last day counts 96
6.3.2 Image Analysis 98

6.3.3 Flow Cytometry 104
6.3.4 Lactate and Glucose Assay 106
6.4 Conclusion 109
Chapter 7 Conclusions and Recommendations 110
7.1 Conclusions 110
7.2 Recommendations 112
7.2.1 Preventing Contamination 112
7.2.2 Limitations and Future Work 113
7.3 Contribution to Scientific Knowledge 114
References 115

List of Figures

Figure 1: Bioprocess for the production of human induced pluripotent stem cells with a proposed short cut through the reprogramming of somatic cells in a dynamic 3D culture. Figure was created with BioRender.com. 10

Figure 2: Attachment of neonatal foreskin fibroblast cells to a commercial microcarrier. The cell nuclei are stained green with a SYTO24 Nucleic Acid Stain after being fixed and permed.....12

Figure 3: Comparison of the horizontal blade and Vertical-Wheel® bioreactors and their CFD model. **(A)** Image of a Horizontal blade bioreactor. **(B)** CFD model of velocity for a 0.1L horizontal blade bioreactor at 80 RPM. Reprinted with permission from Elsevier [44]. **(C)** Image of a Vertical-Wheel® bioreactor **(D)** CFD model of velocity for a 0.1L vertical wheel bioreactor at 80 RPM. Reprinted with permission from John Wiley and Sons [45].....14

Figure 4: hiPSCs (PCPC3) grown as aggregates in a dynamic, 3D bioreactor culture. Image was taken with a Brightfield microscope at 10X with a scale of 200 μm. 15

Figure 5: Differences in differentiated cell versus pluripotent cell metabolism. In the presence of oxygen, differentiated cells will use oxidative phosphorylation while pluripotent cells rely on glycolysis. As somatic cells are reprogrammed, there is a shift from oxidative phosphorylation to glycolysis. Figure was created with BioRender.com. 22

Figure 6: Results published by *Kozlov et al.* comparing expression of glycolytic enzymes using qRT-PCR. Glucose, pyruvate and lactate treatments are compared to the control [5]. A significant increase in the enzymes of PGK1, PDK1and HK2 can be seen in the lactate condition compared to control. 24

Figure 7: Results published by *Kozlov et al*. showing Seahorse Analyzer24 measurements of OCR and ECAR during glycolysis stress test and mitochondrial stress test [5]. **(a)** Lactate treated cells were better at responding to glycolytic energy demand as seen by the increased relative ECAR **(b)** Lactate treated cells had an increased OCR for meeting ATP demand **(c)** Reduced spare respiratory capacity of lactate treated cells indicates ability to use mitochondrial respiration and glycolysis depending on what is available. 25

Figure 8: Sample calculation for the weight of Collagen coated microcarrier needed for 50mL of volume at a microcarrier density of 5.4 cm^2/mL. 35

Figure 9: Timeline for static reprogramming process. MX denotes media change days. 37

Figure 10: Timeline for reprogramming on microcarriers in a dynamic system. MX denotes a 100% media change. 42

Figure 11: Reprogramming timeline with the addition of lactate on Day 4. 43

Figure 12: Similarity and complexity evaluation of the antibody conjugates adapted from Cytek spectrum viewer. 49

Figure 13: Examples of Brightfield images obtained at different microscope configurations. A) Image of static culture at 5X magnification and phase 0. B) Image of static culture at 10X magnification and phase 1. C) Image of suspension aggregate culture at 10X magnification and phase 2.....53

Figure 14: Fluorescent staining of an established hiPSC line PGPC3 with SOX2 (green) and TRA-1-60 (red). 54

Figure 15: Fluorescent staining of an established hiPSC line PGPC3 with OCT4(green) and SSEA4 (red).....55

Figure 16: Settings used for image stitching in FIJI. **A)** FIJI grid stitching pattern used based on output of CellCyte X images. **B)** Configuration of grid size and tile overlap **C)** Example of stitched well image. 58

Figure 17: FIJI scale conversion of pixels to micrometre. 59

Figure 18: FIJI freehand selection tool outlined in red. 59

Figure 19: Example of selected colony using freehand selection tool in FIJI. 60

Figure 20: Built-in analysis of colony selection for a phase contrast image. The yellow mask is the automated selection performed by the software. 61

Figure 21: Experimental set-up for microcarrier screening experiment. 63

Figure 22: Crystal violet counts taken on Day 1, 3 and 5 of microcarrier screening. 64

Figure 23: Fluorescent images of live cells on top four performing microcarriers. Scale bar represents 200 μm. 65

Figure 24: Experiment set-up for comparison of fibroblast cell growth on Hillex and Collagen Coated microcarriers in a 10 mL spinner bioreactor. 66

Figure 25: Comparison of fibroblast growth on Hillex and Collagen Coated microcarriers in 10mL spinner bioreactors. 66

Figure 26: Fluorescent images of live cells stained with SYTO 24 on Collagen coated microcarriers taken on days 1-5. Scale bar represents 100 μm. 67

Figure 27: Fluorescent images of live cells stained with SYTO 24 on Hillex microcarriers taken on days 1-5. Scale bar represents 100 μm. 67

Figure 28: Brightfield images of live cells stained with Crystal violet in MeOH on Collagen coated microcarriers taken on days 1-5. Scale bar represents 200 μm. 68

Figure 29: Brightfield images of live cells stained with Crystal violet in MeOH on Hillex microcarriers taken on days 1-5. Scale bar represents 200 μm.....68

Figure 30: Well plate set up for screening of hiPSCs on Collagen coated and Hillex microcarriers. 69

Figure 31: Fluorescent images of live cells stained with SYTO 24 showing comparison of hiPSC growth on Collagen coated and Hillex microcarriers. Scale bar represents 200 μm.....70

Figure 32: (A) Experimental set-up of factorial experiment with analysed conditions. **(B)** Fold expansion of analysed conditions with statistics performed by one way ANOVA with comparison to each condition. * $P \leq 0.05$. 71

Figure 33: Experimental set-up of reprogramming examining static, shaken and microcarrier conditions in Stage 1. Figure was created with BioRender.com. 72

Figure 34: Total cells counts from the counting wells of the three conditions on Day 0 before transduction. 72

Figure 35: Images of Stage 1 Static and Stage 1 Shaken conditions taken on Day 18 at 10X magnification. 73

Figure 36: The effect of dynamic forces on reprogramming at different stages of the process with optimization of cell density. Figure was created with BioRender.com. 75

Figure 37: Images of cell growth in different combinations of Stage 1 and Stage 2 shaking at different cell densities. Images were obtained on Day 14 at 5X magnification. 76

Figure 38: The effect of shaking at different stages of the reprogramming process at 60,000 cells/well. Figure was created with BioRender.com. 77

Figure 39: Images on Day 19 at cell density of 60,000 cells/ well, 5X magnification. The cell lifting phenomena was again observed in the Shaken-Shaken condition. 78

Figure 40: (A) Images of cells on Day 19 at 5X magnification at Phase 0 and Phase 1. (B) The cells were replated on Matrigel with images shown on Day 1 and Day 3. 79

Figure 41: Summary of cells expressing pluripotency markers in flow cytometry analysis. . 80

Figure 42: Manual counts performed based on the CellCyteX images. Conditions with replicates are identified. 82

Figure 43: Reprogramming timeline with the use of a low attachment plate in Stage 2. Two conditions were tested, one with a media change on Day 8 and one without a media change. Figure was created with BioRender.com. 83

Figure 44: Aggregate formation in low attachment shaking plates with passaging onto static on Day 9. Aggregate images taken at 10X, Phase 2. Static images taken at 5X, Phase 0. Scale bar represents 200 μm. 84

Figure 45: Static recovery of aggregate cells on Day 9 on Matrigel plates. Images taken at 5X magnification. 85

Figure 46: Day 19 cell growth of MX condition demonstrating (A) colony formation and (B) positive alkaline phosphatase staining. 85

Figure 47: Growing aggregates in a well plate suspension at 120,000 cells/well. 86

Figure 48: Proposed bioprocess using aggregate pre-formation and expansion in small scale bioreactors. Figure was created with BioRender.com in collaboration with Tiffany Dang. ...87

Figure 49: Experimental set-up of first lactate experiment testing the effect of lactate exposure on reprogramming. 90

Figure 50: Timeline of the reprogramming process with the addition of lactate. Figure was created with BioRender.com. 91

Figure 51: Cell counts of different treatment lengths taken on Day 7 before the cells were plated at different densities. 91

Figure 52: Images of reprogrammed cells with different lactate treatment lengths, taken on Day 14 at 5X magnification. 93

Figure 53: Examining colony formation after optimal conditions of 13h lactate treatment, Stage 2 shaking and 60,000 cells/well are used. Figure was created with BioRender.com. ...95

Figure 54: Day 7 counts of Experiment 1 and Experiment 2 96

Figure 55: Cells counts performed on the last day of each experiment using a Nuclecounter. The last day for Experiment 1 was Day 23 and for Experiment 2, Day 24. 98

Figure 56: Experiment 1, Day 23 images at 5X magnification. 100

Figure 57: Experiment 2, Day 24 images at 5X magnification. 100

Figure 58: Nanog staining of shaken no lactate condition. 101

Figure 59: Colony counts comparing an automated to manual approach for overall colonies, Nanog+ colonies and Tra-1-60+ colonies. 102

Figure 60: Summary of counted colonies expressing Nanog and Tra-1-60 in Experiment 1 and Experiment 2. Colonies were only counted if they had distinct hiPSC appearance and were larger than 1000 $\mu m^{2.}$ 103

Figure 61: Expression of pluripotent markers using flow cytometry (A) Experiment 1 Day 23 (B) Experiment 2 Day 24. 105

Figure 62: Comparison of CD44 and Tra-1-60 + Nanog expression in Experiment 1 and Experiment 2. 106

Figure 63: Results of the lactate and glucose assay for Experiment 1 and Experiment 2 on Day 7. Flux was used as a comparison of the amount of lactate produced to the glucose consumed. 107

Figure 64: Results of the lactate and glucose assay for the last day of experiment. 108

List of Tables

Table 1: Summary of common reprogramming methods for hiPSC production [2]. 17

Table 2: Surface area of different culture vessels and the required volume of Matrigel solution.....31

Table 3: Recommended reagent volume for T-25 and T-75 flasks.....33

Table 4: Microcarrier Specifications.....36

Table 5: Titer information for Lot No. L2190071 40

Table 6: Comparison of media types and their concentrations of glucose, lactate and pyruvate for use in reprogramming with lactate. 43

Table 7: Flow cytometry markers with fluorophore and supplier information. 48

Table 8: Flow cytometry antibody specifications and required volume. 51

List of Abbreviations

AF – Alexa Fluor

ANOVA - Analysis of Variance

AO - Acridine Orange

AP - Alkaline Phosphatase

c-Myc - Cellular myelocytomatosis oncogene

CC – Collagen Coated

CD44 - Cluster of Differentiation 44

CFD - Computational Fluid Dynamic

cGMP – Current Good Manufacturing Practices

CO_2 - Carbon Dioxide

DAPI - 4',6-diamidino-2-phenylindole

DMEM- Dulbecco's Modified Essential Medium

DMSO - Dimethyl Sulfoxide

DNA- Deoxyribonucleic acid

E8 - Essential 8

ECAR - Extracellular Acidification Rate

EMT – Epithelial Mesenchymal Transition

ESC - Embryonic Stem Cells

FACS - Fluorescence-Activated cell sorting

FBS- Fetal Bovine Serum

hiPSCs - Human Induced Pluripotent Stem Cells

iPSCs - induced Pluripotent Stem Cells

Klf4 - Krüppel-like factor 4

MEFs - Mouse Embryonic Fibroblasts

MET - Mesenchymal epithelial transition

MeOH – Methanol

mM - Millimolar

MOI - Multiplicity of infection

mRNA - Messenger Ribonucleic Acid

MX – Media change

OCR - Oxygen Consumption Rate

OCT 3/4 - Octamer Binding Transcription Factor

OXPHOS - Oxidative Phosphorylation

PBS- Phosphate Buffered Solution

PFA - Paraformaldehyde

Ph - Phase

PPRF - Pharmaceutical Production Research Facility

PSC - Pluripotent Stem Cell

RNA - Ribonucleic acid

ROCKi - Rho-Associated Protein Kinase inhibitor

ROS - Reactive Oxygen Species

RPM – Revolutions Per Minute

SD - Standard Deviation

SOX2 - SRY-Box Transcription Factor 2

SSEA - Stage-Specific Embryonic Antigen

TCA – Tricarboxylic Acid

Thy1 - Thymus Cell Antigen - 1

TRA - Tumor Rejection Antigen

Nomenclature

Symbol	Definition	SI Units
X_v	Cell density	cells/mL
N_v	Number of counted cells	cells
V_B	Volume of bioreactor	mL
X_A	Attached cell density	cells/cm^2
N	Total number of cells	cells

Chapter 1 Introduction

1.1 Motivation

The regenerative medicine field was revolutionized by the discovery of human induced pluripotent stem cells (hiPSCs) and the immense capability these cells offer. The unique potential of these cells is their source of origin. Through a combination of transcription factors, Takahashi and Yamanaka were able to convert somatic cells into pluripotent stem cells, thereby overcoming the moral and ethical implications raised over embryonic stem cells, the traditional source of pluripotent stem cells [1]. Furthermore, the ability to harvest somatic cells from patients provides the opportunity for autologous treatment which has not been previously possible with pluripotent stem cells.

Despite the many possibilities of hiPSCs, there is currently a limited number of clinical trials with their application, vastly due to the challenges of producing clinically relevant cell numbers. The generation of hiPSCs is a costly and time-consuming process in itself without considering the expansion and differentiation stages. While great improvements have been made in the ability to expand and differentiate hiPSCs through 3D suspension cultures, the initial reprogramming stage remains inefficient and poses an obstacle to establishing a bioprocess. Major challenges of reprogramming include virus integration into the genome, time of reprogramming and type of somatic cell used [2][3]. Using a non-integrating reprogramming method that works on multiple cell types, such as Sendai virus, approaches to improving the reprogramming efficiency and integration into a bioprocess can be examined.

It has been shown that metabolism plays a key role in the transition of somatic cells to pluripotency; somatic cells rely on oxidative phosphorylation (OXPHOS) while hiPSCs primarily use glycolysis [4]. Therefore, by increasing the metabolic shift from OXPHOS to glycolysis, the reprogramming efficiency of somatic cells may be increased and recently it has

been shown that cell pre-treatment with lactate may aid in this transition [5]. Additional approaches that may be examined to increase reprogramming efficiency include dynamic culture conditions. A dynamic system has been shown to be beneficial to generation of murine iPSC colonies and the reprogramming of murine cells has been successfully done in a stirred suspension bioreactor [9][10]. Utilizing such an approach for hiPSCs generation would open the opportunity for a comprehensive bioprocess within a 3D dynamic system.

1.2 Scope of Thesis

The objective of this study was to increase colony formation during Sendai Virus reprogramming of human fibroblast cells through a metabolic shift using lactate within a dynamic culture. Increased colony formation is a positive indicator of an increased reprogramming efficiency which would reduce current reprogramming time and expansion in static culture as well as improve integration into a bioprocess.

Hypothesis: Transient exposure of somatic cells (fibroblasts) to lactate in a dynamic system will increase iPSC colony formation and reduce reprogramming time, due to a shift in metabolism from oxidative phosphorylation (OXPHOS) to glycolysis and positive effect of dynamic culture.

Specific Aims:

1: Small-Scale Dynamic Culture Reprogramming: Demonstrate increased colony formation in dynamic culture system.

2: Addition of Lactate to Static Culture Reprogramming: Establish that transient lactate exposure induces a metabolic shift and facilitates reprogramming in static.

3: Small-Scale Dynamic Culture Reprogramming with Addition of Lactate: Determine the effect of lactate exposure in a dynamic culture on reprogramming efficiency.

1.3 Thesis Outline

The literature review and background for this thesis will be covered in Chapter 2. The section will include information on pluripotent stem cells, dynamic culture, methods of reprogramming and the role of metabolism in reprogramming. Chapter 3 will discuss all methodology including static cell culture, dynamic cell culture, microcarrier preparation, reprogramming protocols for static, dynamic and lactate cultures and analytical procedures and protocols for cell counting, flow cytometry and metabolic assays. In addition to this, imaging techniques including brightfield microscopy, confocal microscopy and CellCyteX will be discussed. Aims 1 to 3 will be covered in Chapter 4 through Chapter 6. And lastly, Chapter 7 will cover the conclusions and recommendations to the project and future work.

Chapter 2 Literature Review

2.1 Overview

The following literature review section will cover an introduction to pluripotent stem cells (PSCs) as well as induced pluripotent stem cells (iPSCs) and human induced pluripotent stem cells (hiPSCs). The current challenges related to clinical use of hiPSCs, the need for bioprocess development, the use of bioreactors and impact of dynamic systems on cell growth and quality will be addressed. This will be followed by characterization of pluripotency and the various forms of reprogramming to hiPSCs as well as the advantages and disadvantages of these methods. Lastly, the role of metabolism in hiPSC development from somatic cells and previous results of lactate pre-treatment will be examined in more detail.

2.2 Pluripotent Stem Cells (PSCs)

Stem cells can fall into different categories depending on their capacity to differentiate. Cells with pluripotent ability are termed pluripotent stem cells (PSCs) and have properties of self-renewal and potency [8]. These cells are able to divide indefinitely, producing daughter cells with the same properties and ability to differentiate into specialized cells from the three germ layers: endoderm, mesoderm and ectoderm. The unique characteristics of PSCs make them a valuable asset to regenerative medicine both in drug testing and cell therapy. There are two types of PSCs, the traditional embryonic stem cells (ESCs) and the more recently discovered induced pluripotent stem cells (iPSCs). Despite their long history, the use of ESCs has several drawbacks as the cells are obtained from the inner cell mass of preimplantation embryos therefore raising ethical concerns [9]. iPSCs originate from somatic cells which are then reprogrammed into PSCs allowing for minimally invasive harvesting and avoiding ethical issues. The regenerative medicine field is shifting towards the use of iPSCs due to these advantages as both cell types have the same pluripotent ability.

2.3 Induced Pluripotent Stem Cells (iPSCs)

The first induced pluripotent stem cells (iPSCs) were derived in 2006 by Takahashi and Yamanaka from mouse embryonic and adult fibroblast cells [1]. These cells have pluripotent characteristics, ability to self-renew and can develop into almost any cell type or tissue. Four transcription factors were found to be necessary for inducing pluripotency: Oct3/4, Sox2, c-Myc and Klf4. These factors were identified from 24 genes that were believed to maintain embryonic stem (ES) cell characteristics. Each of the genes was introduced into mouse embryonic fibroblasts through retroviral transduction but no single gene was successful at producing cells with ES cell morphology. However, it was found that the combination of genes introduced together, resulted in a successful outcome. Individual genes were then removed until Oct3/4, Sox2, c-Myc and Klf4 were identified as critical for formation of ES cell-like morphology and coined “Yamanaka factors”.

During the reprogramming process, the establishment of pluripotency is hallmarked by changes in chromatin reorganization, morphology, and metabolism. The emergence of iPSCs is typically identified through formation of tightly packed cell colonies. This morphological change is defined as a mesenchymal – epithelial transition (MET) and is characterized by cells losing mesenchymal features and expressing epithelial ones [10]. The transcription factor Klf4 is responsible for inducing epithelial properties by directly increasing E-cadherin while SOX2 and c-Myc supress mesenchymal characteristics such as migration [11]. Additional epithelial characteristics include well defined intracellular junctions and strong cell – cell interactions which can be seen in emerging iPSC colonies [10]. MET is an essential part of the reprogramming process and its inhibition will prevent the formation of iPSCs [12]. The process is reversible and an epithelial mesenchymal transition (EMT) takes place during embryogenesis and organ development [13].

2.4 Human Induced Pluripotent Stem Cells (hiPSCs)

In 2007, Takahashi and Yamanaka applied their previous findings to the reprogramming of human fibroblast cells to pluripotent cells known as human induced pluripotent stem cells (hiPSCs)[14]. Several groups were able to replicate these findings and create hiPSC lines [15][16]. The discovery of hiPSCs has offered a unique advantage to stem cell research as it allowed for disease-specific cell lines to be established and used for disease modelling and drug validation [17]. Modelling using hiPSCs overcomes the lack of suitable animal models and can identify patient-specific therapies [18]. Not only does this offer an advantage for availability of multi-lineage system testing in preclinical drug safety studies but also opens opportunity for personalized treatment approaches [19]. For disorders that already have a multitude of drug therapies available, it allows for patient-specific screening to ensure the optimal treatment is selected [20] [21]. The tailored treatment approach to medicine is growing in importance due to the rise of adverse side effects from drug treatment [22]. It is estimated that severe adverse side effects are the fourth leading cause of death in the United States, resulting in 100,000 deaths per year and affecting 2 million patients [23]. Therefore, hiPSC based disease models would not only provide a more accurate understanding of disease cause and progression but allow for patient specific treatment to minimize side effects and maximize positive outcomes.

In cell transplantation therapy, hiPSCs offer an advantage to embryonic stem cells (ESCs) by overcoming challenges related to ethical concerns with human embryo use and autologous treatment [24]. Autologous treatment is made possible with hiPSCs as the patient's own somatic cells are collected and reprogrammed into a pluripotent state before generating the needed cell type. Typically, a minimally invasive form of somatic cell collection is used such as a skin punch biopsy or sampling of peripheral blood cells. To be used in clinical applications, the collected, reprogrammed and differentiated cells need to be generated in a robust and reproducible manner as well as satisfy current Good Manufacturing Practices

(cGMP) [25]. Certification of this kind is a laborious process and developed protocols should use integration free methods, xenogeneic material and be conducted in a cGMP-facility [26].

2.4.1 Current Challenges

There are limitations that need to be addressed prior to widespread adoption of hiPSC disease modelling. It is a concern that cells derived from healthy patients already demonstrate heterogeneity and variability in gene expression which would make them unreliable for use in disease modelling. Although some variability between lines is to be expected, standardization of protocols must be done to reduce additional differences in reprogramming, expansion and differentiation [27]. Different methods of reprogramming can be the cause of variability, particularly when the approach involves integration into the genome as there is residual expression of reprogramming factors [28]. To avoid these concerns and adhere to cGMP guidelines, a non-integrating approach with a feeder-free system should be examined. In addition to this, it is beneficial to have the cell culture conditions be highly controlled to ensure a robust and well documented procedure.

When it comes to hiPSC – based therapies, despite the immense potential their use in clinical trials remains very low. Many studies are primarily focused on the expansion of hiPSCs cells and the development of differentiation protocols while the bottleneck of early reprogrammed cell expansion remains. It has been largely agreed that the best method for hiPSC expansion is through 3D dynamic culture systems like bioreactors [29]. Recent studies have shown expansion of upwards 100- fold over 5 days with specialized Vertical-Wheel ® bioreactors [30]. However, the reprogramming efficiency of somatic to induced pluripotent stem cells remains low, labour intensive and often spans several months.

2.4.2 Bioprocess Development

Whether hiPSCs are used for cell therapy or disease modelling, the above presented challenges can be mitigated through a bioprocess that combines a dynamic system with a non-integrating reprogramming approach. A bioprocess is commonly defined as a biological process, involving living cells, to obtain a desired material or product [31]. Typically, cells are expanded in static vessels, such as well - plates or T-flasks, which is labour intensive and time consuming. An alternative to this is a dynamic system. Dynamic systems involve fluid movement which can be induced using an orbital shaker, or a full 3D bioreactor system which uses an impeller for stirring.

Although bioprocesses can be static or dynamic, the use of a 3D dynamic system, such as one using a bioreactor, promotes the production of more homogenous cells due to a well-mixed and highly controlled environment. Factors like agitation speed, pH, CO_2 concentration, and O_2 concentration can be controlled in an automated bioreactor system. A bioreactor-based process also addresses the issue of sufficient cell number for clinical treatments; an adult patient requiring replacement of damaged cardiac tissue due to a myocardial infarction would need 1-2X10^9 cells [32]. To provide patients with a sufficient number of cells and access to autologous cell therapy in a timely manner, a bioreactor-based process needs to be developed and standardized.

The overarching goal of hiPSC expansion is the development of a comprehensive bioprocess such as shown in Figure 1.

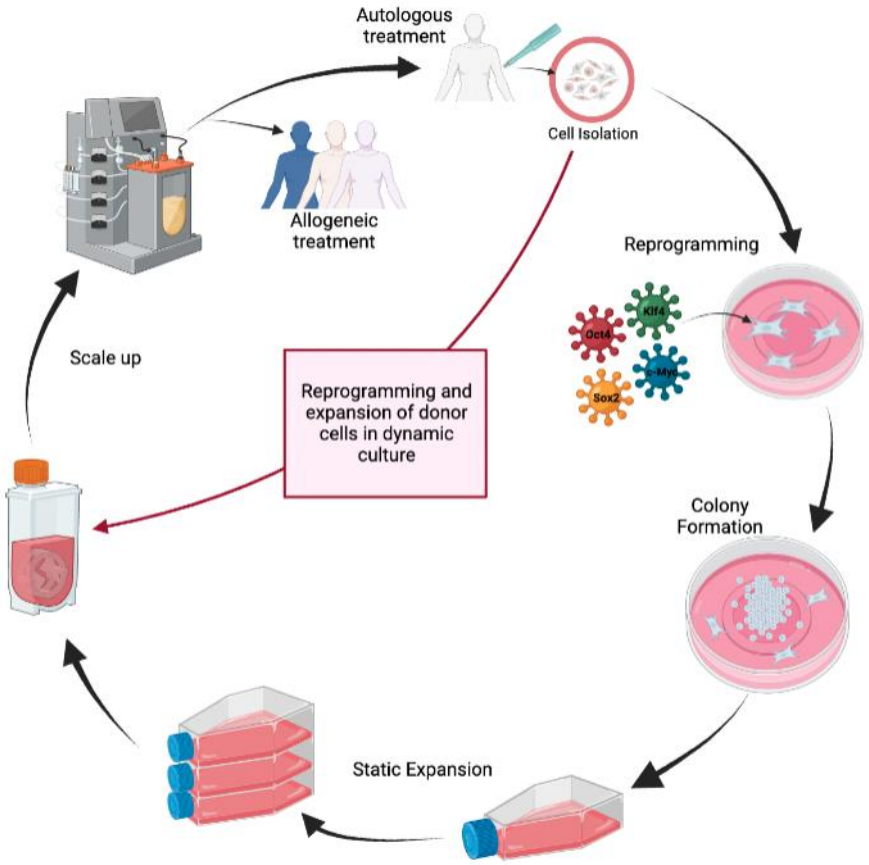

Figure 1: Bioprocess for the production of human induced pluripotent stem cells with a proposed short cut through the reprogramming of somatic cells in a dynamic 3D culture. Figure was created with BioRender.com.

2.5 Dynamic Culture

Dynamic culture systems are primarily characterized by fluid movement. The use of a dynamic system, such as a bioreactor, provides advantages in control of environmental conditions (pH, dissolved oxygen, agitation), scalability potential, and is optimal for producing clinically relevant cell numbers with reduced labour and operating cost. The shear forces caused by stirring have also shown to influence pluripotency and suppress differentiation [7][33]. Additionally, PSCs expanded in dynamic suspension cultures have an increased expression of pluripotency markers, are capable trilineage differentiation and show characteristics of a naïve stem cell [33].

The effect of biophysical factors on cell reprogramming is not well understood but past studies have shown increased reprogramming efficiency in dynamic culture with skin fibroblast cells obtained from transgenic mice [6]. The study used an orbital shaker to simulate a dynamic environment and established an optimal period of shaking to increase reprogramming efficiency. The findings show that the dynamic culture inhibited reprogramming during the early stages of Day 2 – Day 6 and had no significant effect on the later stages of Day 12 – Day 20. The most significant effect was seen when shaking was applied on Day 6 which is hypothesized is when the cells became confluent, and the confluency began having a negative impact. This also led them to examine the effect of cell seeding density on reprogramming which showed that beyond a certain seeding density, there is a negative effect of higher seeding density on reprogramming. The study also determined that within this dynamic culture experiment, convective mixing is the primary dynamic force as opposed to shear stress.

Previous studies have also been done on the reprogramming of mouse cells in a stirred suspension bioreactor [7]. Mouse embryonic fibroblast cells were transduced with retroviral vectors and inoculated in a 100 mL bioreactor at an agitation of 100 rpm. The dynamic culture obtained 50 million cells compared to the 4 million from static culture and 90-100% of these cells expressed pluripotent markers. This study established feasibility of reprogrammed cell expansion in a suspension system and provides foundation for studies involving human cells.

2.6 Microcarriers

Fibroblast cells, which are a common somatic cell type used for reprogramming, are an anchorage dependent cell type. Therefore, these cells require a surface to grow on and in a dynamic 3D system, microcarriers are used to provide a growing surface for cells. Typically, a microcarrier is a microbead that ranges in a diameter of 90–350 μm and allows for cell attachment and growth as can be seen in Figure 2. Common differences in properties of commercialized microcarriers include shape, coating, surface charge, size and composition

[34]. The main advantage of using microcarriers is a high surface to volume ratio which allows for growth of anchorage dependent cells in suspension cultures. Additionally, coatings such as gelatin, collagen and fibronectin promote cell attachment to surface [35].

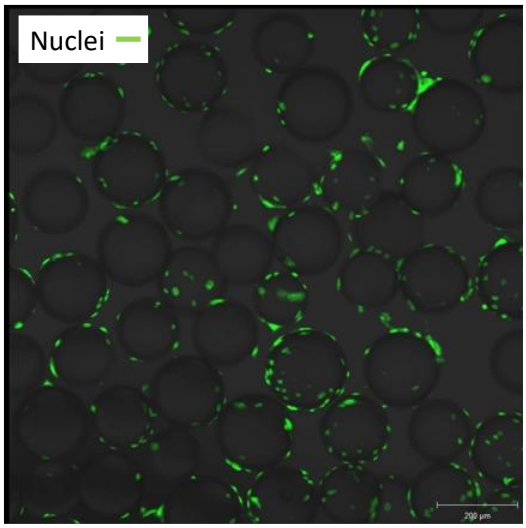

Figure 2: Attachment of neonatal foreskin fibroblast cells to a commercial microcarrier. The cell nuclei are stained green with a SYTO24 Nucleic Acid Stain after being fixed and permed.

Numerous studies have used microcarriers for expansion of various cell types and several groups demonstrated scale up using microcarriers for PSCs in dynamic systems [36]. Microcarrier systems have yielded higher expansion by 2.4-4.3 fold than those of static culture [37] and provided the opportunity for differentiation directly within the dynamic system for various cells such as cardiomyocytes [38][39]. Due to the differences and complexity of the differentiation process, universal protocols for different cultures and cell lines are difficult to establish and standardize. Factors such as type of bioreactor used, oxygen level, growth factors and media composition all play an important role. One disadvantage of microcarrier culture, is the need for dissociation of cells from the microcarriers upon confluency and the additional processing steps to isolate the cells for downstream applications [40].

2.7 Types of Bioreactors

Various bioreactor systems have been developed throughout the years for growing different cell types and biological products. As previously discussed, bioreactor systems have advantages over static culture in reduced labour and cost, increased cell expansion and greater cell homogeneity [29]. The traditional choice for iPSC expansion in 3D culture has been a horizontal blade, stirred suspension bioreactor as shown in Figure 3 A. Over the years, the process within the horizontal blade bioreactor has been optimized but shortcomings of high shear stress, high agitation speed and uneven distribution of forces due to the impeller, have led to the development of an alternative vessel [41]. A computational fluid dynamic model (CFD) of the 100mL horizontal blade bioreactor at 80 RPM can be found in Figure 3 B. The velocity within the bioreactor is either at the high or low end with little range. This is due to the design of the impeller which does not allow for sufficient mixing and causes heterogeneity in the cultivated cells.

The Vertical-Wheel® bioreactor is a novel bioreactor which is characterized by its "waterwheel" style impeller and a U-shaped bottom as shown in Figure 3 C [42]. This design was created to provide more culture homogeneity, a reduced power input and lower fluid forces through having radial and axial mixing [29]. From the CFD model in Figure 3 D, it can be seen that fluid velocity in the cell environment is reduced by more than half in the Vertical-Wheel® compared to the traditional horizontal blade bioreactor. The improved distribution of forces, better mixing, and reduction in shear stress has made a positive impact on cell viability and cell growth, especially for hiPSC expansion [29]. Several studies have reported increased fold expansion, more homogenous aggregate growth and potential for single-cell inoculation compared to the horizontal blade [29][41][43].

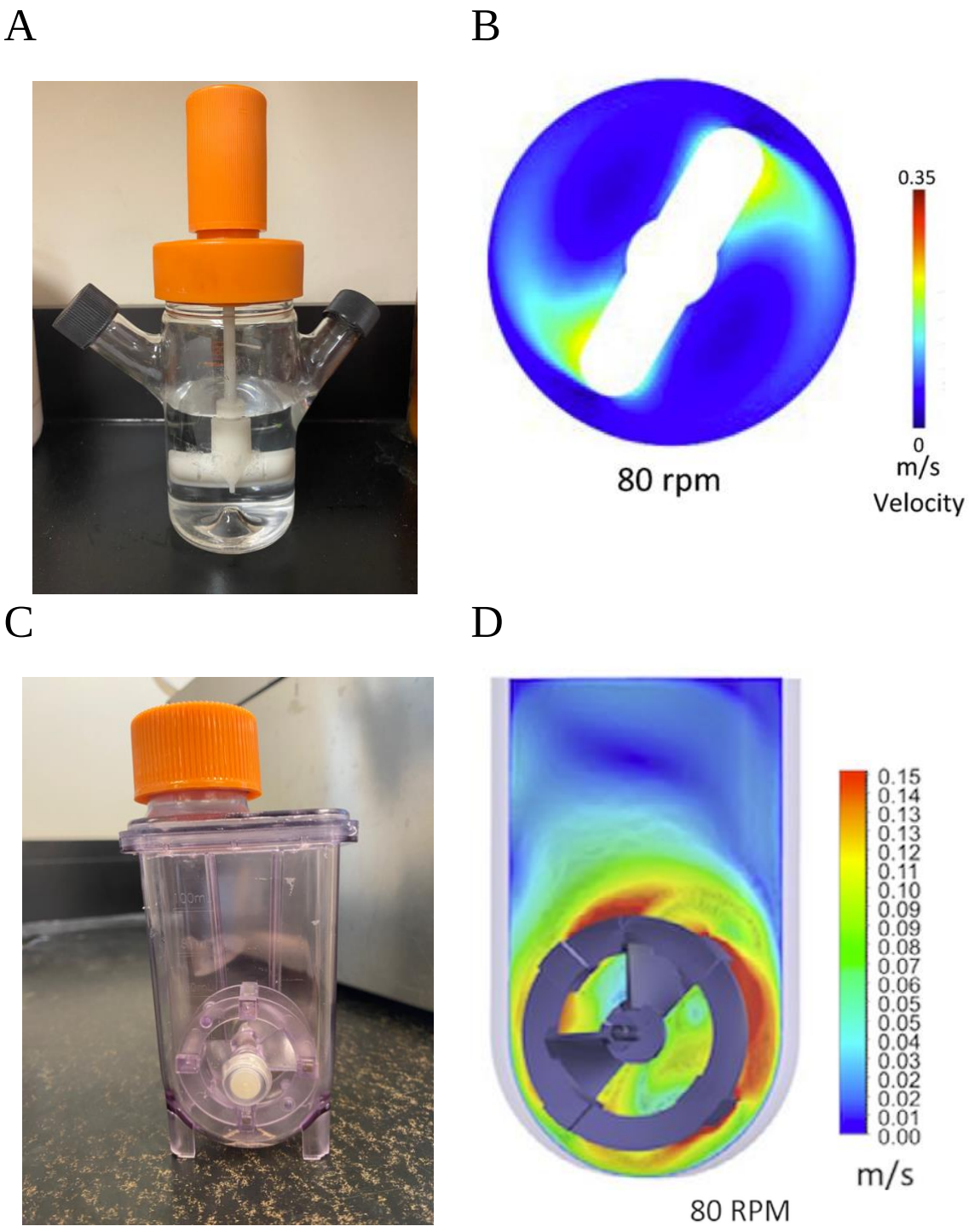

Figure 3: Comparison of the horizontal blade and Vertical-Wheel® bioreactors and their CFD model. **(A)** Image of a Horizontal blade bioreactor. **(B)** CFD model of velocity for a 0.1L horizontal blade bioreactor at 80 RPM. Reprinted with permission from Elsevier [44]. **(C)** Image of a Vertical-Wheel® bioreactor **(D)** CFD model of velocity for a 0.1L vertical wheel bioreactor at 80 RPM. Reprinted with permission from John Wiley and Sons [45].

As previously described, some cell types are adherent and require a surface for growth while others can form aggregates in a suspension environment. hiPSCs fall into a category of cells that are able to aggregate in a stirred suspension bioreactor (with addition of ROCKi) from a single cell suspension when no substrate is present [29][46][47]. A picture of hiPSC aggregates can be found in Figure 4.

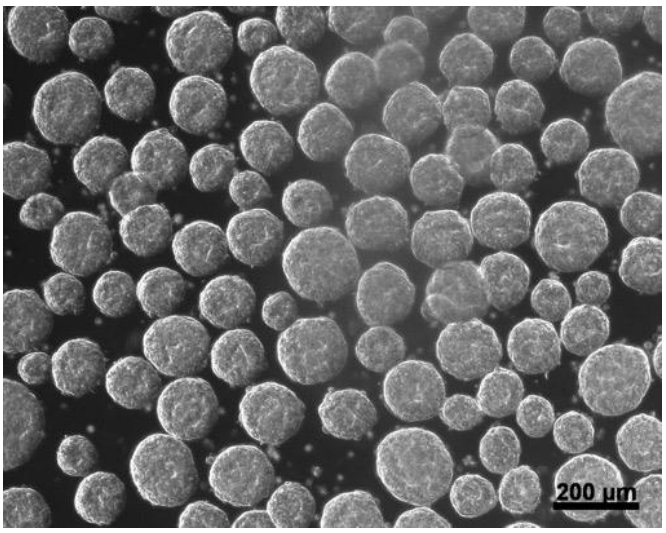

Figure 4: hiPSCs (PCPC3) grown as aggregates in a dynamic, 3D bioreactor culture. Image was taken with a Brightfield microscope at 10X with a scale of 200 µm.

The growth of hiPSCs as aggregates offers many advantages to a 3D dynamic bioprocess development. Prior to being able to culture hiPSCs as aggregates, , cells were grown on microcarriers which led to issues in downstream operations due to difficulties in the harvesting process. Alternatively, aggregates were "pre-formed" prior to inoculation into bioreactors. This approach involved seeding cells between 50,000 – 200,000 cells/cm^2 in a non-adherent six-well plate and waiting approximately 4 hours for cell clusters to form [43]. Following this, the preformed aggregates are inoculated into a bioreactor for growth in a suspension system. Although this approach has been commonly used and achieves good expansion, it produces a problem for scalability. Additionally, there are difficulties in controlling the initial aggregate size which results in heterogeneity. To improve on this approach and remove the bottleneck,

single-cell inoculation was proposed [29]. The growth of pre-formed aggregates to single-cell inoculation in Vertical-Wheel® bioreactors was compared and showed no difference. This led to the conclusion that hiPSCs can be grown in the Vertical-Wheel® bioreactor as aggregates using single cell inoculation.

2.8 iPSC Characterization

Pluripotency is defined by the ability of a cell to differentiate into cells from the three germ layers and it can be characterized by markers such as SSEA4, TRA-1-81, TRA-1-60, SOX2, OCT4 and NANOG [48][49]. In addition to this, CD44, a cell adhesion protein highly expressed in human fibroblasts, can be used to identify non-reprogrammed cells. CD44 is gradually lost during the reprogramming process and is not expressed in iPSCs making it a good negative cell surface marker [50].

Early on in the reprogramming process, successfully reprogrammed cells will downregulate Thy1, a fibroblast marker [51]. In only a fraction of Thy-negative cells, there will then be an upregulation of SSEA1, an embryonic marker, followed by a smaller subset of cells then beginning to express the core pluripotency markers. The expression of pluripotent markers differs throughout the reprogramming process, for example it has been shown that SSEA3 and SSEA4 are detected earlier than TRA-1-60 and TRA-1-81 [52]. This is an important consideration as SSEA3 and SSEA4 may be detectable but do not represent fully reprogrammed cells.

Flow cytometry is a technique that involves the analysis of single cells based on their fluorescent characteristics and visible light scatter [53]. The cells are suspended in a buffered salt-based solution with fluorescent dyes to measure specific markers, a different wavelength of light from the laser is used to excite each marker. Flow cytometry is an effective tool for characterizing iPSCs using the pluripotency markers discussed above.

2.9 Methods of Reprogramming

Takahashi and Yamanaka used retroviral reprogramming to introduce transcription factors into the cell. Over the past 15 years, only a slight improvement in the initial reprogramming efficiency of ~0.02% has been made and concerns over virus integration into the genome remain [54]. Reprogramming efficiency is measured as the number of iPSC colonies generated, divided by the number of starting somatic cells [55]. Currently, available reprogramming methods must trade-off between the source of tissue used for reprogramming, integration of the virus and the reprogramming efficiency [3]. This opens a gap for an improved reprogramming approach that addresses these challenges and produces cells which can be used in clinical applications.

The most common reprogramming methods are summarized Table 1 below and discussed in the next sections.

Table 1: Summary of common reprogramming methods for hiPSC production [2].

Method	Integrating	Time (Days)	Efficiency (%)	Multiple Cell Types Reprogrammed	Reference
Retroviral	Yes	25 - 35	0.02 - 0.08	Yes	[56][57][58]
Lentiviral	Yes	20 - 30	0.02 - 1	Yes	[58] [59]
Adenoviral	No	25 - 30	0.0002	No	[2][59][60][61]
mRNA	No	20	0.6 – 4.4	No	[2][62][63]
Protein Transduction	No	56	0.001	No	[57][59][64]
Episomal	No	30	0.0006 – 0.02	Yes	[65] [66][67]
Sendai virus	No	25	0.5 - 1.4	Yes	[68][69][70]

2.9.1 Retroviral / Lentiviral Reprogramming

The retroviral reprogramming method was the original approach used for reprogramming which relies on factor integration in the genome to transmit gene expression into the host cells [56] [57]. Lentivirus is one type of a retrovirus that is often used and is characterized by the ability to infect non-dividing cells. Retrovirus and lentivirus are both RNA viruses that use reverse transcriptase to convert into DNA and integrate into the host genome [59]. This approach poses many challenges as there is an increased risk of insertional mutagenesis and residual factor expression [59]. Due to integration into the genome, the factors could be activated at any point causing tumorgenicity which poses a risk to clinical applications[58]. In addition to this, there is a low reprograming efficiency with colony development observed as late as day 20-30.

2.9.2 Adenovirus

The Adenovirus reprogramming approach is a non-integrating method that uses cDNA of the Yamanaka factors in a single expression vector [60]. Despite the benefit of being non-integrating, adenovirus only has a short-term expression of transgenes compared other reprogramming approaches, which may be the reason for the reduced the efficiency of 0.0002% in human fetal fibroblasts [2][59][61].

2.9.3 mRNA Reprogramming

This method of reprogramming uses modified RNA (mRNA) which is synthesized with the Yamanaka factors and used to transfect cells. Daily transfections are needed for a period of approximately 17 days to maintain the high levels of transcription factor expression with colonies emerging around Day 20 [62][63]. As this is a non-integrating approach, the genome is not altered and there are no residual exogenous transcription factors remaining. The main drawback of this method is the labour involved with daily transfection and the associated cost [2].

2.9.4 Protein Transduction

An alternative, integration-free approach to virus transduction has been examined in the form of protein transduction which delivers exogenous proteins into cells without transcription from delivered genes [59]. The recombinant proteins are produced in *E.*coli and are fused with a short peptide that facilitates protein transduction (poly-arginine) [64]. Challenges faced by this approach include difficulty in creating and purifying large amounts of bioactive proteins that are able to cross the hydrophobic cellular membrane as well as the short half-life of proteins within the cell [57]. The reprogramming efficiency is also low at 0.001% and this reprogramming method has not been validated on multiple cell types [64].

2.9.5 Episomal Vector Reprogramming

Often described as one of the most economical and easiest ways to reprogram somatic cells into iPSCs, episomal vector reprogramming uses three vectors based on oriP/EBNA (Epstein–Barr nuclear antigen) to deliver six reprogramming factors : Oct4, Sox2, Nanog, Lin28, Klf4 and L-Myc. For the vectors to enter the cell, an electric current is used to open cell channels, a technique which is referred to as electroporation [65]. An additional advantage to this approach is that it has been shown to work with numerous cell types including fibroblast cell, amniotic fluid stem cells, mesenchymal stromal cells and mononuclear cells from adult peripheral blood [66]. Disadvantages of this approach are the low efficiency of under 0.02% [67]

2.9.6 Sendai Virus Reprogramming

The Sendai virus reprogramming method is commercially available and is based on a modified and non-transmissible form of the Sendai virus. This respiratory virus of mouse and rat is non-pathogenic to humans, and has never been linked to human disease [68]. It can be safely used due to the deletion of the Fusion protein (F) which prevents the virus from producing infectious particles [69]. The main advantage of the Sendai virus vectors is that they

replicate only in the cytoplasm of infected cells and do not integrate into the host genome. The virus works by attaching itself to the sialic acid receptor which is present on the surface of many different cells and replicates independent of cell cycle. Following infection, the virus goes through genome replication and protein synthesis and it is slowly diluted through cell division [70].

2.9.7 Comparison of Reprogramming Approaches

There are many reprogramming methods available for the generation of iPSCs, several of which have been discussed in more detail above. Several important factors to consider during reprogramming include length of the reprogramming process, integration of factors into the genome, reprogramming efficiency and types of cells reprogrammed. For translational purposes and clinical use, it is critical that the reprogramming approach is nonintegrative and has GMP potential. Out of the approaches discussed, retro- and lentiviral delivery vectors as well as Piggybac are integrative approaches and would not be suitable for downstream applications. The next consideration is the reprogramming efficiency which out of the remaining footprint-free methods is highest in Sendai virus reprogramming.

One of the current commercially available reprogramming methods is the Sendai virus. The Sendai virus is non-pathogenic to humans and Sendai reprogramming vectors can transduce a wide range of cell types without integration into the chromosomes of the target cells. When compared to reprogramming using retro- and lentiviral delivery vectors, the vectors and transgenes of Sendai virus can be eliminated from cells therefore leaving zero footprint. The virus vectors remain in the cytoplasm of infected cells for a few passages and are completely lost by passage 10 [2]. Sendai virus reprogramming has a relatively high reprogramming efficiency of 1% for fibroblast cells which is greater than for other non-integrating reprogramming approaches like Adenovirus with an efficiency of 0.0002%, and protein overexpression and episomal vectors with <0.02% efficiency [2][57][68]. Additionally,

this reprogramming approach has been successful on multiple cell types unlike mRNA which only has published results using fibroblast. Due to these advantages, reprogramming with the Sendai virus is one of the most applicable methods for translational purposes and will be the focus of this project.

2.10 Role of Metabolism in Reprogramming

As a general definition, metabolism refers to the biochemical processes that produce or consume energy within living organisms [71]. Metabolism changes within different cells; for example somatic cells use mitochondrial oxidation phosphorylation (OXPHOS) while pluripotent cells use glycolysis [72]. During OXPHOS, somatic cells that are in the presence of oxygen, will metabolize glucose to carbon dioxide. This occurs through the oxidation of pyruvate within the tricarboxylic acid cycle (TCA). When there is a lack oxygen, lactate will be produced instead through anaerobic glycolysis [73]. In pluripotent cells, such as those in proliferative tissue and tumors, there is no requirement for oxygen to produce large amounts of lactate which is referred to as aerobic glycolysis or Warburg effect. This was first observed in cancer cells which have also displayed metabolic plasticity, the ability to switch from one type of metabolism to another. Although pluripotent and cancer cells primarily use glycolysis, the metabolic plasticity allows cells to switch to OXPHOS and for the mitochondria to remain functional [74].

The change from glycolysis to OXPHOS is also characteristic of embryonic and adult stem cells during differentiation [75]. As the cells differentiate, a remodelling of the mitochondria occurs; the mitochondria is restructured from a globular shape to more elongated [76]. In addition, higher amounts of energy are needed to sustain specialized functions of the cell so the need for OXPHOS is increased while the reliance on glycolysis is reduced. Consequently, this results in downregulation of glycolytic enzymes. The opposite phenomenon is observed as somatic cells are reprogrammed to iPSCs as illustrated in Figure 5 [77].

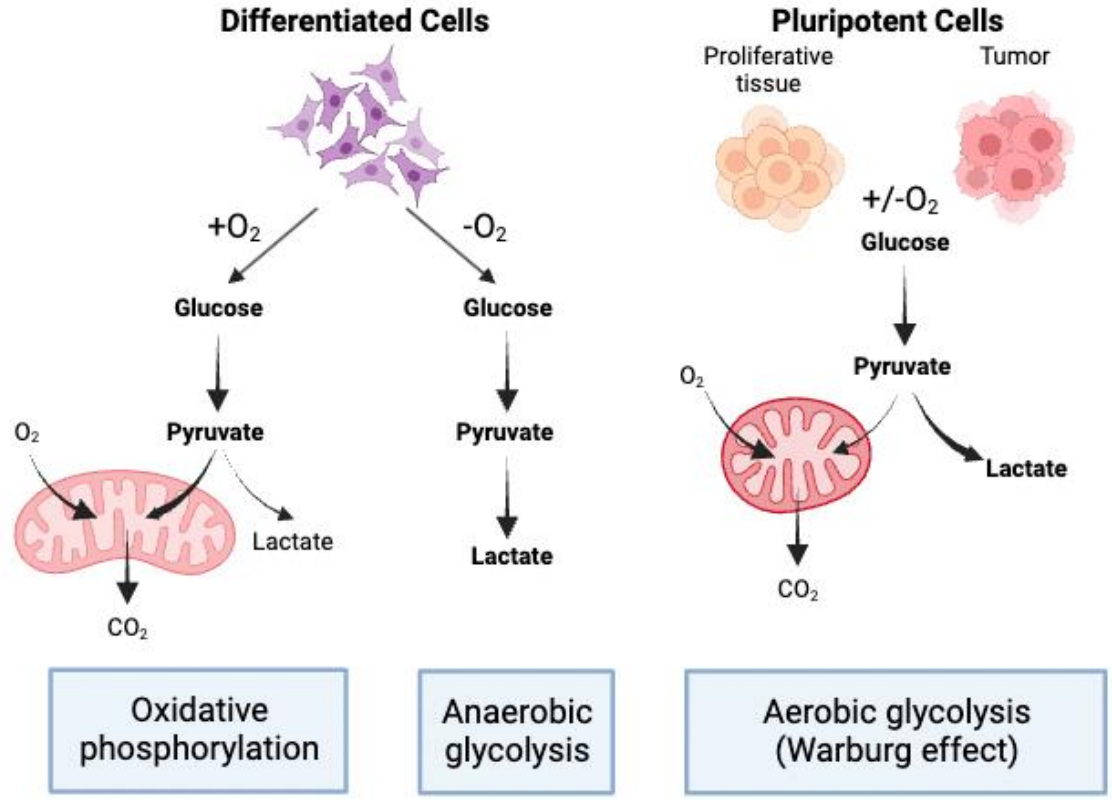

Figure 5: Differences in differentiated cell versus pluripotent cell metabolism. In the presence of oxygen, differentiated cells will use oxidative phosphorylation while pluripotent cells rely on glycolysis. As somatic cells are reprogrammed, there is a shift from oxidative phosphorylation to glycolysis. Figure was created with BioRender.com.

For somatic cells to become pluripotent, a shift in metabolism from OXPHOS to glycolysis must take place. This metabolic shift may contribute to the reprogramming process as somatic cells that display greater glycolic capacity and lower oxidative capacity result in a higher reprogramming efficiency [75]. There is potential that this is also connected to production of reactive oxygen species (ROS) which occurs during OXPHOS.

Studies have been done to better understand the changes in metabolism during reprogramming. One such study examined ROS production during the reprogramming of mouse iPSCs. ROS is a by-product of OXPHOS and an important signalling molecule in multiple pathways, but its build up can be toxic, causing oxidative damage and inducing

apoptosis [78]. When manipulating ROS levels during reprogramming, it was found that lower levels of ROS during early reprogramming resulted in fewer alkaline phosphatase positive colonies but elevated levels also impaired reprogramming [79]. ROS levels are most critical during the first 2-3 days of reprogramming as the somatic cells are more oxidative after transduction and require a high level of ROS signalling for successful reprogramming [80]. In later stages of reprogramming, ROS signalling was no longer needed and potentially had a negative impact. Although pluripotent and cancer cells primarily use glycolysis, the metabolic plasticity allows cells to switch to OXPHOS and for the mitochondria to remain functional [74].

2.11 Metabolism of Cancer Cells

Cancer cells and pluripotent cells share some similarities in their metabolism; both cell types have demonstrated metabolic plasticity, the potential to alter metabolic pathways. In pluripotent cells this occurs during reprogramming when metabolism shifts from OXPHOS to glycolysis [75]. Through studying metabolic behaviour of cancer cells, more insight can potentially be gained into pluripotent cell metabolism.

Originally, cancer cells were thought to demonstrate the Warburg Effect and aerobic glycolysis, which is the utilization of glucose in the presence of oxygen and production of lactate [81]. This proposed mechanism explained the increase of glucose uptake by cancer cells compared to that of surrounding tissue but was limited in the understanding of how biosynthesis and mitochondrial functions were performed [82]. The connection between glycolysis and mitochondrial oxidation can now be explained with the reverse Warburg effect which suggests a relationship between the two pathways [83]. In the dual model, it is proposed that cancer cells induce oxidative stress in neighbouring tissue through high ROS production (secretion of hydrogen peroxide) which enables the cancer-associated fibroblasts to undergo aerobic glycolysis [84]. The result is a high level of pyruvate and ketones which are energy

rich intermediate metabolites that can be used by the cancer cells for OXPHOS and production of ATP. This therefore provides cancer cells with energy to support proliferation. Further proof of metabolic plasticity of cancer cells was shown through a restriction of the cells to a single fuel source. Cancer cells which were restricted to pyruvate, showed a metabolic switch from glycolysis to OXPHOS [85].

2.12 Addition of Lactate to Reprogramming Process

Recently, the restriction of fuel source to shift metabolism was evaluated on somatic cells similar to the previously described cancer cell research. Fibroblast cells were preconditioned in static with several fuel sources including glucose, pyruvate, and lactate. qRT-PCR analysis, found in Figure 6, showed a significant increase in expression of glycolytic enzymes HK2, PGK1 and PDK1 for the lactate treatment group compared to control [5]. This suggests that lactate treatment results in upregulation of these metabolic enzymes and primes the cells for glycolysis.

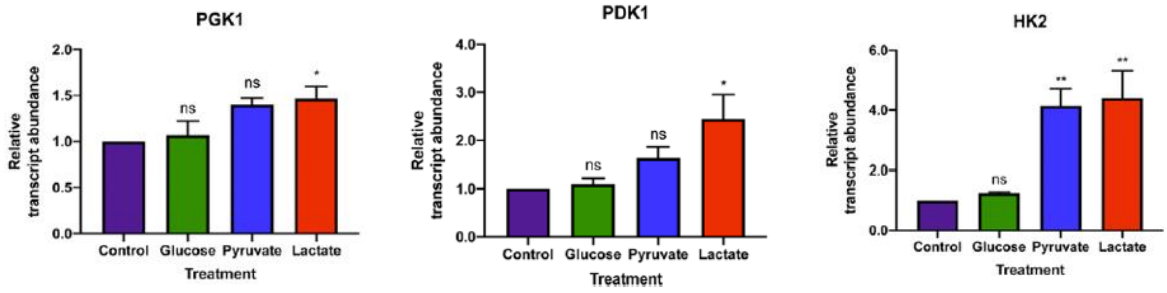

Figure 6: Results published by *Kozlov et al*. comparing expression of glycolytic enzymes using qRT-PCR. Glucose, pyruvate and lactate treatments are compared to the control [5]. A significant increase in the enzymes of PGK1, PDK1and HK2 can be seen in the lactate condition compared to control.

Further testing was done using a Seahorse Analyzer24 to measure oxygen consumption rate (OCR) and extracellular acidification rate (ECAR) using the glycolysis stress test and mitochondrial stress test as can be seen in Figure 7. The two described measurements are

representative of metabolism, OCR is an indicator of mitochondrial respiration while ECAR is largely the result of glycolysis. The measurements obtained showed that lactate-treated cells had a significantly greater glycolytic reserve when compared to pyruvate-treated cells, this refers to the capability to respond to glycolytic energy demand. Lactate treated cells also exhibited a significantly greater basal respiration which is the cell's oxygen consumption to meet ATP demand under normal conditions. In addition to this, when compared to pyruvate-treated cells, the lactate treated cells had a significantly reduced spare respiratory capacity (how closely the cell is to respiring to its theoretical maximum). These results suggest that the lactate treatment primes the cells for the glycolytic pathway and enables metabolic plasticity in the presence of glucose much like the cancer cells previously demonstrated.

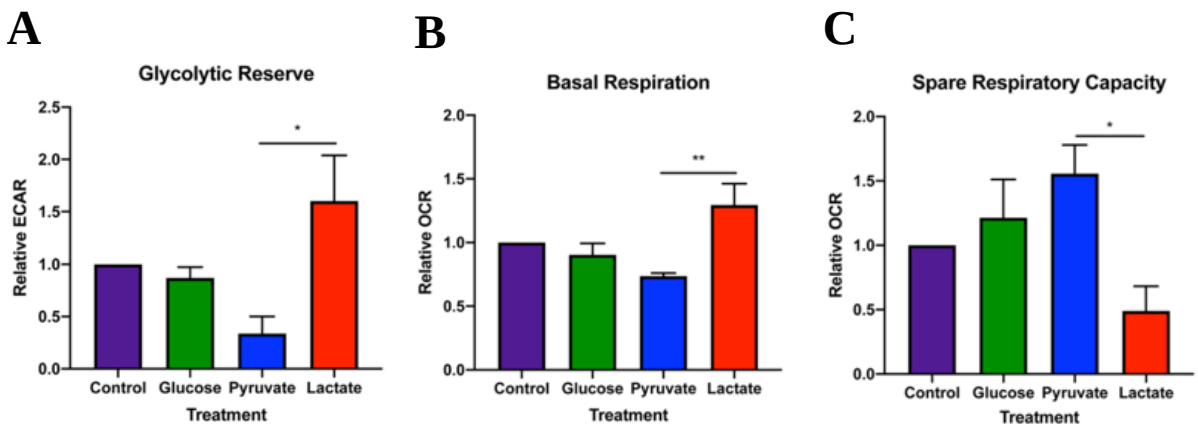

Figure 7: Results published by *Kozlov et al*. showing Seahorse Analyzer24 measurements of OCR and ECAR during glycolysis stress test and mitochondrial stress test [5]. **(a)** Lactate treated cells were better at responding to glycolytic energy demand as seen by the increased relative ECAR **(b)** Lactate treated cells had an increased OCR for meeting ATP demand **(c)** Reduced spare respiratory capacity of lactate treated cells indicates ability to use mitochondrial respiration and glycolysis depending on what is available.

The other effect of lactate pre-treatment is the significantly higher levels of total cellular ROS compared to pyruvate treated cells. As was previously discussed, ROS levels play a critical role in the reprogramming of cells and require a delicate balance. ROS levels are elevated in the beginning stages of reprogramming and have a direct impact on reprogramming efficiency with levels that are too low or too high impairing reprogramming. However, it is hypothesized that the increase in ROS has advantages when it comes to stabilizing HIF-1α which thereby promotes an increase in glycolytic metabolism and therefore the upregulation of metabolic enzymes. In all, this indicates that lactate pre-treatment may promote a bivalent metabolic state and thereby increase reprogramming efficiency.

Chapter 3 Methodology

3.1 Cell Source

3.1.1 CRL 2522

This cell line is established from fibroblast cells taken from foreskin of a neonatal male (BJ ATCC CRL-2522). This line was used for reprogramming to hiPSCs.

3.1.2 PGPC3

The PGPC3 line is a male human induced pluripotent stem cell line reprogrammed from volunteers of the Personal Genome Project Canada [86].

3.2 Culture Media

Cells require a source of energy and nutrients to support their metabolic and development needs which is provided by a culture media. Typical culture media components include serum, glucose, amino acids, vitamins and growth factors [87]. Different cell types have varying requirements of culture media; this project mainly used fibroblast media for growth of fibroblast cells and Essential 8 or mTeSR1 for growth of hiPSCs.

3.2.1 Fibroblast Media

The fibroblast media is composed of:

- DMEM (Gibco, 10569-010)
- FBS (ATCC, 30-2020)

The DMEM is aseptically supplemented with 10% FBS for a complete media.

3.2.2 hiPSC Media

Several types of hiPSC media are available for commercial use. The following two were used within this project:

- **Essential 8 Media** (Gibco, A1517001):

    1. Thaw frozen Essential 8™ Supplement at 2–8°C overnight before using it to prepare complete medium. Do not thaw the frozen supplement at 37°C.
    2. Mix the thawed supplement by gently inverting the vial a couple of times, remove 10mL from the bottle of Essential 8™ Basal Medium, and then aseptically transfer the entire contents of the Essential 8™ Supplement to the bottle of Essential 8™ Basal Medium. Swirl the bottle to mix and to obtain 500 mL of homogenous complete medium.
    3. Complete Essential 8™ Medium can be stored at 2–8°C for up to 2 weeks.
    4. Media should be warmed at room temperature until it is no longer cool to the touch. Do not warm the medium at 37°C.

- **mTeSR** (STEMCell Technologies, Cat# 85850):

    1. Thaw mTeSR1 5X supplement and warm to room temperature. Mix thoroughly. Do not thaw the frozen supplement at 37°C. Supplement must be free of cloudiness before adding to basal medium.
    2. To prepare media, combine supplement and basal medium at a ratio of 1:4. Mix thoroughly and store at 2–8°C for up to 2 weeks.

Note: When working with single - cell suspension of hiPSCs, ROCKi (STEMCell Technologies, Cat # 72308) should be added to all reagents. Add 1 µL ROCKi per 1 mL of complete medium/enzyme, for a final concentration of 10 µM. Reagents should be filtered as the ROCKi aliquots are not sterile.

3.3 Static Culture Procedure for CRL 2522

The following protocols were adapted from the manufacturer suggested protocol for BJ fibroblast cells (ATCC CRL-2522).

3.3.1 Thawing

1. Thaw the cell vial in a 37°C water bath. Ensure that the O-ring and cap are kept out of the water to reduce the possibility of contamination. Thawing should be rapid (approximately 2 minutes).
2. Under sterile conditions, transfer the contents of the vial to a centrifuge tube with 9 mL of media.
3. Centrifuge for 10 minutes at 125g. Discard the supernatant and resuspend the cells in 1 or 2 mL of complete growth medium.
4. Perform cell counts to determine number of cells. Seed at 5000 cells /cm^2. Transfer the cell suspension into the culture vessel containing the complete growth medium and mix thoroughly by gentle rocking.
5. Incubate the culture at 37°C.

3.3.2 Passaging

The following volumes are given for a 75 cm^2 flask. Increase or decrease the amount of dissociation medium needed proportionally for culture vessels of other sizes. Manufacturer recommends Corning T-75 flasks (Corning, 430641) for subculturing.

1. Remove and discard culture medium.
2. Rinse the cell layer with 3 mL of PBS to remove all traces of serum that contains trypsin inhibitor.
3. Add 2.0 to 3.0 mL of Trypsin-EDTA 0.25% (ThermoFisher, 25200056) solution to flask and place in 37°C incubator. Observe cells under a microscope until cell layer is dispersed (usually within 5 to 15 minutes).

4. Pipette cell solution three times to break up aggregates and transfer to 15 mL conical tube.
5. Rinse the T-flask with media (1:1 volume ratio to Trypsin used) and transfer to conical tube.
6. Centrifuge at 500g for 5 min.
7. Remove supernatant and resuspend in 1 mL of media.
8. Perform cell counts to determine number of cells. Seed at 5000 cells /cm^2. Transfer the cell suspension into the culture vessel containing the complete growth medium and mix thoroughly by gentle rocking.
9. Incubate cultures at 37°C.
10. Replace media every 2 to 3 days.

3.3.3 Cryopreservation

1. Perform protocol for passaging, stopping after counts on step 6.
2. The cells can be frozen at 1E6 – 2E6 cells/mL. Resuspend the appropriate aliquot of the cell suspension in 1mL of cryogenic media within a cryogenic vial.

Note: Cryogenic media is complete growth medium supplemented with 5% (v/v) DMSO (ATCC, 4-X)

3. Store cells in liquid nitrogen storage.

3.4 Static Culture Procedure for PGPC3

The following protocols were adapted from the PPRF lab, developed by Tiffany Dang.

Note: ROCKi should be added to any culture media in which there are single cells. The ratio is 1 µL ROCKi per 1 mL of complete medium/enzyme, for a final concentration of 10 µM.

3.4.1 Matrigel Preparation

A Matrigel or vitronectin coating is needed to support hiPSC cell attachment and expansion in static culture. Corning® Matrigel® hESC-qualified Matrix (Corning, 354277) was used for coating of surfaces for hiPSC growth within this project.

Note: For Matrigel coating, the ratio is 50 μL aliquot of Matrigel to 5 mL DMEM / F12 (Thermo Scientific, 11320033).

1. Aliquot the required amount of DMEM/F12 into 50 mL conical tube.
2. Add 100 μL of cold DMEM to the Matrigel aliquot and pipette up and down to mix.
3. Add the mixture of DMEM/F12 + Matrigel into the 50 mL conical tube with DMEM/F12.
4. Add the appropriate amount of mixture to coat the surface, see Table 2 below for volume amounts . A coating concentration of 0.5 μg/cm^2 is needed.

Table 2: Surface area of different culture vessels and the required volume of Matrigel solution.

Culture vessel	Surface area	Volume of Matrigel solution
6-well plate	10 cm^2 per well	1.0 mL/well
12-well plate	4 cm^2 per well	0.4 mL/well
24-well plate	2 cm^2 per well	0.2 mL/well
T-25 flask	25 cm^2	2.5 mL
T-75 flask	75 cm^2	7.5 mL

5. Incubate for a minimum of 2 hours, ideal is 24 hours. However, it can be left in the incubator for up to 7 days as long as there is a Matrigel and DMEM/F12 mixture. Do not allow the Matrigel to sit dry. If not ready to add media, do not remove DMEM/F12 after rinsing.
6. When ready to add cell suspension, aspirate unbound material.

7. Rinse with equal amount of DMEM/F12 previously added.
8. Add complete media and cell suspension.

3.4.2 Thawing

1. Thaw the cell vial in a 37°C water bath. Ensure that the O-ring and cap are kept out of the water to reduce the possibility of contamination. Thawing should be rapid (approximately 2 minutes).
2. Under sterile conditions, transfer the contents of the vial to a conical tube with 2 mL of pre-warmed media. Ensure the pipette tip is submerged and slowly transfer the cells to reduce stress.

Note: The speed of the pipette controller can be reduced to minimize pipette velocity.

3. Rinse the cryovial with 1 mL of ROCKi containing media and transfer to the conical tube. Do not vigorously pipette or mix cell solution.
4. Centrifuge at 300g for 5 min
5. Remove supernatant without disturbing the cell pellet. Resuspend the cell pellet with 1 mL of prepared media using a P1000 micropipette. Pipette 5 times or until the cell pellet appears dissolved. Be gentle during this step as the cells are very sensitive.
6. Perform cell counts to determine the total number of cells. Typical cell seeding density is 5000 cells /cm^2. Use a serological pipette to inoculate the resuspended cells to avoid contamintation. Ensure the pipette tip is submerged in the media while transferring into the flask.
7. Incubate in standard culture conditions of 37 °C and 5% CO_2.

3.4.3 Passaging

The recommended volumes for T-25 and T-75 flasks can be found in Table 3 below.

Table 3: Recommended reagent volume for T-25 and T-75 flasks

T-flask Size	Media Volume	PBS & Accutase Volume
25 cm^2	5-9 mL	3 mL
75 cm^2	25 mL	7 mL

1. Add ROCKi (STEMCELL Technologies, 72304) to media and Accutase (STEM CELL Technologies, 07920) in a ratio of 1 mL solution to 1 uL ROCKi. Filter and warm in the incubator or water bath.
2. Remove and discard media. Wash with specified volume of 1xPBS (Gibco, 14200166).
3. Pipette the Accutase a few times and add needed volume. Incubate at 37 °C for 5-6 min.
4. Tap the edges of the flask to assist with detachment and check under a microscope to ensure cells have detached.
5. Pipette Accutase cell solution three times to break up aggregates and transfer to 15 mL conical tube.
6. Rinse the T-flask with media (1:1 volume ratio to Accutase used) and transfer to conical tube.
7. Centrifuge at 300g for 5 min.
8. Remove supernatant and resuspend in 1 mL of media.
9. Perform cell counts to determine number of cells. Seed at 5000 cells /cm^2. Transfer the cell suspension into the culture vessel containing the complete growth medium and mix thoroughly by gentle rocking.
10. Incubate in standard culture conditions of 37 °C and 5% CO_2.
11. Replace media every day.

3.5 Glassware Preparation for Microcarrier Culture

Glassware such as bioreactors and Erlenmeyer flasks should be siliconized with Sigmacote (Sigma, SL2) prior to use to prevent microcarriers from sticking to the sides.

1. Ensure the bioreactor is completely dry. Any water residue will contaminate the Sigmacote. Kimwipes can be used to remove remaining water.
2. Using a pipette, dispense 5mL of Sigmacote for a 10mL spinner bioreactor.
3. Ensure bottom of the vessel (including glass indent on bottom) is covered in Sigmacote.
4. Aspirate Sigmacote and dispense down sides of the bioreactor to ensure all sides are covered.
5. Aspirate Sigmacote and dispense over the impeller, impeller shaft and any probes.
6. Aspirate any residual Sigmacote and return to storage bottle. The Sigmacote can be reused for future bioreactors provided it is has not come into contact with water.
7. Leave bioreactors to dry for at least 4 hours.
8. Fill bioreactors with 1XPBS and leave for at least 4 hours.
9. Fill the bioreactors up to the arms or the highest point where Sigmacote came into contact with the bioreactor.
10. Rinse bioreactors with distilled water a few times, fill bioreactors with water and leave for at least 4 hours, before removing the water

3.6 Microcarrier Preparation

1. Calculate the necessary weight of needed microcarriers. See Figure 8 for sample calculation.

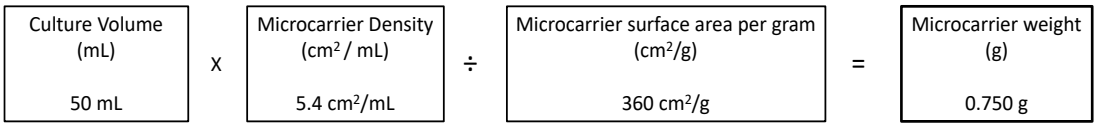

Figure 8: Sample calculation for the weight of Collagen coated microcarrier needed for 50mL of volume at a microcarrier density of 5.4 cm^2/mL.

2. Add microcarriers to a siliconized Erlenmeyer flask. Then hydrate with 50mL 1X PBS and 1% Pen-Strep (Gibco, 15140122) per gram of microcarrier.

Example: If 2 g microcarrier is required for a 1 L bioreactor, add 100mL 1X PBS with 1% Pen-Strep.

3. Leave for at least 4 hours or overnight at room temperature to soak.
4. Remove PBS from flask, careful to not aspirate the microcarriers, then add another 50mL/g microcarrier into the flask.

Note: The best method to remove the PBS without disturbing the microcarriers is to tilt the Erlenmeyer flask so the microcarriers settle into a corner. Remove PBS from the top.

5. Let microcarriers settle and remove PBS. Repeat for a total of 2 times.
6. Add 50mL 1X PBS / per gram of microcarrier into flask and cover top with aluminum foil for autoclaving.

3.6.1 Autoclaving Procedure

Note: Only glass vessels should be autoclaved.

1. Cover all plastic parts and any exposed probe parts on bioreactors with aluminium foil. Slightly loosen caps to allow for venting before autoclaving.
2. Autoclave for at least 30 minutes on liquid cycle.

3.7 Microcarrier Screening

3.7.1 Experiment Set-up

A microcarrier screening was performed to determine the best microcarrier type for growth of fibroblast cells and hiPSCs. The list of microcarriers and specifications can be found in Table 4.

Table 4: Microcarrier Specifications

Microcarrier	Material	Animal Product	Particle Size µm	Density (g/cm^3)	~Area per g dry weight	Surface Charge	Cat No.
Cytodex 1	Dextran	No	190	1.03	4400cm^2	Yes	GE Healthcare, 17–0448-01
Cytodex 3	Dextran	Yes	>175	1.04	2700cm^2	No	GE Healthcare, 17–0485-01
Plastic Plus	Cross-linked Polystyrene	No	125 - 212	1.022 - 1.030	360 cm^2	Yes	Sartorius, 102-521
Hillex	Modified Polystyrene	No	160 – 200	1.080 - 1.150	515 cm^2	Yes	Sartorius, H-170-050
Collagen Coated	Cross-linked polystyrene	Yes	125-212	1.026 ± 0.004	360 cm^2	No	Corning, 3786
Fact III	Cross-linked polystyrene	Yes	125–212	1.022–1.030	360 cm^2	Yes	Sartorius, F-221-020
Star-Plus	Cross-linked Polystyrene	No	125 - 212	1.020 - 1.035	360 cm^2	Yes	Sartorius, SP-221-080

The growth kinetics of cells on microcarriers were assessed using Crystal Violet staining and a hemacytometer. Brightfield images using Crystal Violet in MeOH and Confocal fluorescent images after staining with SYTO 24 Green Nucleic Acid stain (Invitrogen, S7559) were also taken to observe cell attachment.

The best two performing microcarriers were then tested within a 10mL horizontal blade bioreactor to determine performance and establish a growth curve for both fibroblast and hiPSCs. Following this, the reprogramming process was completed in a shaken 6-well plate with modifications to the CytoTune™-iPS 2.0 (Invitrogen, A16518) protocol.

3.8 Reprogramming Timeline Overview

The reprogramming protocol used for static reprogramming was adapted from ThermoFisher for the CytoTune™-iPS 2.0 kit (Invitrogen, A16517) and is described below. The timeline for the process, Figure 9, is as follows:

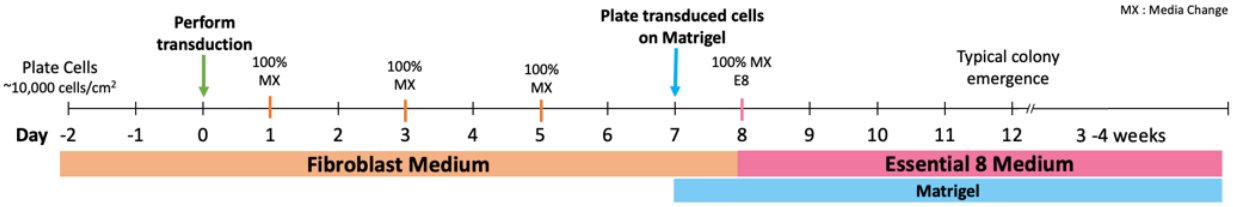

Figure 9: Timeline for static reprogramming process. MX denotes media change days.

Day –2: Human fibroblasts were plated into a 6-well plate with fibroblast medium to achieve confluency of 30–60% on the day of transduction (Day 0). Two extra wells were plated to be used for counts.

Day 0: Counts were performed on two of the wells and the cell number averaged. The cells were transduced using the CytoTune™ 2.0 Sendai reprogramming vectors at the appropriate MOI and virus volume based on the cell count. Cells were then incubated overnight.

Day 1: Medium was replaced with fresh complete fibroblast medium to remove the CytoTune™ 2.0 Sendai reprogramming vectors.

Day 2–6: Spent medium was replaced every other day.

Day 7: The transduced cells were passaged and plated on Matrigel coated culture dishes in fibroblast medium.

Day 8: Medium was changed to complete Essential 8 Medium.

Day 9–28: Spent medium was replaced every day and the culture vessels were monitored for the emergence of iPSC colonies.

3.9 Static Reprogramming Protocol

When starting with frozen cells, ensure they have undergone one passage in static prior to reprogramming. This is referred to as a seed train.

3.9.1 Static Seed Train

1. Thaw cells as described in section: Static Culture Procedure for CRL 2522.
2. Perform cell counts to determine number of cells. Seed at 5000 cells /cm^2 in a T-75.

Note: 1 vial of 1E6 cells should seed about two - three T-75 flasks.

3. Transfer the cell suspension into a T-75 culture vessel containing 15mL of complete growth medium and mix thoroughly by gentle rocking.
4. Incubate the culture at 37°C for 2-3 days.
5. Passage cells and begin Day -2 of reprogramming protocol.

3.9.2 Static Reprogramming

Day –2:

1. Plate human fibroblasts into a 6-well plate with fibroblast medium (DMEM (Gibco; #10569-010) and 10% FBS (ATCC, 30-2020). Cell seeding density should be between 5000 - 10,000 cells/cm^2 to achieve confluency of 30–60% ($2x10^5$–3x105 cells per well) on the day of transduction (Day 0).

2. Plate two extra wells to be used for counts. The count wells will be averaged and used to calculate the correct volume of each needed virus.

Day 0:

Harvest 2 of the wells (count wells) to obtain an average cell number:

1. Remove media from wells.
2. Wash each well with 0.5 mL of 1X PBS (Gibco, Cat# 14040133) to remove all traces of serum that contains trypsin inhibitor.
3. Add 0.5 mL Trypsin-EDTA 0.25% (ThermoFisher, Cat# 25200056) and incubate at 37°C for 2-5 minutes.
4. Check cells under microscope to ensure detachment. Tap the vessel surface to promote detachment if needed. Transfer the cell suspension to separate 15 mL conical tubes.
5. Rinse each well twice with 0.5 mL of media and transfer to the corresponding conical tube. Pipette cell solution three times to break up aggregates.
6. Centrifuge at 500g for 5 min.
7. Remove supernatant and resuspend in 1 mL of media.
8. Take two samples of 100µL from each tube and dilute at 2X with 100µL of media. Perform cell counts to determine the total number of cells.
9. Calculate the volume needed of each CytoTune reprogramming vector based on the average cell number of the counting wells.

   The volume of virus can be found as follows:

$$Volume\ of\ virus\ (\mu L) = \frac{MOI\ (CIU/cell)\ x\ number\ of\ cells}{titer\ of\ virus\ (CIU/mL) x\ 10^{-3} (mL/\mu L)}$$

Note: The titer information differs by Lot number. An example is found in Table 5.

Table 5: Titer information for Lot No. L2190071

Component	Titer* (CIU/mL)	MOI
hKOS	1.10E8	5
hc-Myc	1.20E8	5
hKlf4	1.10E8	3

10. Thaw one set of CytoTune reprogramming vectors in a 37°C water bath for 5-10 seconds and then allow to thaw at room temperature. Briefly centrifuge.
11. Add the calculated volumes of each vector to 1 mL (per well) of fibroblast media pre-warmed to 37°C. Pipette the mixture to ensure the solution is thoroughly mixed.

Note: To ensure all wells are getting the same amount of vector, prepare a master mix.

12. Perform the following step within 5 minutes: Aspirate the fibroblast media from the cells and add the reprogramming virus mixture.
13. Incubate the cells at standard culture conditions of 37 °C and 5% CO_2 overnight.

Day 1: 24 hours after transduction, replace the medium with fresh complete fibroblast medium to remove the CytoTune™ 2.0 Sendai reprogramming vectors.

Day 2–6: Replace the spent media on Day 3 and 5.

Day 6: Prepare a sufficient number of Matrigel coated 6 well plates. See protocol for Matrigel preparation.

Day 7: Passage and plate the transduced cells on Matrigel-coated culture dishes in fibroblast medium.

1. Remove media from wells and wash each well with 0.5 mL of 1X PBS.
2. Add 0.5 mL Trypsin-EDTA 0.25% and incubate at 37°C for 2-5 minutes. Check cells under microscope to ensure detachment. Use a cell scraper (VWR, 10062-908) if cells are not detaching.
3. Collect cells into separate 15 mL conical tubes. Rinse each well twice with 1 mL of media and transfer to conical tube.
4. Centrifuge at 200g for 4 min.
5. Remove supernatant and resuspend in 1 mL of media.
6. Take two samples of 100μL from each tube and supplement with 100μL of media. Perform cell counts to determine number of cells.
7. Plate cells at the appropriate cell density in 2mL of media. Incubate overnight in a 37°C incubator with a humidified atmosphere of 5% CO_2.

Day 8: Change the medium to complete Essential 8 Medium (Gibco, A1517001) at 2mL per well.

Day 9–28: Replace spent medium every day and monitor the culture vessels for the emergence of iPSC colonies.

3.10 Dynamic Reprogramming

The dynamic reprogramming process included use of a shaker (Eppendorf, E5 M1353-0004) to simulate a dynamic environment. An agitation rate of 100 RPM was used to produce fluid movement without lifting cells. The conditions regarding transduction, media changes and cell passaging remained the same as in the static protocol.

3.10.1 Reprogramming on Microcarriers

Figure 10 shows a timeline of the reprogramming process on microcarriers.

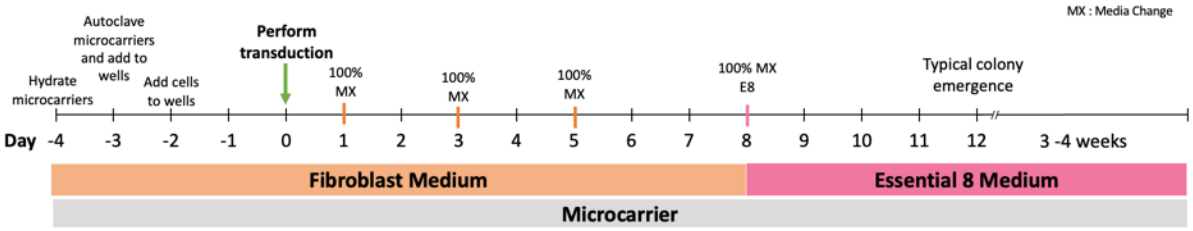

Figure 10: Timeline for reprogramming on microcarriers in a dynamic system. MX denotes a 100% media change.

Several steps need to be added to the reprogramming process when microcarriers are involved:

Day -4: Microcarriers were prepared by hydrating in 1XPBS and 1% Pen Strep (Gibco, 15140122) for 24 hours.

Day -3: The mixture was autoclaved and once cooled, the microcarriers were added to the wells and left for 24 hours to acclimate in the cell culture medium.

Day -2: Cells were added to the microcarrier wells and monitored for attachment.

Following this, the reprogramming protocol proceeded the same as for static culture.

3.10.2 Media change in Suspension

Media changes in suspension culture pose an obstacle as microcarriers/cells are present in the spent media. To overcome this, all media was removed from the well and centrifuged. The supernatant was discarded, and cell pellet resuspended in fresh media. The suspension was then be added back to the wells.

3.11 Addition of Lactate to Reprogramming Process

Lactate was added at a 20mM concentration on day 4 of the reprogramming process. The selected concentration is the common concentration of lactate found in tumour microenvironments which demonstrate the ability of metabolic flux between glycolysis and

OXPHOS. Table 6 shows a comparison of different media types used when lactate treatment is added within the reprogramming process and Figure 11demonstrates the timeline.

Table 6: Comparison of media types and their concentrations of glucose, lactate and pyruvate for use in reprogramming with lactate.

Day	Medium	Glucose	Lactate	Pyruvate
-2 to 4	Fibroblast	25 mM	-	1.25 mM
4	Lactate	-	20 mM	-
5-7	Glucose	20 mM	-	
7-8	Fibroblast	25 mM	-	1.25 mM
8+	E8	17.5 mM	-	0.6 mM

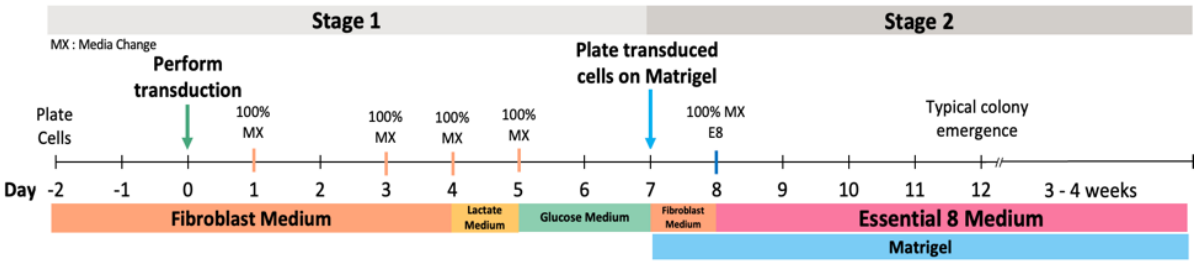

Figure 11: Reprogramming timeline with the addition of lactate on Day 4.

3.11.1 Lactate Medium

To prepare 20mM lactate medium: Combine 8.6 mL DMEM base medium, 200uL 1M lactate solution, and 1 mL dialyzed FBS (Gibco, A33820-01). Filter through a 0.2 um syringe filter.

- *Lactate 1M solution stock*

Dissolve 0.56 g Sodium-L-lactate (Sigma, 71718-10G) in 5 mL of cell culture grade water (Cytiva, SH30529) and sterilize through a 0.2 um syringe filter using a 5 mL syringe. Store at 4°C.

3.11.2 Glucose Medium

To prepare 20mM glucose medium: Combine 8.6 mL DMEM base medium, 200uL 1M glucose solution, and 1 mL dialyzed FBS. Filter through a 0.2 um syringe filter.

- *Glucose 1M solution stock*

Dissolve 0.9 g D-glucose (Sigma, G7021-1KG) in 5 mL of cell culture grade water (Cytiva, SH30529) and sterilize through a 0.2 um syringe filter using a 5 mL syringe.

3.11.3 Lactate Reprogramming Protocol

The static reprogramming protocol is modified starting on Day 4.

Day 4: Replacement with lactate medium.

1. Remove media from cell wells that will be treated with lactate.
2. Rinse twice with 1 mL PBS.
3. Add 2mL lactate medium per well. Record the time.
4. Wait the needed amount of time (10h,13h,16h depending on the experiment)
5. Rinse twice with 1mL PBS.
6. Add 2mL glucose medium per well.

Cells are left to recover in glucose medium until passaging on Day 7.

3.12 Counting Techniques

There are various methods available for counting cells and determining cell density of a sample. The following project used Crystal violet assay and the automated Nucleocounter (Chemometec, NucleoCounter NC-200). The Crystal violet assay was mainly used during the microcarrier screening of Aim 1 as its easier to adjust dilution. The Nucleocounter was used for all other applications unless otherwise stated.

3.12.1 Crystal Violet Assay

Staining with a 0.1% crystal violet solution allows for the quantification of attached adherent cells to a culture surface. Cells adherent to a surface indicate live cells, while those not attached, are not viable [88]. During the assay, dead cells are washed away and the crystal violet dye binds to proteins and DNA therefore staining the nuclei of attached cells. The stained cells can then be counted with a hemocytometer.

Protocol

1. Obtain sample and wait for microcarriers to settle. Remove supernatant without disturbing the settled pellet.
2. Add 1X PBS.
   - Amount of PBS should be equal to ½ volume of sample.
   - Example: If sample volume is 2ml, use 1 mL of PBS
3. Wait again for microcarriers to settle, remove 1X PBS.
4. Repeat again: Add 1X PBS and allow microcarriers to settle.
5. After microcarriers have settled, remove PBS and add 1mL of 0.1% Crystal violet in 0.1M citric acid to each tube.
   - Volume of Crystal violet added should be ½ volume of the sample.
6. Incubate samples preferably 24 hours before counting.

To count each tube:

1. Agitate sample 20 times with 1mL pipette to ensure all nuclei have been lysed from microcarriers.
2. Add PBS to dilute sample for counting if necessary.
3. Samples are counted using a hemocytometer and the cell density (Xv) in cells/mL, is calculated using equation 1. N_v is the number of counted cells.

$$X_v = \frac{N_v}{\#\ of\ chambers} * \frac{chamber}{0.1\ mm^3} * \frac{10^3 mm^3}{1\ mL} * \frac{volume\ of\ count\ (Crystal\ Violet+PBS)}{volume\ of\ sample\ removed} \quad (1)$$

4. The total number of cells is calculated using equation 2 below, where V_B is the volume of the bioreactor.

$$N = X_V * V_B \quad (2)$$

The attached cell density, X_A in cells/cm^2, can then be found with equation 3:

$$X_A = N * \left(MC\ surface\ area\ \frac{g}{cm^2}\right) * \left(\frac{1}{g\ microcarrier}\right) \quad (3)$$

3.12.2 NucleoCounter

The NucleoCounter (Chemometec, NucleoCounter NC-200) is an automated cell counting device which uses acridine orange (AO) and 4',6-diamidino-2-phenylindole (DAPI) to label total number of cells and determine cell viability, respectively [89]. The device uses single-use cassettes which are preloaded with the dyes and uptake a pre-calibrated sample volume. When inserted into the device, the software analyses the fluorescence data from the dyes to output the total number of cells and cell viability. Results of the NucleoCounter have been shown to be more reproducible when compared to conventional counting methods using Trypan blue [90].

Protocol for single cell suspension

1. Aliquot 2 x 50 µL samples for counting. Dilute with 50 µL of media.
2. Vortex sample before running on Nucleocounter NC-200.

Protocol for microcarrier culture

1. Take a 2 mL sample.
2. Concentrate the sample by removing 1.8mL of supernatant.

3. Add 200 µL of Reagent A.
4. Flick and wait 2 min.
5. Add 200 µL of Reagent B.
6. On the NucleoCounter Select the protocol: Count Aggregate cells A100 and B100 Assay and enter the following information:

Sample: 2000 µL, Dilution: -1800 µL, A100: 200 µL, B100: 200 µL

3.13 Validation of Pluripotency

One of the main outcomes of this project is the generation of hiPSCs through reprogramming. Several methods can be used to validate the pluripotency of generated cells which include alkaline phosphatase (AP) live staining, pluripotent marker immunocytochemistry and flow. Additional methods such as teratoma assay and PCR can be performed to validate pluripotency but will not be covered in this project.

3.13.1 Alkaline phosphatase live stain

Alkaline phosphatase live stain is most widely used as an easy and fast method to identify iPSC colonies in the early stages of reprogramming as AP is expressed at high levels and is a good initial indicator [91]. This approach is ideal for continued cell growth as the stain is eliminated from cells 60-90 minutes after removal from the media and stained colonies preserve their morphology and maintain cell health. AP live stain (Invitrogen, A1435) can be used as an initial indicator to identify iPSC colony formation and allow for pick passaging of those colonies as needed. Manufacturer protocol will be followed to perform staining. However, it should be noted that AP staining alone is not a definitive marker of pluripotency and further validation is needed.

3.13.2 Immunocytochemistry

Immunocytochemistry involves staining of proteins or markers and can be used to identify cells positive for pluripotency markers. This form of validation is not a live stain and requires the fixing of cells which is best performed after sufficient colony formation is observed. Common pluripotency markers are SSEA4, TRA-1-81, TRA-1-60, SOX2, Oct4 and NANOG [92]. It is important to note that OCT4 and SOX2 are pluripotent markers that are also two of the transcription factors which are introduced exogenously during the transduction process in reprogramming. Therefore, the use of OCT4 and Sox2 with immunocytochemistry should be avoided as positive expression would be misleading.

3.13.3 Flow Cytometry

A list of markers used for flow cytometry can be found in Table 7. The following markers were validated on the Cytek spectrum viewer to ensure their unique fluorophore signature. As can be seen from Figure 12, the similarity index is below 0.9 for each combination, indicating they are compatible for use within the panel. Detailed protocols for sample preparation can be found in Flow Cytometry Procedure.

Table 7: Flow cytometry markers with fluorophore and supplier information.

Marker	Fluorophore	Supplier (cat#)
SOX2	Alexa Fluor 700	Novus Biologicals, NB110-37235AF700
Nanog	DyLight™ 488	Thermo Scientific, MA1017D488
Tra-1-60	PE	Invitrogen, MA1023PE
Tra-1-81	APC	Invitrogen, 17888342
Oct4	Alexa Fluor 405	Novus Biologicals, NB100-2379AF405
SSEA4	PerCP-eFluor™ 710	Invitrogen, 46884342
CD44	SuperBright 702	Invitrogen, 67-0441-82

Super Bright 780	1						
PerCP-eFluor 710	0.25	1					
Alexa Fluor 405	0.05	0	1				
APC	0.03	0.29	0	1			
PE	0	0.03	0	0.04	1		
DyLight 488	0	0	0	0	0.07	1	
Alexa Fluor 700	0.09	0.47	0	0.49	0	0	1
	Super Bright 780	PerCP-eFluor 710	Alexa Fluor 405	APC	PE	Alexa Fluor 488	Alexa Fluor 700
Complexity™ Index: 2.35							

Figure 12: Similarity and complexity evaluation of the antibody conjugates adapted from Cytek spectrum viewer.

3.14 Flow Cytometry Procedure

The following protocol has been produced by Tiffany Dang, Juyeon Cha and Emilie Gysel.

1. Harvest cells and perform cell counting.
2. Adjust the suspension to a concentration of 1 x 10^6 cells/mL in 1 X PBS.

<u>If not staining right away:</u>

1. Fix cells in 0.25ml of 1% PFA (Invitrogen, 00-8222-49) for 20 minutes in fridge protected from light.
2. Remove PFA, wash cells with PBS and resuspended in PBS.
3. Store at 4 degrees until ready for staining (about 7 days). Then continue at step 2 of the staining protocol.

If staining right away:

1. Spin down the cell and PBS mixture at 2000 rpm for 5 mins.
2. Decant supernatant leaving behind a small amount of medium. Loosen pellet with gentle tapping.
3. Top up tubes with 1 mL of 1 X PBS and spin down at 2000 rpm for 5 mins.
4. Remove the supernatant by decanting, leaving behind a small amount of PBS. Loosen pellet with gentle tapping.
5. Resuspend in 100 µL of 1 % PFA for 20 mins in fridge protected from light.
6. Top up with 1 mL of 1 X PBS and spin down at 2000 rpm for 5 mins.
7. Remove the supernatant by decanting. Loosen pellet with gentle tapping.
8. Resuspend in 100 µL permeabilization buffer (1% Saponin/PBS) for 20 mins in fridge protected from light.
9. Top up the tubes with 1 mL of 1 X PBS and spin down at 2000 rpm for 5 mins.
10. Remove the supernatant by decanting, leaving behind a small amount of PBS. Loosen pellet with gentle tapping.
11. Resuspend in master mix and incubate for 1 hour in fridge protected from light.

Master Mix:

a. Total volume of 100 µL.
b. Calculate volume of each antibody. See Table 8.
c. Add corresponding volume of flow staining buffer/block (3% BSA/PBS) to tube, then add volume of each antibody.

Note: Unstained control will use 100 µL of flow staining buffer (3% BSA/PBS)

12. Top up tubes with 1 mL of 1X PBS and spin down at 2000 rpm for 5 mins.
13. Remove the supernatant by decanting, leaving behind a small amount of PBS. Loosen pellet with gentle tapping.
14. Resuspend in 0.3 mL of 1 X PBS in FACS tube. Cover the tubes with foil.

Table 8: Flow cytometry antibody specifications and required volume.

Marker	Fluorochrome	Type	Volume of Antibody µL
SOX2	Alexa Fluor 700	intracellular	1
Nanog	DyLight™ 488	intracellular	1
Tra-1-60	PE	surface	1
Tra-1-81	APC	surface	1
Oct 4	Alexa Fluor 405	intracellular	1
SSEA4	PerCP-eFluor™ 710	surface	1
CD44	SuperBright 702	surface	1

3.15 Reprogramming Efficiency

The common metric of iPSC reprogramming success is the reprogramming efficiency. This percent is typically calculated as the number of iPSC colonies generated, divided by the number of input cells [55].

The calculation is presented as follows:

$$Efficiency = \frac{iPSC\ colonis\ obtained}{Fibroblasts\ exposed\ to\ the\ virus}\ x\ 100\%$$

The number of iPSC colonies obtained is typically performed by expanding colonies that are stained with AP live stain and counting the ones that have survived.

For the purposes of this project, several approaches were explored for obtaining a reprogramming efficiency. Colonies were counted from images of the whole well obtained using the CELLCYTE X imaging system. Additionally, immunocytochemistry was used to distinguish colonies positive for certain pluripotency markers. Lastly, percentage of cells expressing pluripotent markers were determined by flow cytometry.

3.16 Lactate and Glucose Assay

A colorimetric assay (Abcam, ab65330) was used to determine the concentration of lactate in media samples. The manufacturer protocol was followed, and a microplate reader was used to measure the output at OD570 nm.

Another colorimetric assay (Abcam, ab65333) was used for determining the concentration of glucose in media samples. The manufacturer protocol was followed, and a microplate reader was used to measure the output at OD570 nm.

3.16.1 Sample Preparation

A 0.5mL sample of media should be collected into a centrifuge tube. The sample needs to be deproteinized before storing due to a high number of proteins from FBS in the media. Deproteinization of samples was done using an ultrafiltration centrifugation device (Thermo Scientific, 88513).

1. Collect 0.5 mL of media sample in centrifuge tube.
2. Insert the filter and close tube.
3. Centrifuge at 12,000 for 5 min.
4. Discard filter and store at -80C

3.17 Brightfield Imaging

To monitor cell growth, a brightfield microscope (Zeiss, Axiovert 200M) was used. The typical settings for a static culture are at 5X or 10X magnification with Phase 0 or 1 respectively. When imaging a suspension culture such as that of aggregates, Phase 2 at 10X is used. An example of these images can be seen in Figure 13.

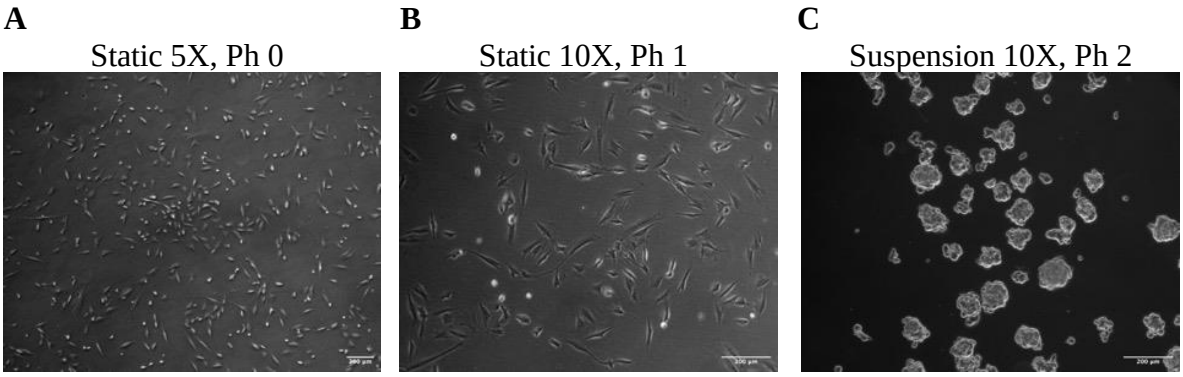

Figure 13: Examples of Brightfield images obtained at different microscope configurations. A) Image of static culture at 5X magnification and phase 0. B) Image of static culture at 10X magnification and phase 1. C) Image of suspension aggregate culture at 10X magnification and phase 2.

3.18 Confocal Imaging

The confocal fluorescent microscope system (Zeiss, LSM 700) allows for acquisition of fluorescent stain images. A laser is used to excite cells labelled with a specific fluorophore. The nuclei of cells were stained with SYTO 24 (Invitrogen, S7559), according to manufacturer protocol, to visualize cell nuclei and determine cell attachment to microcarriers. The microscope was also used to perform immunocytochemistry.

3.18.1 Protocol for iPSC immunocytochemistry

Protocol adapted from ThermoFisher for the Pluripotent Stem Cell 4-Marker (Immunocytochemistry Kit (Invitrogen, A24881)

1. Remove media from the cells.
2. Add Fixative Solution (Invitrogen, A24344) and incubate for 15 minutes at room temperature.
3. Remove Fixative Solution.

Optional stopping point: After removing Fixative, add Wash Buffer (diluted to 1X with water), parafilm the sample to prevent it from drying out, and store at 4°C for up to 1 month.

4. Add Permeabilization Solution (Invitrogen, A24878) and incubate 15 minutes at room temperature.
5. Remove Permeabilization Solution.
6. Add Blocking Solution (Invitrogen, A24353) and incubate in incubator overnight.
7. Add desired antibody directly to the Blocking Solution covering the cells to yield a 1X final dilution and mix gently.
8. Wet a regular paper towel and cover wells followed by the well plate cover. Place in refrigerator (at 4°C) for at least 4 hours (best overnight).
9. Remove the solution. Add Wash Buffer (diluted to 1X with water) and wait for 2–3 minutes. Repeat the wash procedure 2 more times so that the cells are washed a total of 3 times. Do not remove the last wash.
10. Image the cells immediately or store cells at 4°C in the dark, wrapped with parafilm to prevent the samples from drying out, for up to 1 month.

Examples of images stained with this protocol can be found in Figure 14 and Figure 15.

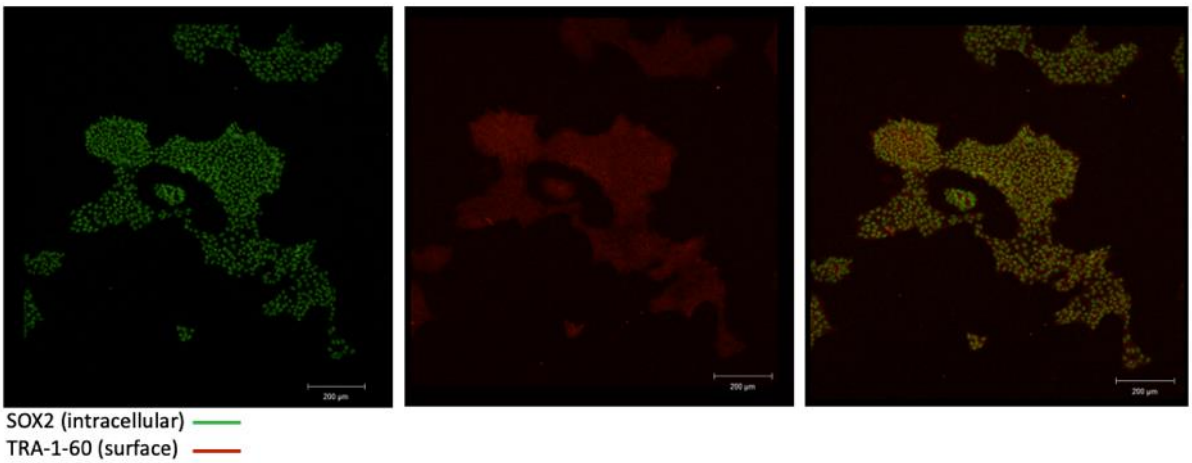

Figure 14: Fluorescent staining of an established hiPSC line PGPC3 with SOX2 (green) and TRA-1-60 (red).

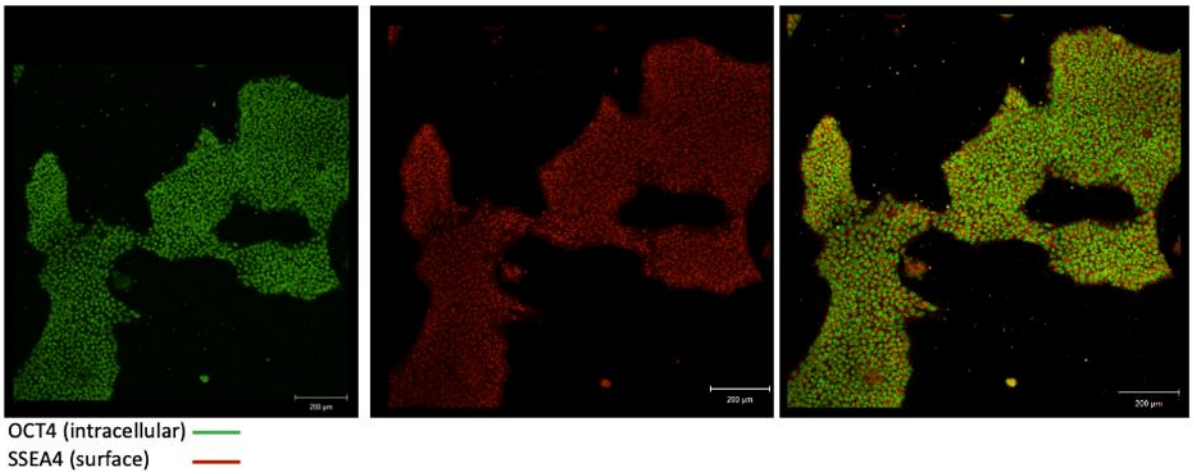

Figure 15: Fluorescent staining of an established hiPSC line PGPC3 with OCT4(green) and SSEA4 (red).

3.19 CellCyte X Imaging

The CellCyte X (Cytena) imaging system was created as a user-friendly and efficient method of obtaining images of a whole well. The system is able to obtain 64-images per well at 10X magnification with enhanced contour and 3 fluorescent channels. Additionally, the software has built-in analysis tools for determining cell confluence and area.

The Live Cell Imaging Facility provided the services of CellCyte X for the purposes of this project. The same protocol as optimized for the confocal fluorescent system was used for the preparation of cells imaged by the CellCyte X.

3.19.1 Stitching images

64 images per well were obtained resulting in an 8x8 configuration. The images were stitched using a plugin for the open source imaging software FIJI [93]. The images were stitched with the grid pattern shown in Figure 16 A based on the numbered order outputted by CellCyte X. Figure 16 B shows a summary of the stitching settings including a 35% overlap which was found to be optimal in ensuring proper image position. An example of a stitched image can be seen in Figure 16 C.

Protocol

1. Obtain images using the CellCyte at 64 images per well. Settings of the machine will need to be adjusted each time. Ensure that each well of a 6-well plate has 3 mL of media to prevent blurriness around the edges.
2. Save images from CellCyte in tiff image type. Sort the downloaded images into folders based on each well.
3. Stitch images using ImageJ by going to Plugins -> Stitching-> Grid/Collection stitching.
4. Use the settings as shown in Figure 16 A and B.
5. Ensure that the directory leads to the corresponding well folder and the file name is directly copied. Replace number after p with {i} and add “tiff” to the end of the file name.

Note: If an error is encountered, double check the directory and file name.

A

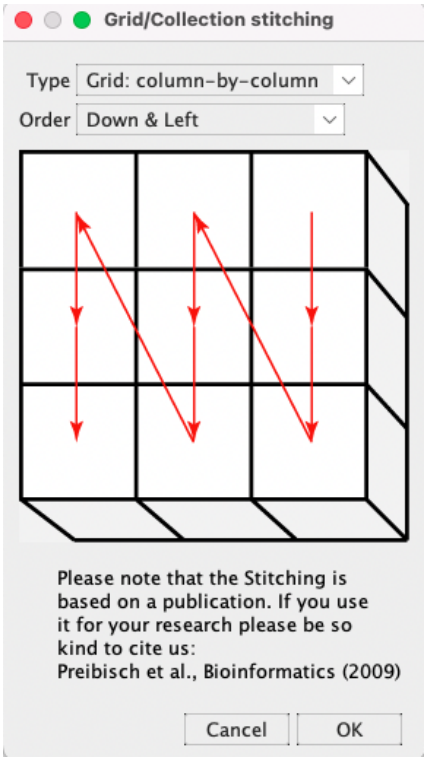

B

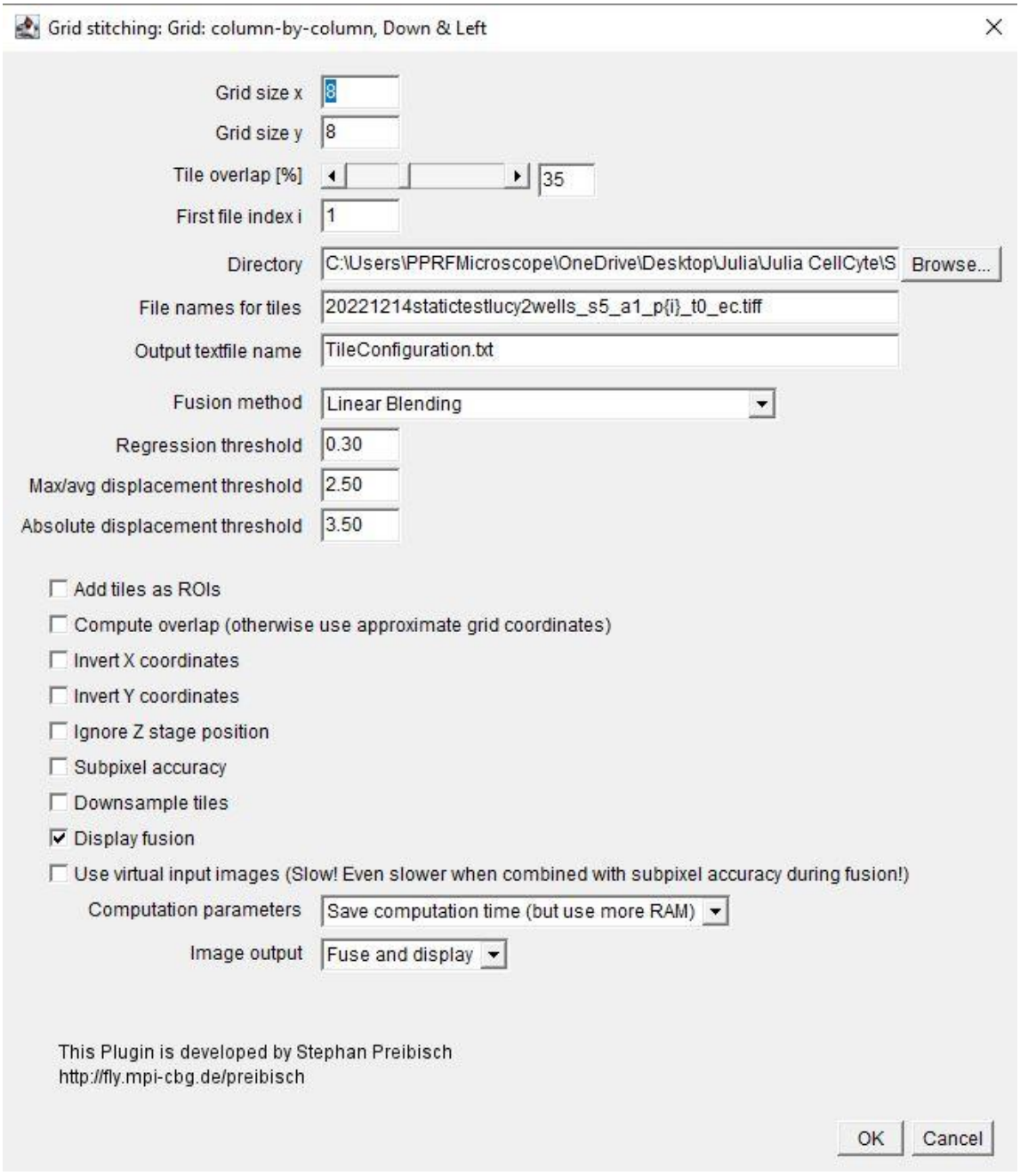
Grid stitching: Grid: column-by-column, Down & Left
Grid size x
8
Grid size y
8
Tile overlap [%]
35
First file index i
1
Directory
C:\Users\PPRFMicroscope\OneDrive\Desktop\Julia\Julia CellCyte\S
Browse...
File names for tiles
20221214statictestlucy2wells_s5_a1_p{i}_t0_ec.tiff
Output textfile name
TileConfiguration.txt
Fusion method
Linear Blending
Regression threshold
0.30
Max/avg displacement threshold
2.50
Absolute displacement threshold
3.50
Add tiles as ROIs
Compute overlap (otherwise use approximate grid coordinates)
Invert X coordinates
Invert Y coordinates
Ignore Z stage position
Subpixel accuracy
Downsample tiles
Display fusion
Use virtual input images (Slow! Even slower when combined with subpixel accuracy during fusion!)
Computation parameters
Save computation time (but use more RAM)
Image output
Fuse and display
This Plugin is developed by Stephan Preibisch
http://fly.mpi-cbg.de/preibisch
OK
Cancel

C

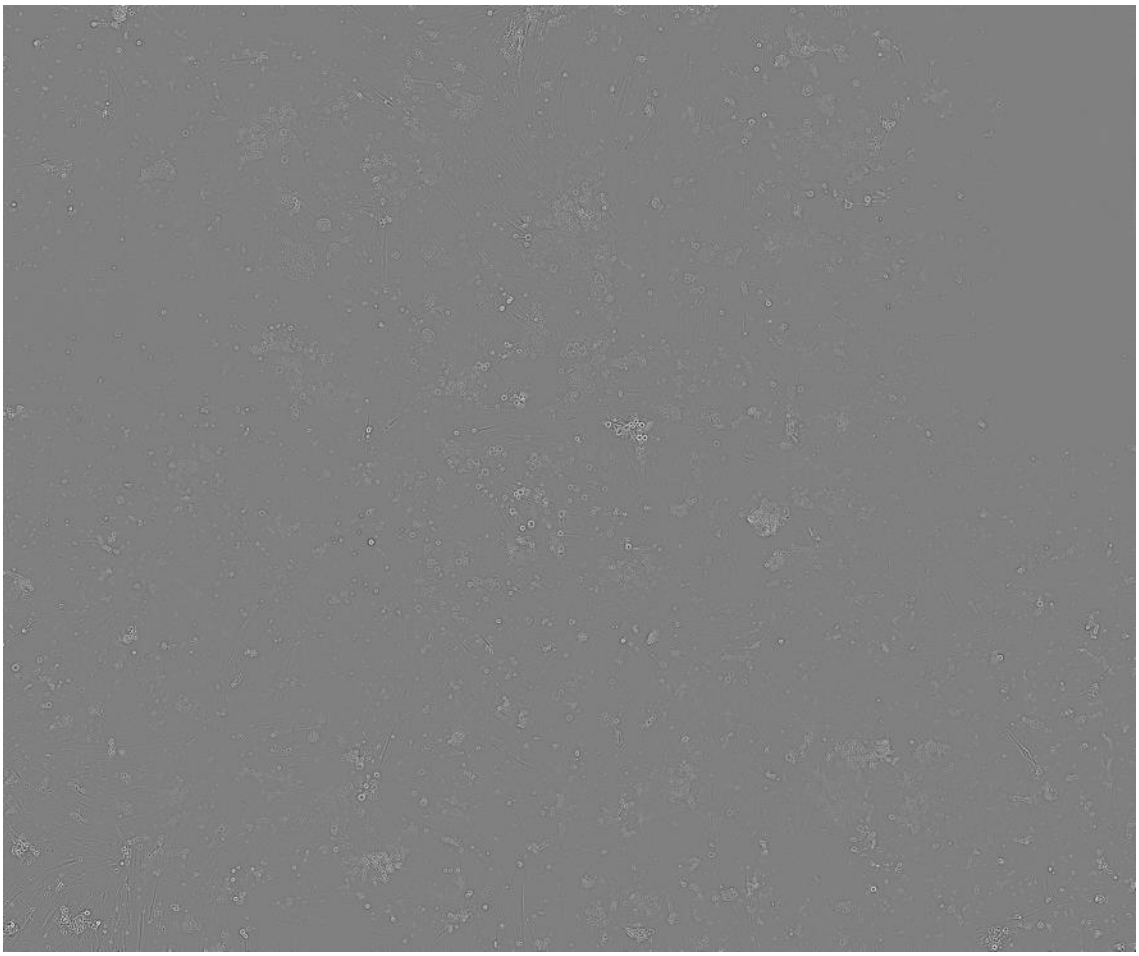

Figure 16: Settings used for image stitching in FIJI. **A)** FIJI grid stitching pattern used based on output of CellCyte X images. **B)** Configuration of grid size and tile overlap **C)** Example of stitched well image.

3.19.2 Manual Colony Selection

The stitched images are used to determine the number of colonies in each well. To ensure that the correct colony size can be obtained, the scale within FIJI needs to be set. The settings used for this project are found in Figure 17.

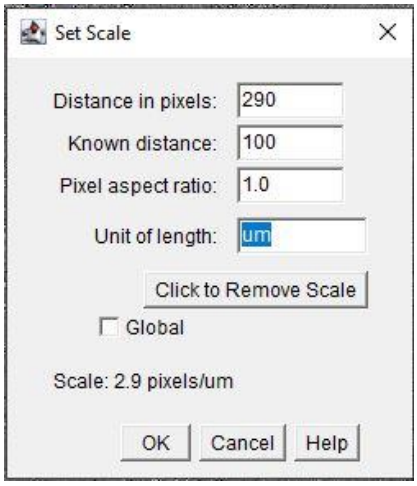

Figure 17: FIJI scale conversion of pixels to micrometre.

To keep track of colonies counted and their measurements, the FIJI freehand selection tool, shown in Figure 18, is used to circle appropriate colonies. hiPSC cells are identified by their high nucleus to cytoplasm ratio and distinct colony formation with clear edges [94]. An example of a selected colony can be found in Figure 19.

A

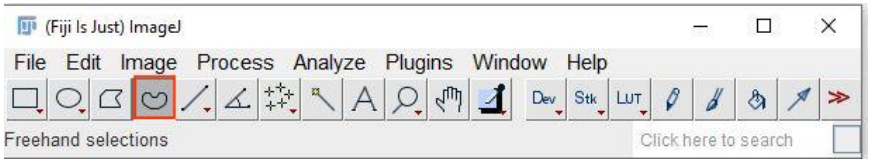

Figure 18: FIJI freehand selection tool outlined in red.

B

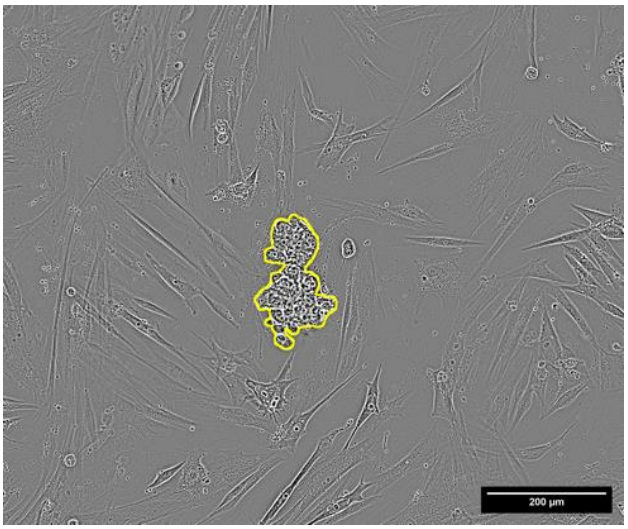

Figure 19: Example of selected colony using freehand selection tool in FIJI.

Protocol to count and measure colonies:

1. Ensure the correct scale is set for the image.
2. Under Analyze select “Set Measurements”. Select “Area“ and any other parameters of interest.
3. Open ROI manager: Analyze -> Tools -> ROI Manager
4. Use the freehand selection tool to trace the colony. Add to the ROI manager. Select “Show All” and “Labels” to see what has already been selected
5. When all colonies have been selected, click “Measure”.

Note: Adding scale can be done through a macro.

3.19.3 Automated Colony Selection

An automated approach to colony counting was examined. Automation of colony selection has many advantages as it does not dependent on the operator therefore eliminating bias and improving reproducibility while reducing the time of analysis.

To evaluate the automated approach, the CellCyte X built-in analysis tool was used.

The built-in tool allows for areas of interest to be selected from several images which creates a mask based on this input. Figure 20 shows the yellow mask being correctly applied to the colony but additional areas that would not be considered a colony as also being selected. This suggests that comparison to the manual approach needs to be done and an area range should be established.

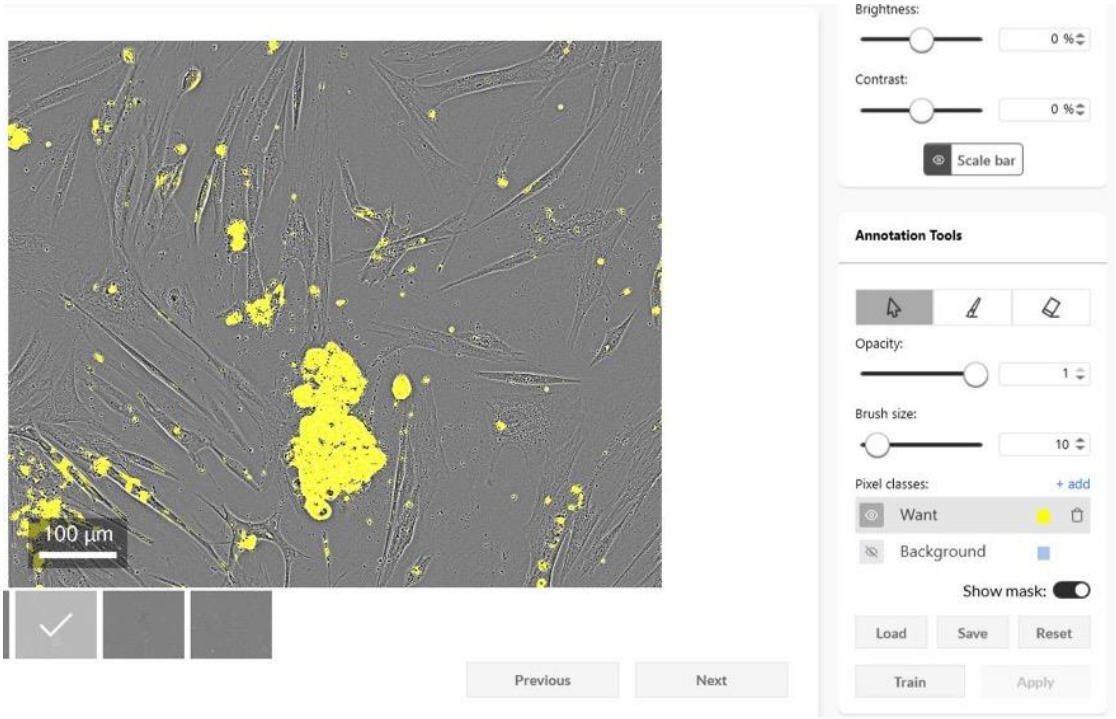

Figure 20: Built-in analysis of colony selection for a phase contrast image. The yellow mask is the automated selection performed by the software.

Chapter 4 Aim 1- Small-Scale Dynamic Culture Reprogramming

4.1 Overview

The objective of this aim was to adapt the manufacturer reprogramming process to a dynamic system. As fibroblast cells are an adherent cell type and require a surface for growth, the approach was to select a microcarrier for cell growth in a dynamic environment. Several microcarrier screening experiments were performed to select the optimal microcarrier. This was followed by an experiment to isolate the effect of a dynamic system on cell growth during Stage 1 and determine the best seeding density in Stage 2. The best combination of static and dynamic systems for the reprogramming process was then evaluated in Stage 1 and Stage 2. Additional experiments were performed to determine the feasibility of integrating the reprogramming process into a small-scale bioreactor system.

4.2 Introduction

The biophysical cell environment plays an important role in cell growth kinetics and phenotype. This is particularly important for pluripotent cells as dynamic forces can influence pluripotency and differentiation [7][33]. The positive effect of a dynamic system when applied to the expansion and differentiation of hiPSCs has previously been observed [30][95]. Additionally, studies have focused on reprogramming fibroblast cells on microcarriers or using mouse embryonic fibroblasts (MEFs) within a dynamic system [6][96]. The effect of a dynamic system on reprogramming of human fibroblast cells to hiPSCs has not been evalauted. The objective of this aim was to use a commercially available, non-integrating reprogramming approach and evaluate its effect within a dynamic system.

4.3 Results and Discussion

4.3.1 Microcarrier Screening

Fibroblast cells are an adherent cell type which require a surface to grow on. To support fibroblast growth in a dynamic system and be able to perform reprogramming, a microcarrier must be used. The selected microcarrier must perform well in both fibroblast medium as well as E8 medium and support fibroblast and hiPSC growth. A microcarrier screening was performed as described in Chapter 3.

The microcarrier set up can be found in Figure 21.

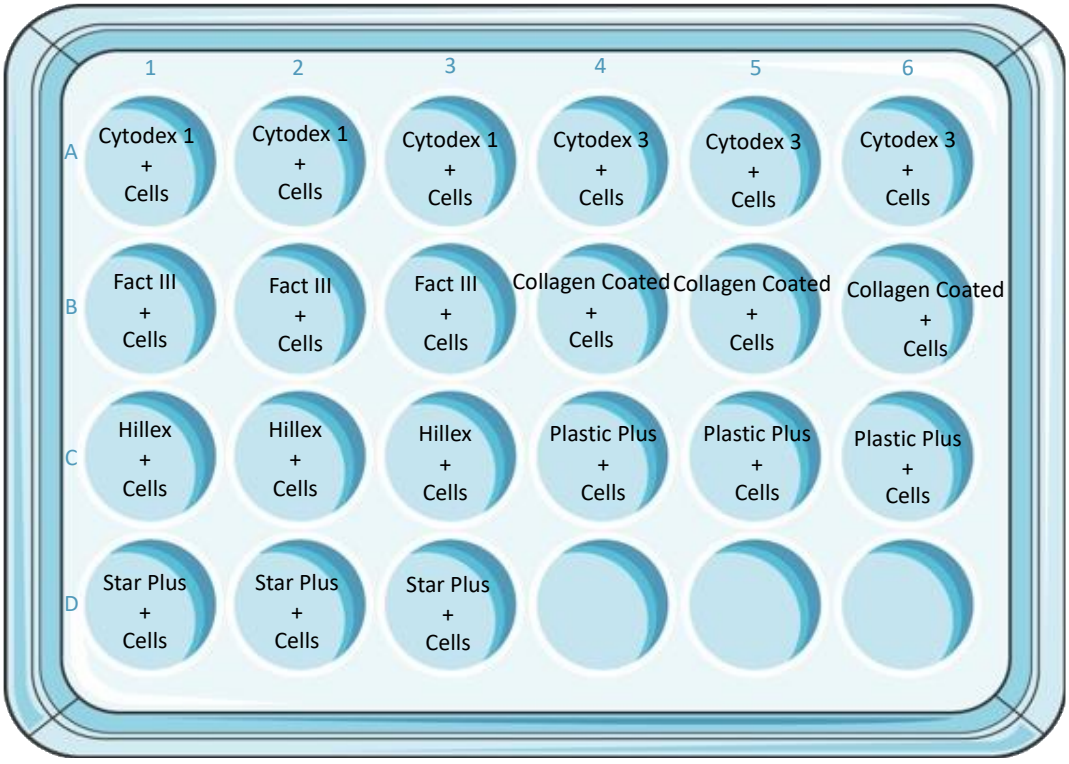

Figure 21: Experimental set-up for microcarrier screening experiment.

This experiment used a non-adherent 24 well plate, placed on an orbital shaker to simulate a dynamic environment. A microcarrier density of 5.4 cm^2/mL was used with cells seeded at 5000 cells /cm^2 (27000 cells /mL) in a fibroblast medium consisting of DMEM (Gibco; #10569-010) and 10% FBS (ATCC, 30-2020).

Growth kinetics were assessed on Days 1, 3 and 5 using Crystal Violet staining and a hemacytometer as shown in Figure 22.

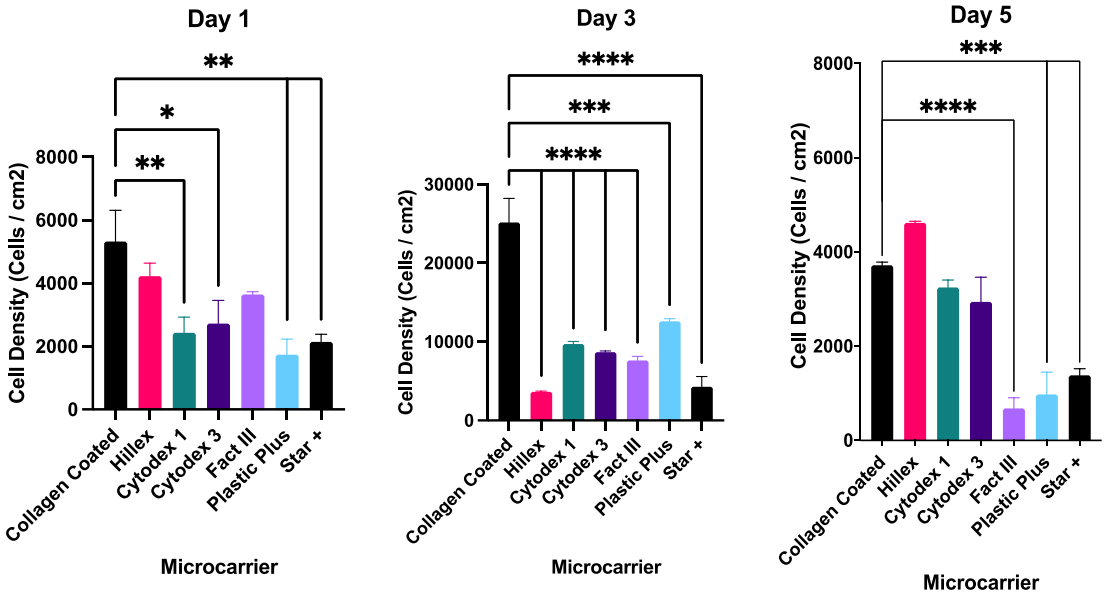

Figure 22: Crystal violet counts taken on Day 1, 3 and 5 of microcarrier screening.

Statistics performed by one way ANOVA with comparison to Collagen coated microcarrier.

$* P \leq 0.05,\ ** P \leq 0.01,\ *** P \leq 0.001,\ ****P \leq 0.0001.$

Confocal fluorescent images after staining with SYTO 24 Green Nucleic Acid stain were taken to observe cell attachment. The imaging conditions were optimized using a negative control of microcarriers with no cells (not pictured). The top four performing microcarriers on Days 1,3 and 5 are pictured in Figure 23. The combined microcarrier screening results of Crystal violet counts and fluorescent images suggest that the top three performing microcarriers include Cytodex 1, Collagen Coated and Hillex. Unfortunately, Cytodex 1 is no longer available for purchase and therefore would not be feasible for prolonged use. Therefore, Collagen Coated and Hillex were selected for further comparison.

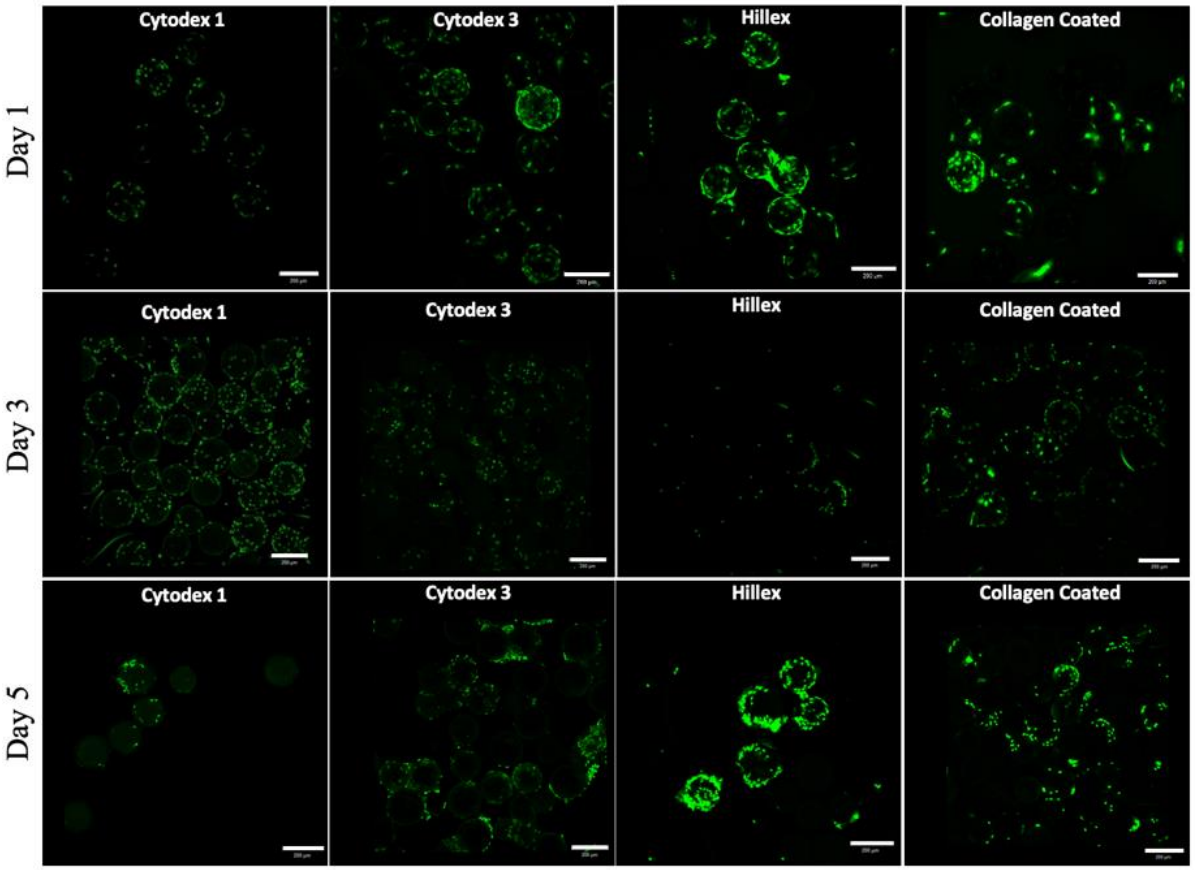

Figure 23: Fluorescent images of live cells on top four performing microcarriers. Scale bar represents 200 μm.

4.3.1.1 Performance Comparison of fibroblast cells on Hillex and Collagen Coated Microcarriers

An experiment was performed to compare cell growth of fibroblast cell line CRL2522 on Hillex and Collagen Coated microcarriers using 10 mL spinner bioreactors. Six bioreactors were seeded with one sacrificed for counts each day (5 Days total) and an additional one used for contingency. A static control was used to ensure no abnormalities in cell growth. The experiment set-up can be found in Figure 24.

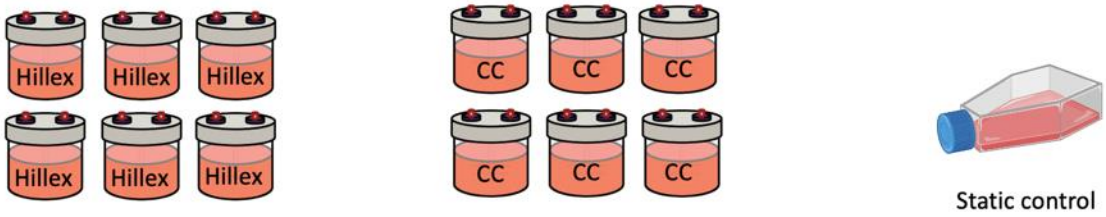

Figure 24: Experiment set-up for comparison of fibroblast cell growth on Hillex and Collagen Coated microcarriers in a 10 mL spinner bioreactor.

Crystal Violet staining and hemacytometer counts were used to generate a 5-day growth curve as seen in Figure 25. The growth curve results show that there was a drop in cell density from the initial seeding density of 5000 cells/cm^2 for both microcarrier types. This could be due to poor initial cell attachment and requires further optimization of factors such as cell seeding density, microcarrier density and serum concentration in media. Overall, the growth curve shows a higher cell density of cells on collagen coated microcarriers compared to Hillex.

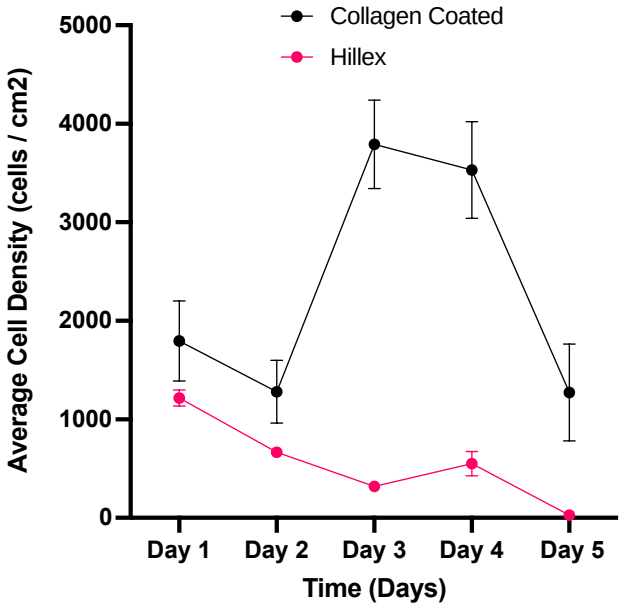

Figure 25: Comparison of fibroblast growth on Hillex and Collagen Coated microcarriers in 10mL spinner bioreactors.

To evaluate the microcarriers qualitatively, fluorescent images were taken on each day as seen in Figure 26 and Figure 27. Negative controls were imaged with no cells (not pictured).

Collagen Coated

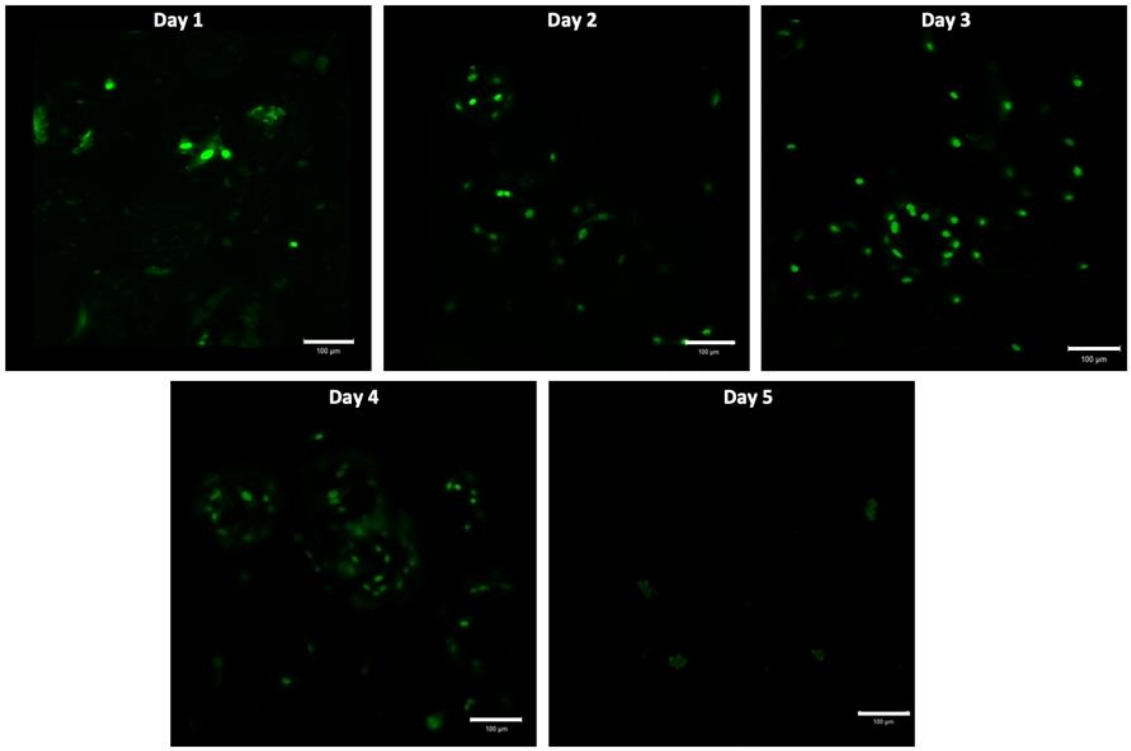

Figure 26: Fluorescent images of live cells stained with SYTO 24 on Collagen coated microcarriers taken on days 1-5. Scale bar represents 100 μm.

Hillex

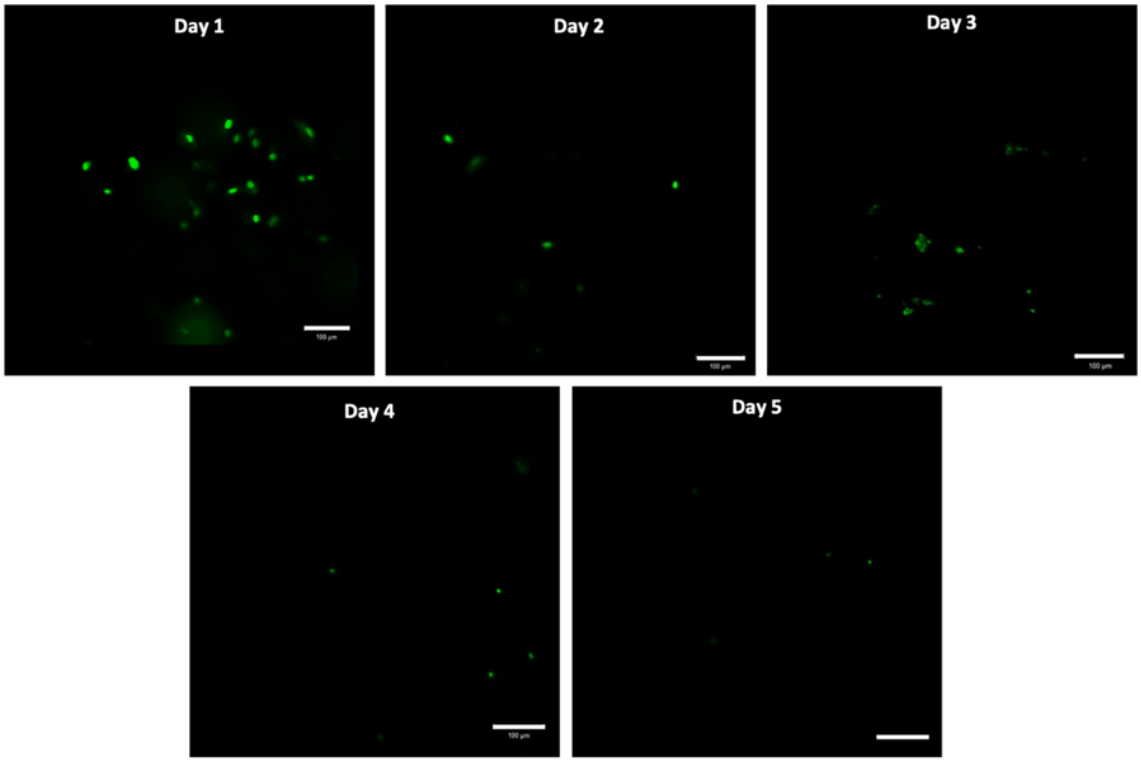

Figure 27: Fluorescent images of live cells stained with SYTO 24 on Hillex microcarriers taken on days 1-5. Scale bar represents 100 μm.

Brightfield images of live cells stained with Crystal violet in MeOH can be found in Figure 28 and Figure 29. These images further support that Collagen coated microcarriers perform better as there are more stained cells.

Collagen Coated

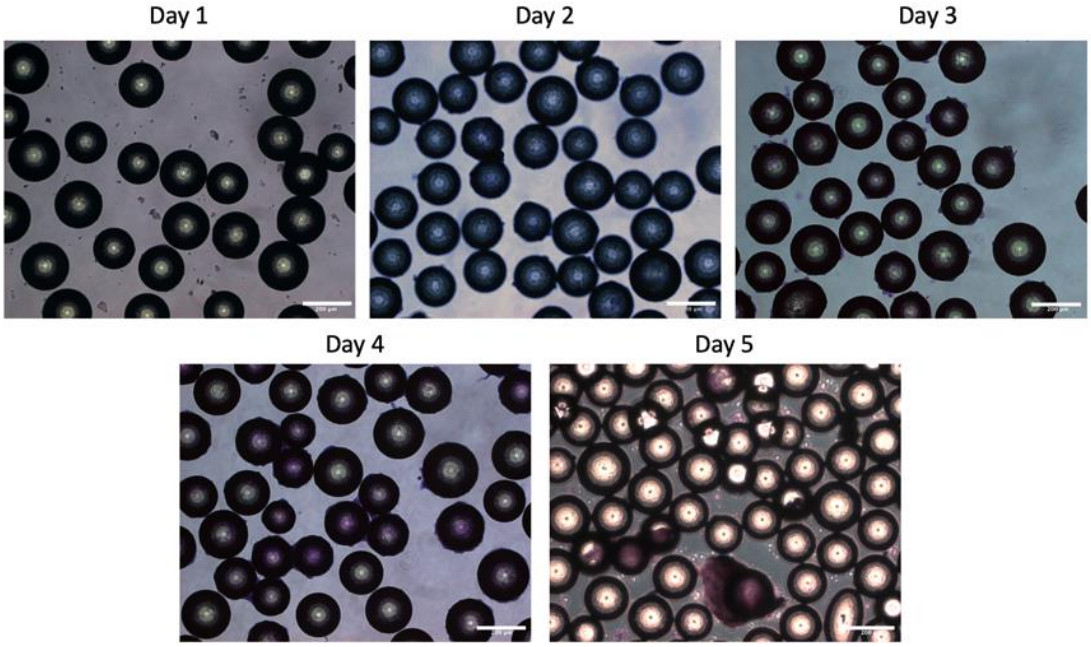

Figure 28: Brightfield images of live cells stained with Crystal violet in MeOH on Collagen coated microcarriers taken on days 1-5. Scale bar represents 200 μm.

Hillex

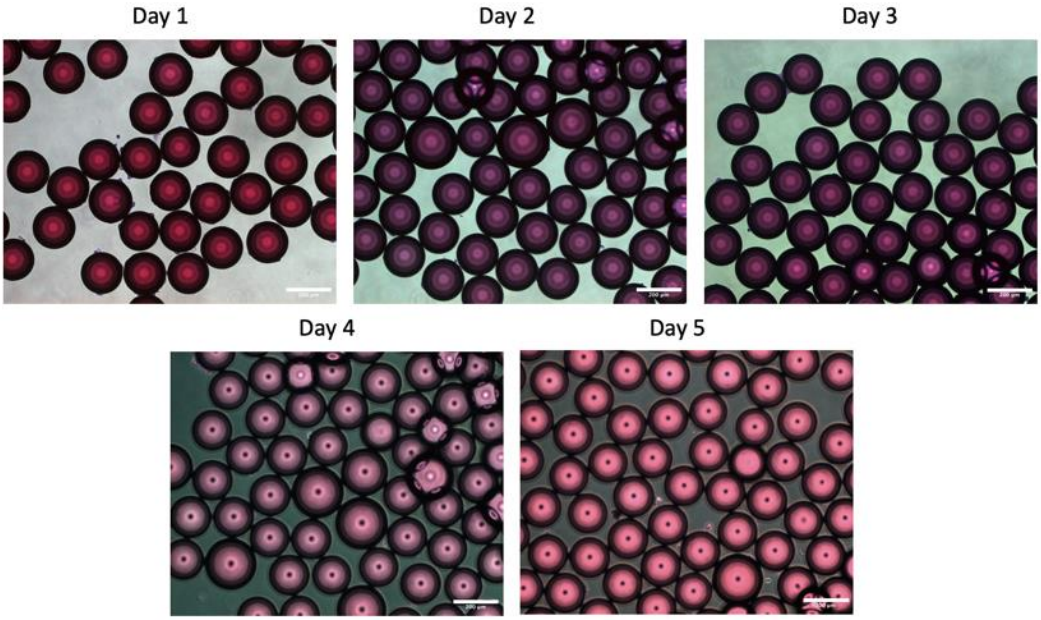

Figure 29: Brightfield images of live cells stained with Crystal violet in MeOH on Hillex microcarriers taken on days 1-5. Scale bar represents 200 μm.

4.3.1.2 Comparison of Hillex and Collagen Coated Microcarriers with hiPSCs

An additional experiment was performed to evaluate the cell attachment and growth of iPSCs on microcarriers. As the objective of reprogramming is to obtain hiPSCs, the chosen microcarrier should also be able to support hiPSC growth in serum free E8 media. The set-up of this screening is shown in Figure 30.

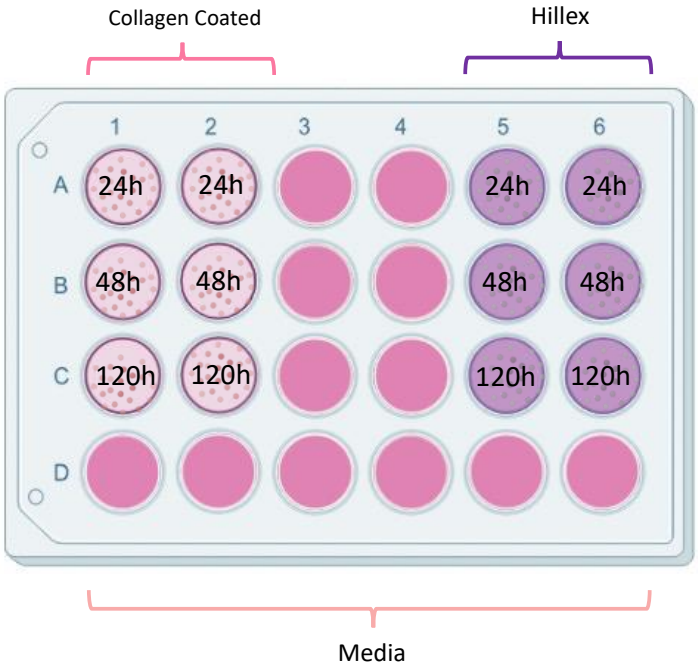

Figure 30: Well plate set up for screening of hiPSCs on Collagen coated and Hillex microcarriers.

As was previously done, a shaken plate was used to simulate a dynamic culture. The cells were stained with SYTO 24 Green Nucleic Acid stain at 3 time points: 24h, 48h and 120h. Confocal fluorescent images were then taken to determine cell attachment as seen in Figure 31. Negative controls of empty Collage coated and Hillex microcarriers were but are not pictured.

The fluorescent images show an initially better cell attachment to Hillex microcarriers with more nuclei visible at the 24h time point. However, by the 120-hour mark, both microcarrier types show significant cell growth.

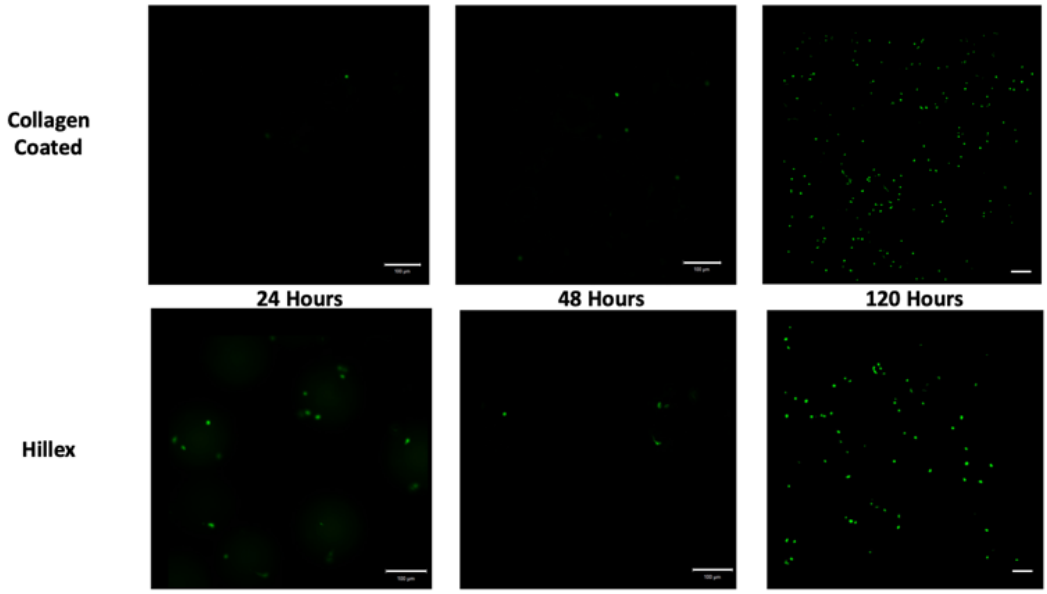

Figure 31: Fluorescent images of live cells stained with SYTO 24 showing comparison of hiPSC growth on Collagen coated and Hillex microcarriers. Scale bar represents 200 μm.

The objective of the microcarrier screening was to select an optimal microcarrier for the growth and expansion of fibroblast cells and hiPSCs. Based on the combination of obtained results icnluding cell counts, fluorescent images and Brightfield images, it can be determined that Collagen coated performed the best and will be used in further experiments.

4.3.1.3 Improvement of Cell Attachment to Microcarriers

A key factor of performing reprogramming in a 3D suspension such as a bioreactor, is ensuring an adequate attachment of cells to microcarriers. To optimize cell attachment, a factorial experiment was performed evaluating the effect of serum content, cell density and microcarrier density. The cells were seeded in a non-adherent 24-well plate with images taken at 24h, 48h, 72h. The experimental design and results are found in Figure 32.

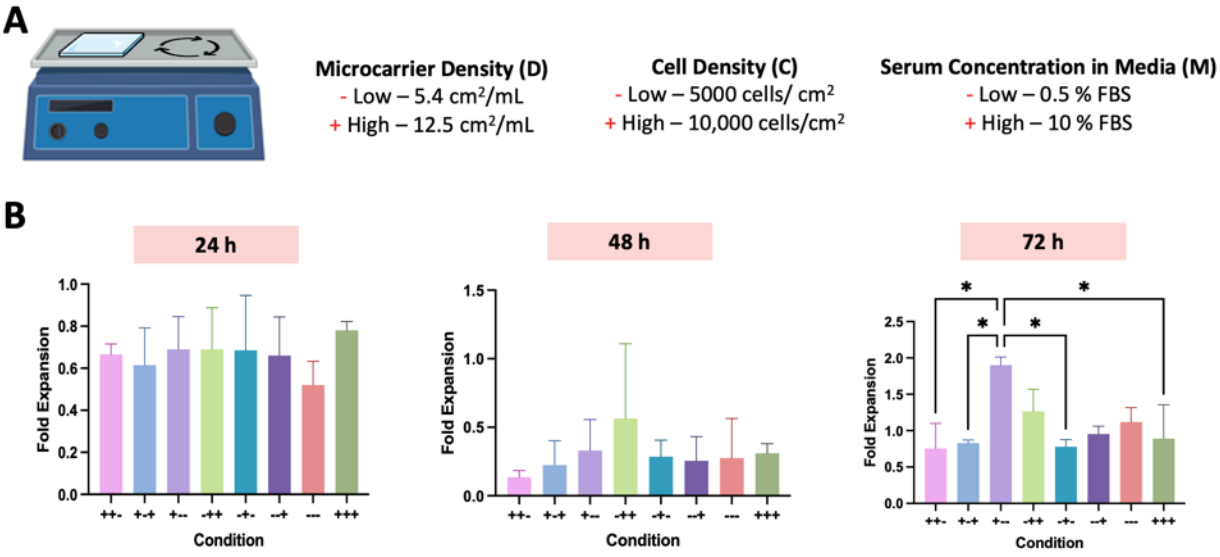

Figure 32: (A) Experimental set-up of factorial experiment with analysed conditions. **(B)** Fold expansion of analysed conditions with statistics performed by one way ANOVA with comparison to each condition. * $P \leq 0.05$.

4.3.1.4 Conclusions

There appeared to be no statistical differences between the conditions at 24h and 48h. Additionally, no statistical difference was found at 72h between condition +-- and conditions -++, --+, ---. The fold expansion of <1 in most conditions suggests that there is poor initial cell attachment and fibroblast cells do not grow well on microcarriers in a suspension environment. Next steps would include testing intermittent agitation during the attachment stage.

4.3.2 Reprogramming on microcarriers

Despite the poor attachment of cells to microcarriers, an experiment was conducted to examine the effect of shaking on the reprogramming process during Stage 1. The experiment timeline and set-up can be found in Figure 33. The microcarrier condition was tested along with a shaker plate and static control.

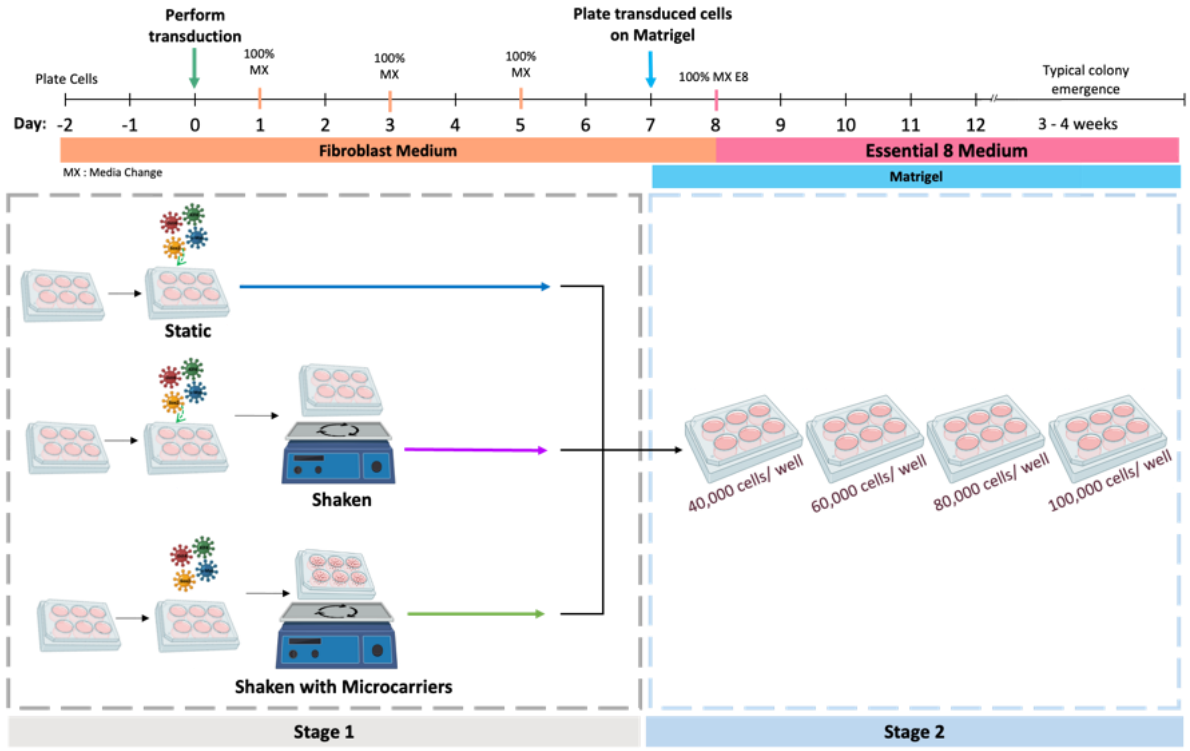

Figure 33: Experimental set-up of reprogramming examining static, shaken and microcarrier conditions in Stage 1. Figure was created with BioRender.com.

The two counting wells from each condition were harvested and counted. The average cell count was then used to determine the required volume of virus. The total cell number can be seen in Figure 34.

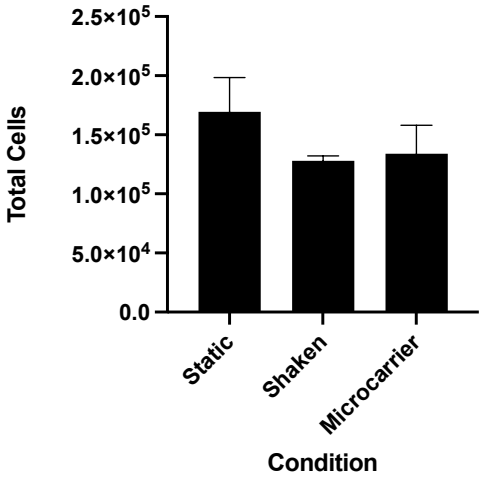

Figure 34: Total cells counts from the counting wells of the three conditions on Day 0 before transduction.

The total cell number obtained was lower than the recommended cell number of $2x10^5$–$3x10^5$ cells per well. Despite this, cells were able to grow in the static and shaken conditions at Stage 1 and when passaged into static for Stage 2.

On Day 7, the passaged cells were plated at four different densities to determine how density impacts colony formation. Images of Day 18 colonies can be seen in Figure 35. The first colony was observed in the 60,000 cells/well shaken condition on Day 11.

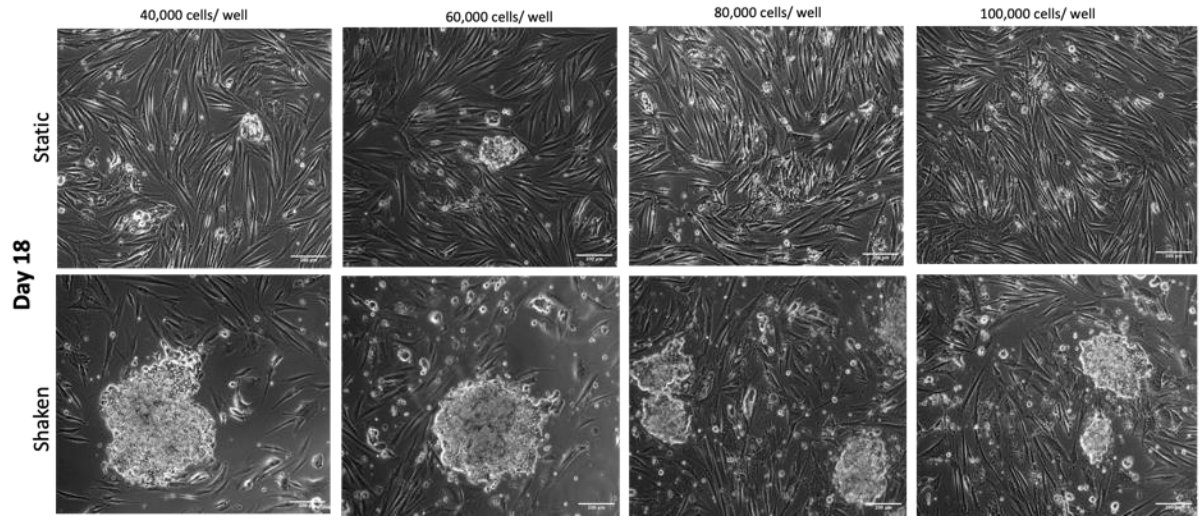

Figure 35: Images of Stage 1 Static and Stage 1 Shaken conditions taken on Day 18 at 10X magnification.

4.3.2.1 Results and Discussion

Based on the Day 0 count, it is observed that the microcarrier condition did not support cell growth and reprogramming. This could be due to the poor initial cell to microcarrier attachment and therefore poor growth or the negative impact of shaking in general in the beginning stages of the process. It can be postulated that the shaking environment is too stressful for the cells when undergoing reprogramming and they are unable to stay attached to the microcarrier. The Stage 1 shaking condition with no microcarriers resulted in earlier colony emergence with overall larger colonies than the Stage 1 static condition. This was observed across all cell densities.

When observing cell growth across the various cell densities of Stage 2, it is observed that higher cell density conditions (80,000 cells/well and 100,000 cells/well) resulted in smaller and fewer colonies compared to the lower cell density conditions (40,000 cells/well and 60,000 cells/well). This result was expected as a negative correlation between seeding density and reprogramming efficiency has been previously described in literature [6].

4.3.2.2 Conclusion

This experiment demonstrated the effect of Stage 1 shaking on cell growth and colony development. The microcarrier condition was unsuccessful in supporting cell growth and is potentially too stressful for proper cell attachment and reprogramming. The shaken condition was more successful and resulted in earlier and larger colony formation than the static control in all four densities. This observation leads to the conclusion that the forces induced by the shaking condition may be beneficial to the reprogramming process but have a negative impact on cells being reprogrammed on microcarriers. Overall results suggest that the 40,000 cells/well and 60,000 cells/well conditions may be the most optimal cell densities for Stage 2.

4.3.3 Effect of shaking at different Stages of Reprogramming process

To further observe the effect shaking has on the reprogramming process, combinations of shaking in Stage 1 and Stage 2 were evaluated. The cell density in Stage 2 was also examined to determine the optimal density for colony development. The reprogramming timeline for this experiment can be found below in Figure 36.

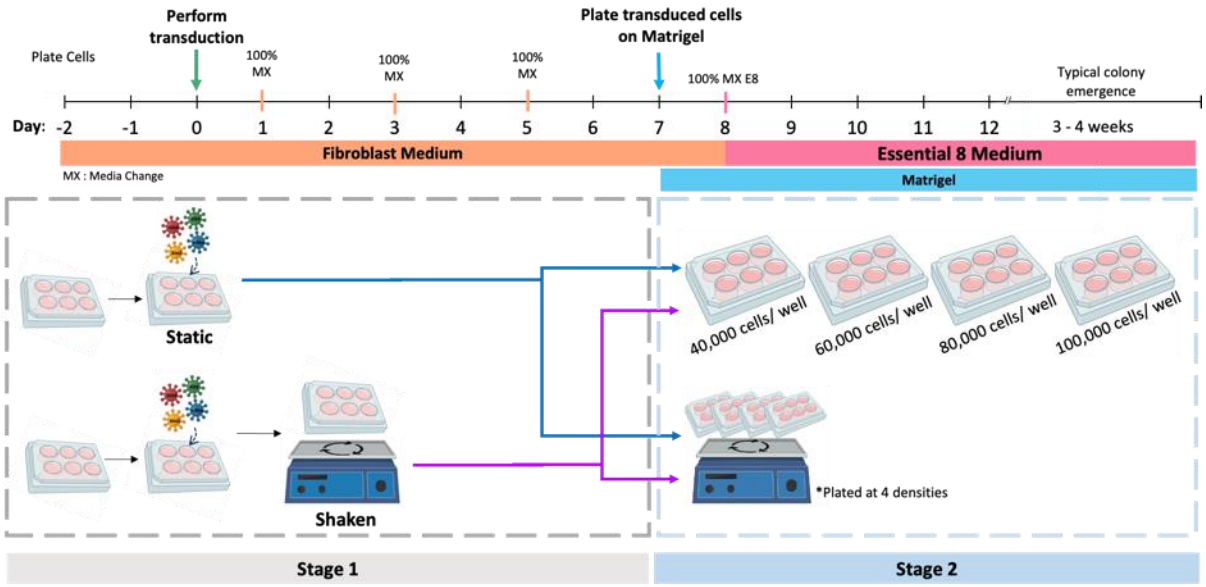

Figure 36: The effect of dynamic forces on reprogramming at different stages of the process with optimization of cell density. Figure was created with BioRender.com.

4.3.3.1 Results and Discussion

Images of the cell growth can be found in Figure 37. The cell growth was very similar in the Static –> Static and Shaken –> Static conditions. Colonies in these conditions did form but were slower to emerge compared to Static –> Shaken. The Static –> Shaken condition had the most colonies formed with visible colonies emerging as early as Day 10.

The Shaken -> Shaken condition had the most interesting result as cells were starting to lift off and clump together. It is presumed that these lifted off cells may be colonies and their viability will need to be further examined as there may be potential to plate these cells for expansion in static. The lifting of cells may indicate an occurrence of EMT which is characterized by the breaking down of the basement membrane and migration of cells away from the epithelial layer, very similar to what was observed within this condition [13]. More close monitoring will need to be done to determine if the cells are lifting off as colonies or as single cells which then attach to each other.

Previous studies have shown that although hiPSCs are generally anchorage dependant, they are able to aggregate in suspension with the addition of ROCKi [96][97]. It is hypothesized that the addition of ROCKi increases adhesive properties through cell-cell interaction thereby enhancing aggregate formation [47][98]. ROCKi was not added during the reprogramming process but its addition may improve cell-cell interaction of the detached cells thereby forming aggregates. However, if the detached cells are not viable, it may be a sign that the shaking environment is too stressful, and the cells cannot sustain healthy growth.

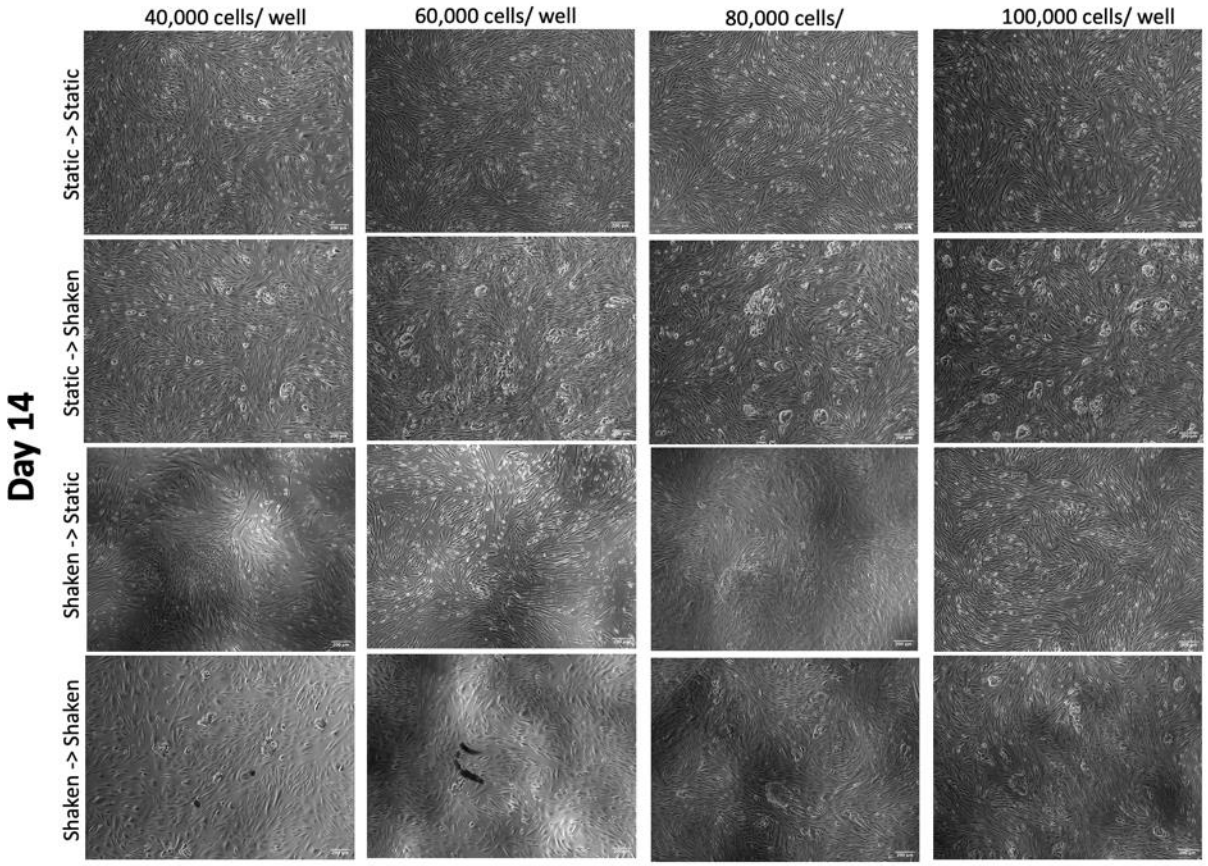

Figure 37: Images of cell growth in different combinations of Stage 1 and Stage 2 shaking at different cell densities. Images were obtained on Day 14 at 5X magnification.

Comparison of cell growth at different cell densities yielded similar results to the previous experiment, with densities of 40,000 cells/well and 60,000 cells/well performing the best. All cell density conditions resulted in colony formation however the lower seeded conditions are optimal due to fewer cells required. When comparing between the two

conditions, the 40,000 cells/well density was less consistent with slower colony emergence compared to the 60,000 cells/well condition.

4.3.3.2 Conclusion

The Static -> Shaken condition resulted in colony emergence at the earliest point of Day 10. The 60,000 cells/well density has again shown the optimal ratio of starting cell number to colony formation. Further steps should include a more quantitative approach to evaluating the best condition and determining reprogramming efficiency. Additionally, the lifted cells of the Shaken -> Shaken condition should be examined, and their viability determined if the lifting phenomena is repeated.

4.3.4 Shaking at different Stages of Reprogramming process at 60,000 cells/well

The previous experiment examining the effect of shaking at different stages was repeated with a focus on cell density of 60,000 cells/well. Fluorescent imaging and flow cytometry were chosen to provide a more quantitative method for evaluating the conditions. The timeline and set-up for this experiment can be found in Figure 38.

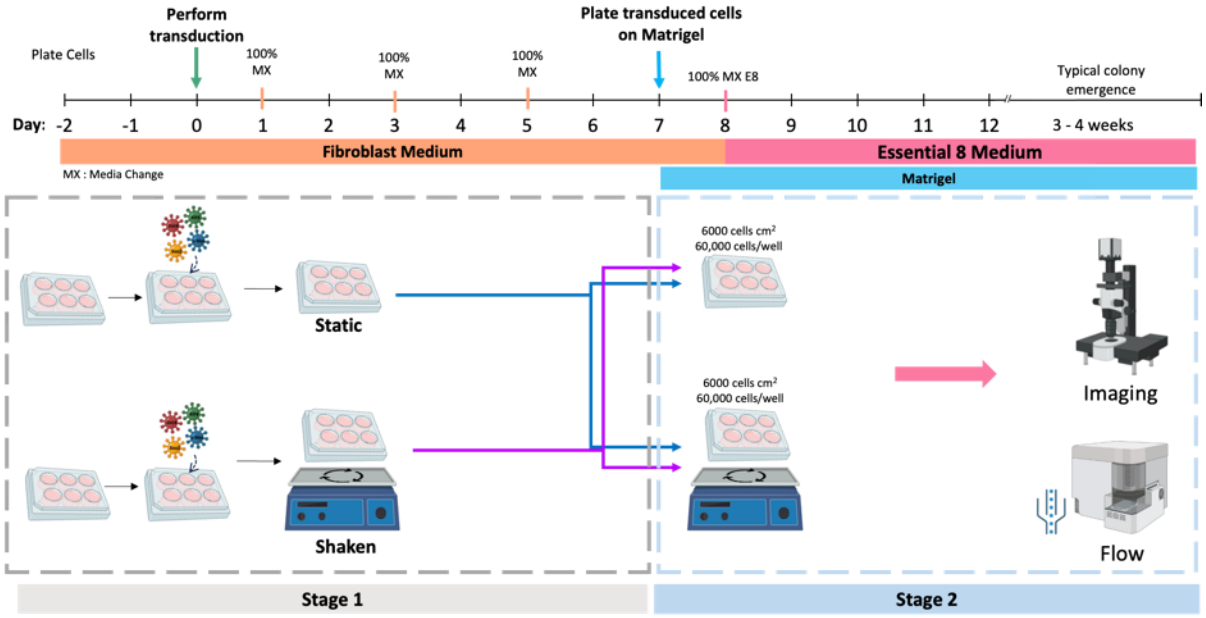

Figure 38: The effect of shaking at different stages of the reprogramming process at 60,000 cells/well. Figure was created with BioRender.com.

4.3.4.1 Results and Discussion

The cell growth and colony emergence during this experiment was slightly slower than was previously observed. Images for this experiment can be found in Figure 39. Aside from the Shaken –> Shaken condition, the other conditions looked very similar to each other on Day 19.

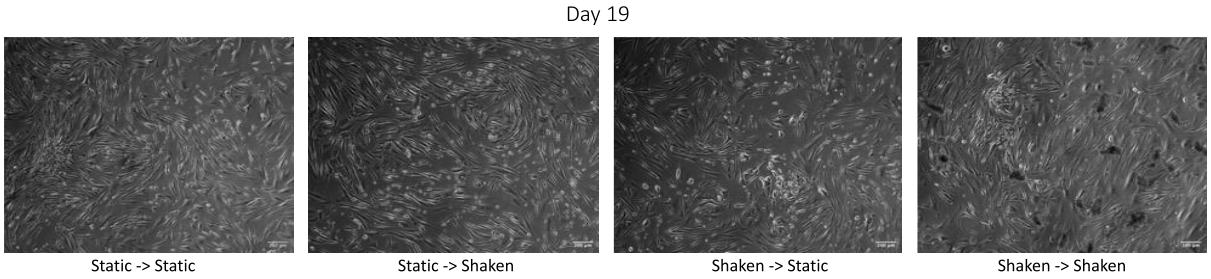

Figure 39: Images on Day 19 at cell density of 60,000 cells/ well, 5X magnification. The cell lifting phenomena was again observed in the Shaken-Shaken condition.

The Shaken -> Shaken condition again exhibited the lifting of cells. A closer look of the cells on Day 19 and after replating can be seen in Figure 40.

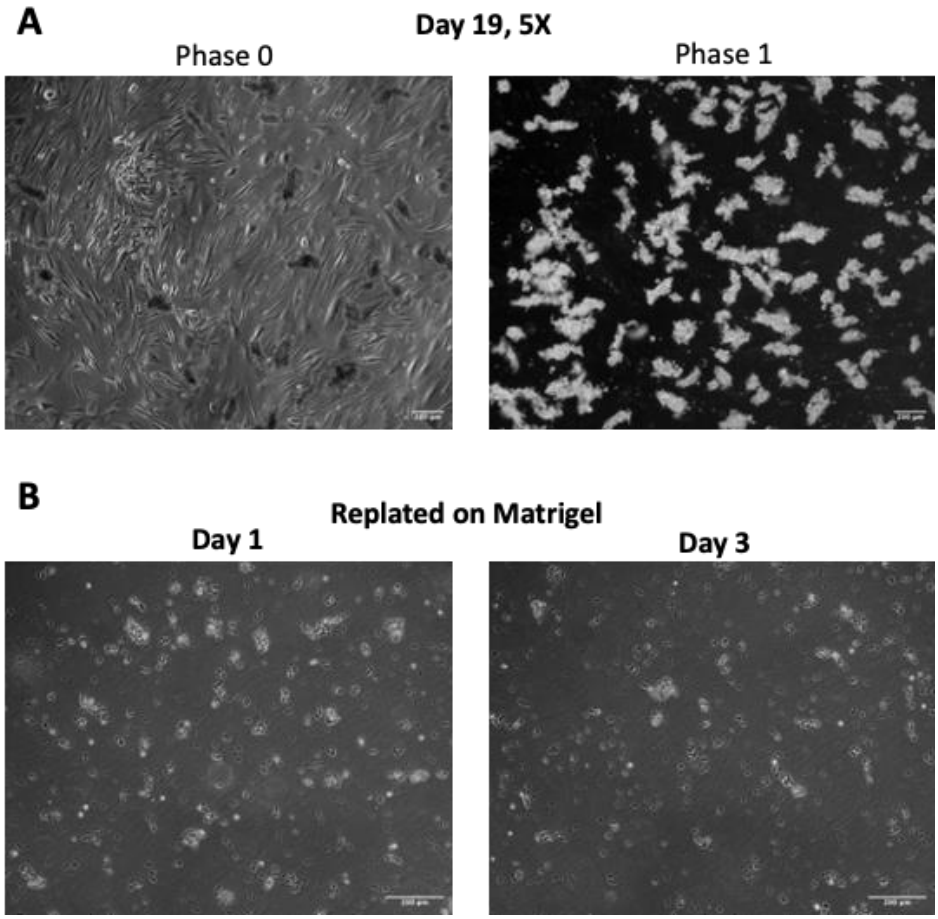

Figure 40: (A) Images of cells on Day 19 at 5X magnification at Phase 0 and Phase 1. (B) The cells were replated on Matrigel with images shown on Day 1 and Day 3.

The Figure 40 (A) phase 1 image, shows that cells lifted and were no longer attached. These cells were collected as part of the supernatant and viability was assessed. There was a total of ~70,000 cells with <30% viability. The cells were replated on Matrigel as shown in Figure 40 (B) and grown for 3 days. There was little cell attachment and no cell growth by Day 3. Due to low viability of the lifted off cells and no cell growth in static, it can be concluded that these cells cannot be recovered once they have lifted.

4.3.4.1.1 Flow Cytometry

On Day 19, the cells from several wells of the same condition were harvested and pooled together to be prepared for flow cytometry as described in the Analytical Procedures

section. The percent of cells expressing pluripotency markers including Tra-1-60, SSEA4, Nanog and Tra-1-81 can be found in Figure 41.

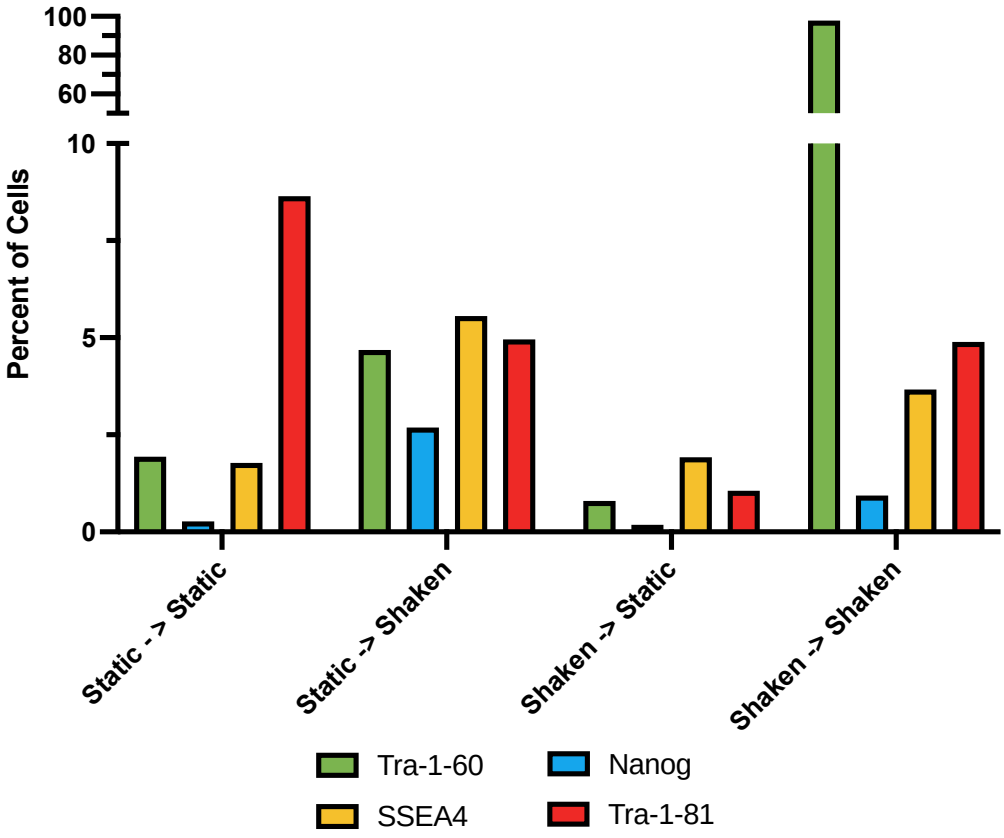

Figure 41: Summary of cells expressing pluripotency markers in flow cytometry analysis.

The flow cytometry results support previously published data from a similar experiment done with mice fibroblast cells [6]. In that study, a negative effect of shaking during Stage 1 was observed which hindered the expression of pluripotency markers and resulted in lower expression than the Static -> Static control. The same result was seen in this experiment with the Shaken –> Static condition having the lowest pluripotency marker expression. Additionally, the mice study demonstrated a positive impact of shaking during Stage 2. This is consistent with the findings of this experiment in which the Static –> Shaken condition had the most even distribution of pluripotency marker expression. It is hypothesized that this is due to the dynamic forces preventing over confluency. As was previously discussed, cell density in

Stage 2 is negatively correlated to the reprogramming efficiency [6]. Overall, the best condition was Static –> Shaken, followed by Shaken –> Shaken, Static –> Static and Shaken –> Static.

One of the most interesting findings of these results was the high expression of Tra-1-60 in the Shaken –> Shaken condition, the same condition which had a large number of lifted cells. It was expected that this condition would not have a high expression of pluripotency markers due to a large number of dead cells and perhaps unviable conditions for healthy cell growth. However, the expression of pluripotent markers in this condition was high, potentially due to the survival of cells with a predisposition to pluripotency. Literature suggests that TRA-1-60 is one of the earlier markers of pluripotency while Nanog is expressed in later stages which may explain why Nanog expression is not as high as Tra-1-60 [49][52].

The reproducibility of cell lifting within the Shaken -> Shaken condition suggests a mechanism is involved, perhaps related to EMT. The cells appeared to be migrating away from the base layer and losing cell junctions which is characteristic of EMT. As the cells did not have a high viability, it is possible that the environment is lacking factors that would support mesenchymal - like cells therefore causing cell death.

4.3.4.1.2 Image Analysis

The CellCyteX was used to obtain images of the whole well for the purpose of colony counting. A more detailed account of image acquisition and processing can be found in 3.19 CellCyte X Imaging.

For this experiment, two wells were designated per condition for image acquisition but unfortunately some of the conditions required more cells for flow analysis which resulted in only one well left for imaging. The summary of colony counts can be found in Figure 42.

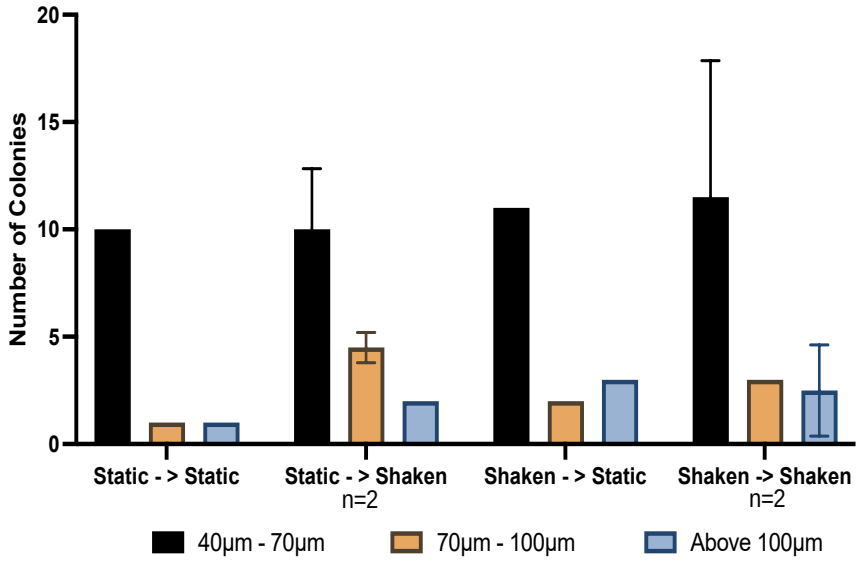

Figure 42: Manual counts performed based on the CellCyteX images. Conditions with replicates are identified.

The overall number of colonies in the range 40µm - 70µm was very similar across all the conditions. In the 70µm - 100µm range, the Static–> Shaken condition had the most colonies and Static –> Static had the least. The Static –> Static condition also had the least number of colonies greater than 100µm. This is an interesting result as the Static –> Static condition had a greater pluripotent marker expression than the Shaken –> Static condition which has more colonies. This could be explained by the cells within the smaller Static –> Static condition colonies strongly expressing markers or the Shaken –> Static cells exhibiting iPSC morphology but not expressing the markers.

4.3.4.2 Conclusion

The analysis of the Static – > Shaken and Shaken –> Shaken conditions demonstrated consistent results from flow cytometry and image analysis. The main concern with the Shaken –> Shaken condition is large number of cells lifting off the surface. It has been shown that iPSCs are able to grow in an aggregate morphology [7][43], but these lifted cells did not resemble aggregates and were not able to produce viable cells. Perhaps there is potential for aggregate formation post Stage 1 that can be explored.

4.3.5 Reprogramming on an orbital shaker plate with Low Attachment plate

As discussed in the previous section, iPSCs have the potential to grow as aggregates in a suspension environment. Preliminary experiments have showed that this is not possible for fibroblast cells which are an adherent cell type and therefore require a surface. This experiment established a proof of concept that aggregate formation was possible on Day 7 of the reprogramming process as can be seen in Figure 43. After two days in a suspension environment, the cells were recovered in static.

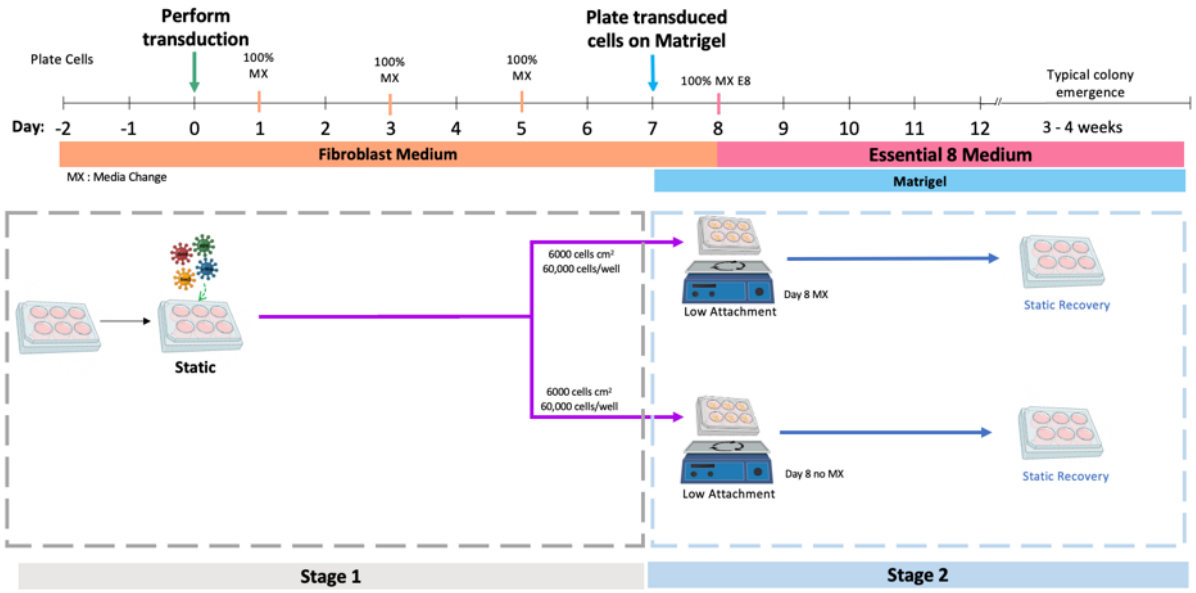

Figure 43: Reprogramming timeline with the use of a low attachment plate in Stage 2. Two conditions were tested, one with a media change on Day 8 and one without a media change. Figure was created with BioRender.com.

In the previously shown timelines, reprogrammed cells are passaged onto a Matrigel plate on Day 7. For this experiment, reprogrammed cells were instead passaged in a low attachment plate at 60,000 cells/well which prevented attachment of cells to the culture ware. It was hypothesized that because fibroblast cells are adherent, they were not unable to survive in a suspension environment while hiPSCs formed aggregates.

4.3.5.1 Results and Discussion

Images of the cells were taken 24h and 48h after inoculation (Day 8 and Day 9 respectively) as can be seen in Figure 44. Two conditions were tested, one included a media change on Day 8 (MX) and one without it (no MX). Cell aggregates formed in both conditions, but higher cell numbers were observed in the no media change condition. The reduction in cell number between conditions may be explained by cell loss during the media change as the cell pellet is very small. Adjustments will have to be made to protocols to reduce cell losses during this stage and an optimization of aggregate preformation should be completed.

Assuming an initial seeding density of 60,000 cells/well and that the cells which aggregated and survived are hiPSCs, 7.07% of the MX condition and 17.4% of the no MX condition cells were recovered.

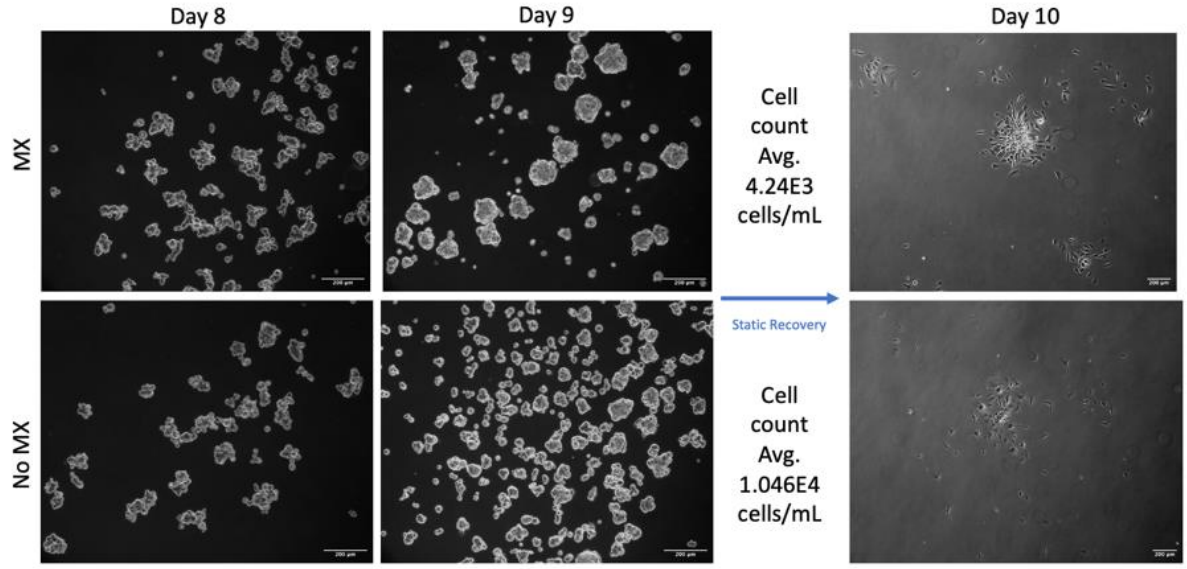

Figure 44: Aggregate formation in low attachment shaking plates with passaging onto static on Day 9. Aggregate images taken at 10X, Phase 2. Static images taken at 5X, Phase 0. Scale bar represents 200 μm.

On Day 9, the aggregates were passaged on to Matrigel plates in static to observe growth as seen in Figure 45. Colony formation was observed in both conditions.

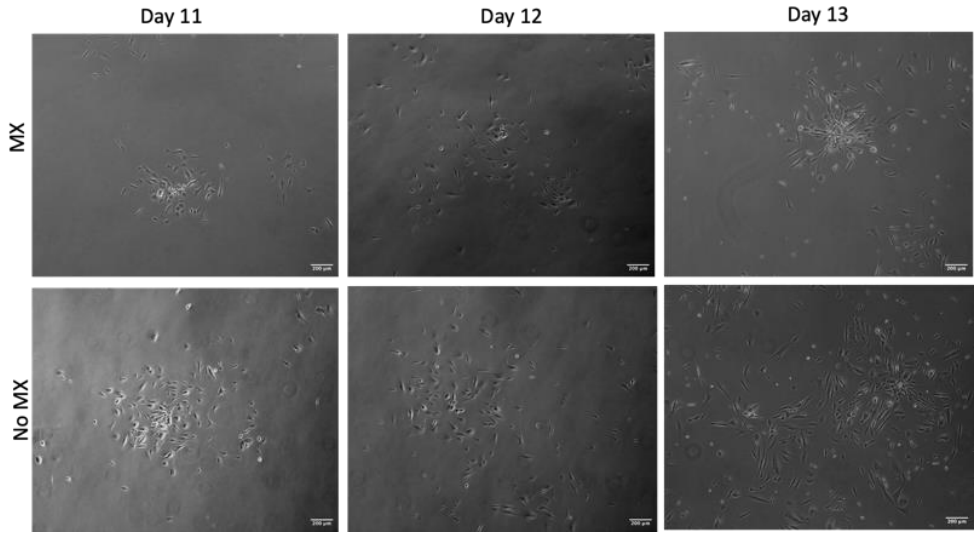

Figure 45: Static recovery of aggregate cells on Day 9 on Matrigel plates. Images taken at 5X magnification.

The newly plated static cells were cultured until Day 19 at which point alkaline phosphatase staining was completed. Figure 46 shows a brightfield image of a potential hiPSC colony on Day 19 of the MX condition (A) and the alkaline phosphatase staining (B). The positively stained colony suggests pluripotency and the potential of recovering reprogrammed cells in static after aggregate formation.

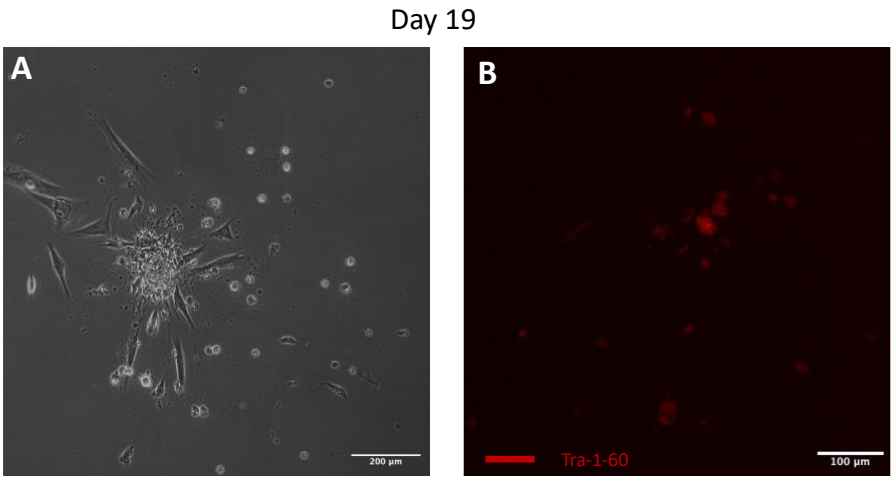

Figure 46: Day 19 cell growth of MX condition demonstrating (A) colony formation and (B) positive alkaline phosphatase staining.

As the aggregate formation showed promise for the culturing of newly reprogrammed cells in suspension, a higher cell density was tested. Following Day 7 passaging, the cells were seeded in a low attachment at 120,000 cells/ well and placed on a shaker. Images were taken daily with a brightfield microscope and media changes of 100% were performed as previously described. These cells were cultured until Day 13, images of which can be found in Figure 47.

The images demonstrate that aggregate formation was successful, and cells continued growing albeit the number of aggregates diminished as time went on. As previously hypothesized, this was most likely due to the inevitable loss of cells during media changes. The morphology of the aggregates also changed, and development of necrosis centres begun on Day 10. As can be expected, the culturing of aggregates in a low attachment plate is not the ideal suspension culture. The development of necrosis in aggregates of such small size suggests that there is poor distribution of oxygen and nutrients. Issues such as these may be addressed with a small-scale bioreactor system that requires a low initial number of cells.

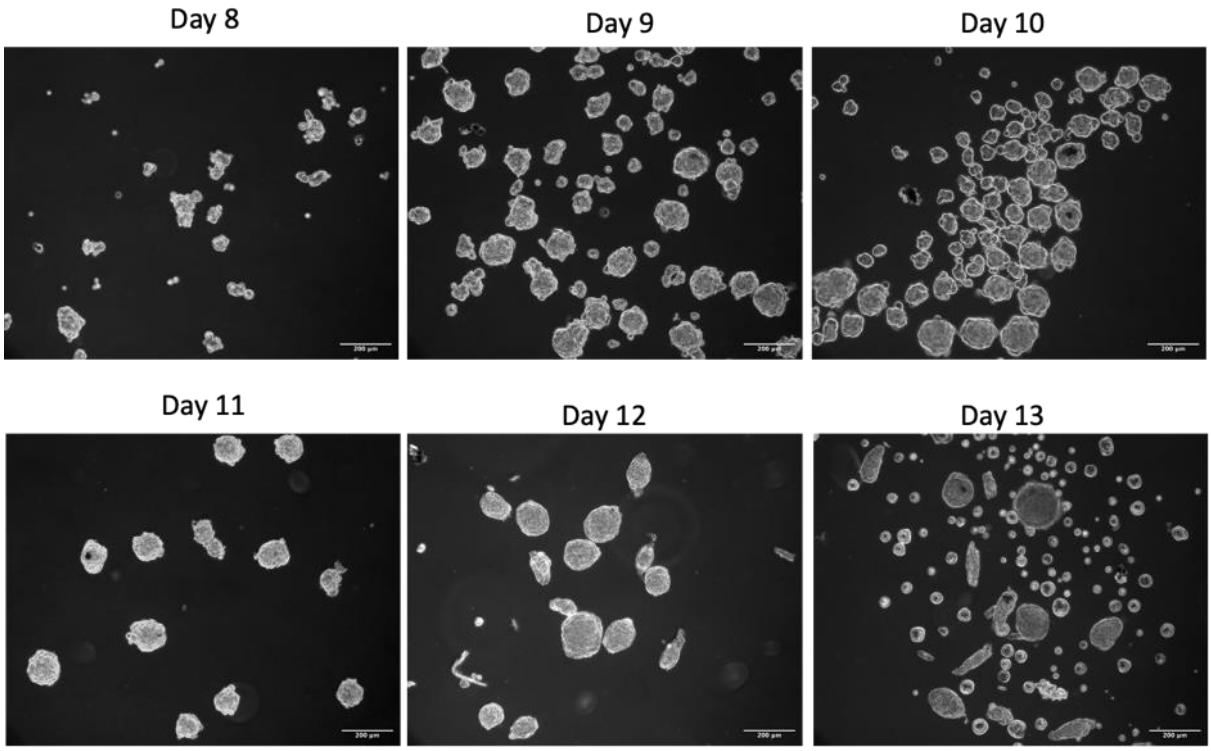

Figure 47: Growing aggregates in a well plate suspension at 120,000 cells/well.

4.3.6 Potential for reprogramming in 10mL stirred suspension bioreactor

The previously observed recovery of cells following aggregation in low attachment plates is averaged at 12%. Based on the optimized protocols developed by James Colter at the PPRF, preformed aggregates should be seeded in 10mL spinner at a total of 650,000 cells with a cell density of 35,000 cells/mL. Given the 12% recovery, a staggering 5.4 million reprogrammed cells would be needed which is the equivalent of ~5 wells on Day 7 of reprogramming. A diagram of the potential bioprocess using aggregate pre-formation is shown in Figure 48.

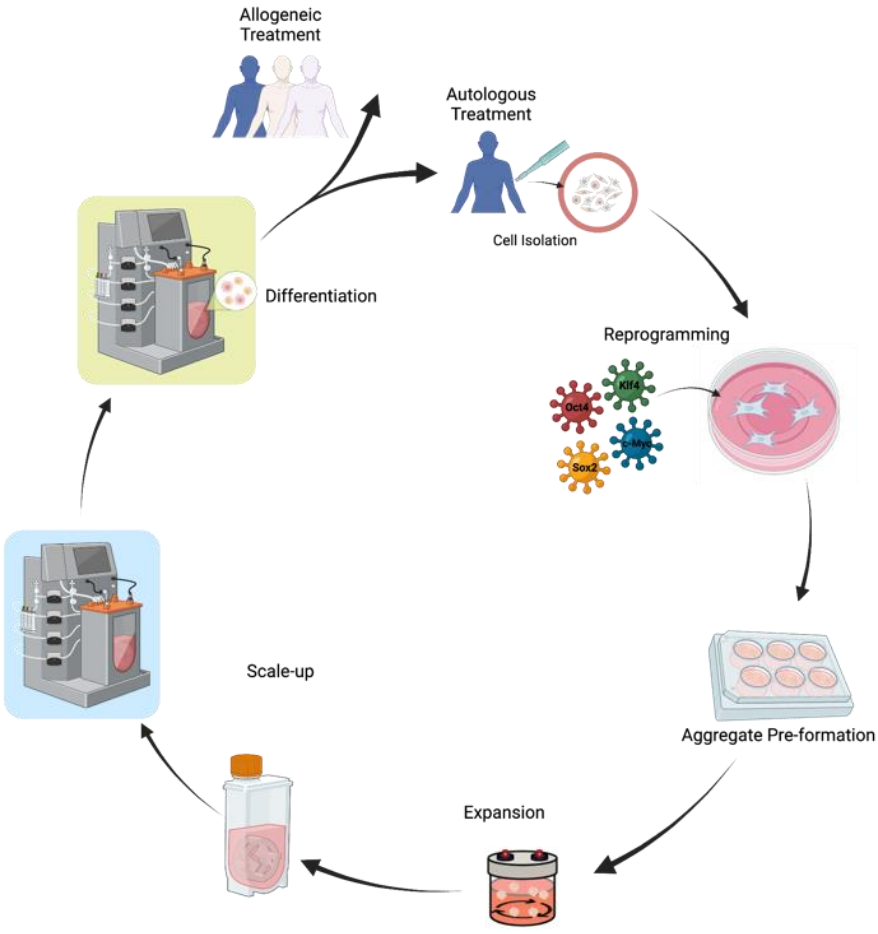

Figure 48: Proposed bioprocess using aggregate pre-formation and expansion in small scale bioreactors. Figure was created with BioRender.com in collaboration with Tiffany Dang.

The use of 5 million cells to achieve the necessary seeding density for a 10mL bioreactor may not be feasible or practical, especially during initial stages of bioprocess development. Given this roadblock, the cells may need to be expanded in static to increase cell number and allow for development of hiPSC markers.

4.4 Conclusion

The objective of this aim was to develop a reprogramming process for a dynamic system. The initial approach was to select a microcarrier for growth of fibroblast cells, anchorage dependant, in a bioreactor. After several screenings, the Collagen Coated microcarrier was selected. A factorial experiment was then conducted to optimize cell growth, but fold expansion remained low, and reprogramming on microcarriers was not possible. During this time, the effect of a dynamic system on reprogramming was evaluated and the optimal seeding density for Stage 2 determined. The dynamic system was created using a shaker to induce fluid motion and 60,000 cell/well was found to be the optimal density. A combination of static and shaking conditions was evaluated with static during Stage 1 and shaking during Stage 2 providing the best result.

To address the issue of reprogramming in a bioreactor system, the reprogrammed cells passaged on Day 7, were used to create preformed aggregates. This created potential for early inoculation of reprogrammed cells into a bioreactor as well as a way to separate out the remaining fibroblast cells which would not aggregate. Initial findings of aggregate preformation followed by static recovery showed positive staining with AP. Further work will need to focus on testing the feasibility of growing these aggregate cells in a bioreactor.

Chapter 5 Aim 2 - Addition of Lactate to Static Culture Reprogramming

5.1 Overview

The objective of this aim was to evaluate the effect of lactate on cell growth through: 1) Investigating effect of lactate treatment length on colony formation and 2) Determining optimal cell seeding density for Stage 2. In this aim, the effect of lactate treatment length was examined to validate previous collaborator results and determine the optimal time of treatment. Collaborator experiments have used 12h and 16h treatment lengths which had a positive effect on reprogramming efficiency. The treatment lengths included in this experiment were 10h, 13h and 16h. The cell density of Stage 2 was also examined, and the best combination of treatment length and cell density selected. Changes between the conditions were compared based on cell morphology.

5.2 Introduction

Metabolism has been shown to play a significant role in the reprogramming process of somatic cells to pluripotency through the shift from OXPHOS to glycolysis [72] [77]. Somatic cells displaying greater glycolic capacity and lower oxidative capacity have been shown to have a higher resulting reprogramming efficiency [75]. Therefore, priming cells for glycolysis may be the key to increasing reprogramming efficiency. A recent study has demonstrated that pre-treatment of cells with the metabolite lactate can upregulate glycolytic enzymes and increase the capabilities of cells to respond to glycolytic energy demand. These results suggest that the lactate treatment primes cells for glycolysis which would result in higher reprogramming efficiency to pluripotent cells.

5.3 Results and Discussion

An initial experiment was performed examining three lengths of time for the lactate treatment to validate previous collaborator results.

One 6-well plate was used for a static control of reprogramming with no lactate treatment and count wells. A second 6-well plate followed the same reprogramming protocol except for the addition of lactate treatment at a concentration of 20mM on day 4. The initial study testing lactate pre-treatment observed a significant decrease in cell growth after 24h, so shorter lengths of time (10h, 13h, 16h) were selected for evaluation, as cells post-transduction are more sensitive.

The experiment set-up can be seen in Figure 49. Following the lactate treatment, the cells were recovered in a base DMEM media supplemented with 20mM of glucose. The timeline of the reprogramming process with lactate is shown in Figure 50.

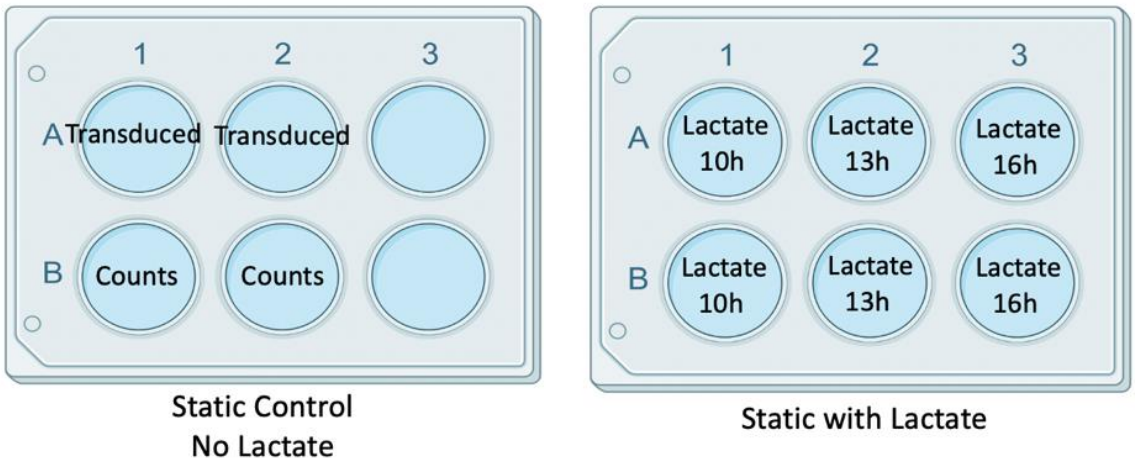

Figure 49: Experimental set-up of first lactate experiment testing the effect of lactate exposure on reprogramming.

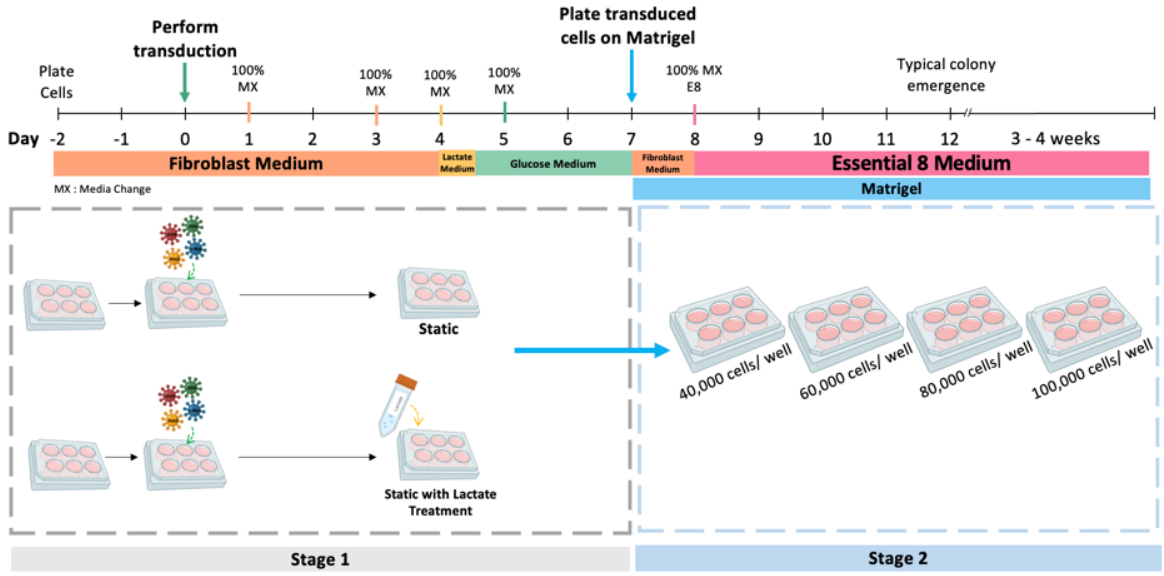

Figure 50: Timeline of the reprogramming process with the addition of lactate. Figure was created with BioRender.com.

On Day 7, cell counts were preformed, Figure 51, and the cells plated at four different densities for Stage 2.

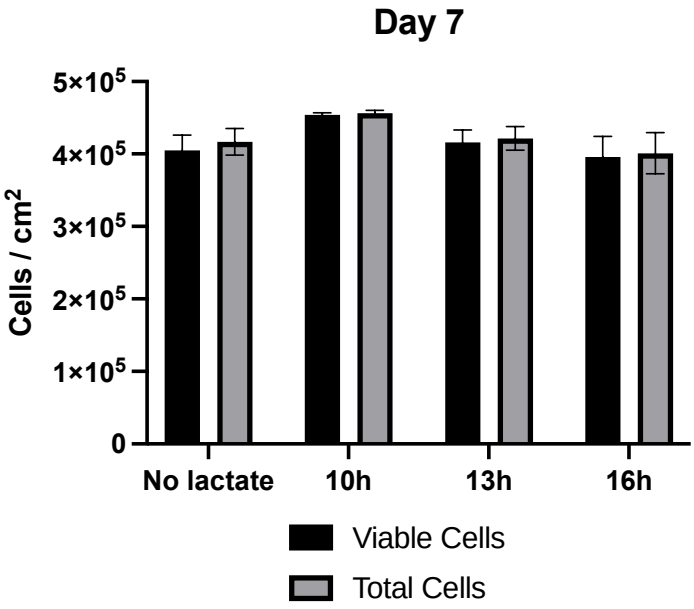

Figure 51: Cell counts of different treatment lengths taken on Day 7 before the cells were plated at different densities.

The initial study testing lactate pre-treatment observed a significant decrease in cell growth after 24h of treatment [5]. Based on the counts of this experiment, it can be observed that the lactate treatment did not have a significant negative impact on cell growth. The longest time of treatment used was 16h and although there appears to be a slight trend between increased lactate treatment and lower cell number by Day 7, the standard deviation of the results minimizes this significance. Overall, as the cell viability and growth were not impacted, it is hypothesized that ROS levels did not significantly increase, or the increase was not high enough to cause toxicity. Based on the cell counts alone, it is hard to determine whether this effect is positive or negative. ROS levels are a critical factor in reprogramming and levels that are too low or too high can impact reprogramming efficiency [79].

5.3.1 Brightfield Images

As was previously described, the cells were plated at four different densities in Stage 2 and Brightfield images were taken every two days. Images at the four cell densities on Day 14 can be found in Figure 52.

Colony formation was most evidently seen in the 80,000 cells/well and 100,000 cells/well conditions however colonies of smaller size were present in the 40,000 cells/well and 60,000 cells/well conditions at the 13h and 16h treatment times. Visibly more colonies formed in the 13h and 16h lactate treatment conditions compared to the 10h treatment and control (no lactate). This suggests that not only the addition of lactate treatment but also the length of exposure has an impact on colony formation. The initial study examining effect of lactate treatment on ROS levels found that lactate had a significant, negative impact on cell viability after 24h [5]. Due to these findings, the experiment described here used shorter lengths of treatment as reprogrammed cells are already stressed and sensitive. However, it appears that the 10h treatment was not long enough to have an impact on ROS levels and thereby colony formation.

The 13h treatment was the shortest period of time in this experiment that yielded a noticeable change in the number of colonies formed. It was therefore deemed the best condition for further investigation of lactate treatment effect on colony formation. It is suggested that future experiments aim to better understand the effect of lactate treatment length between 10h and 24h on ROS levels.

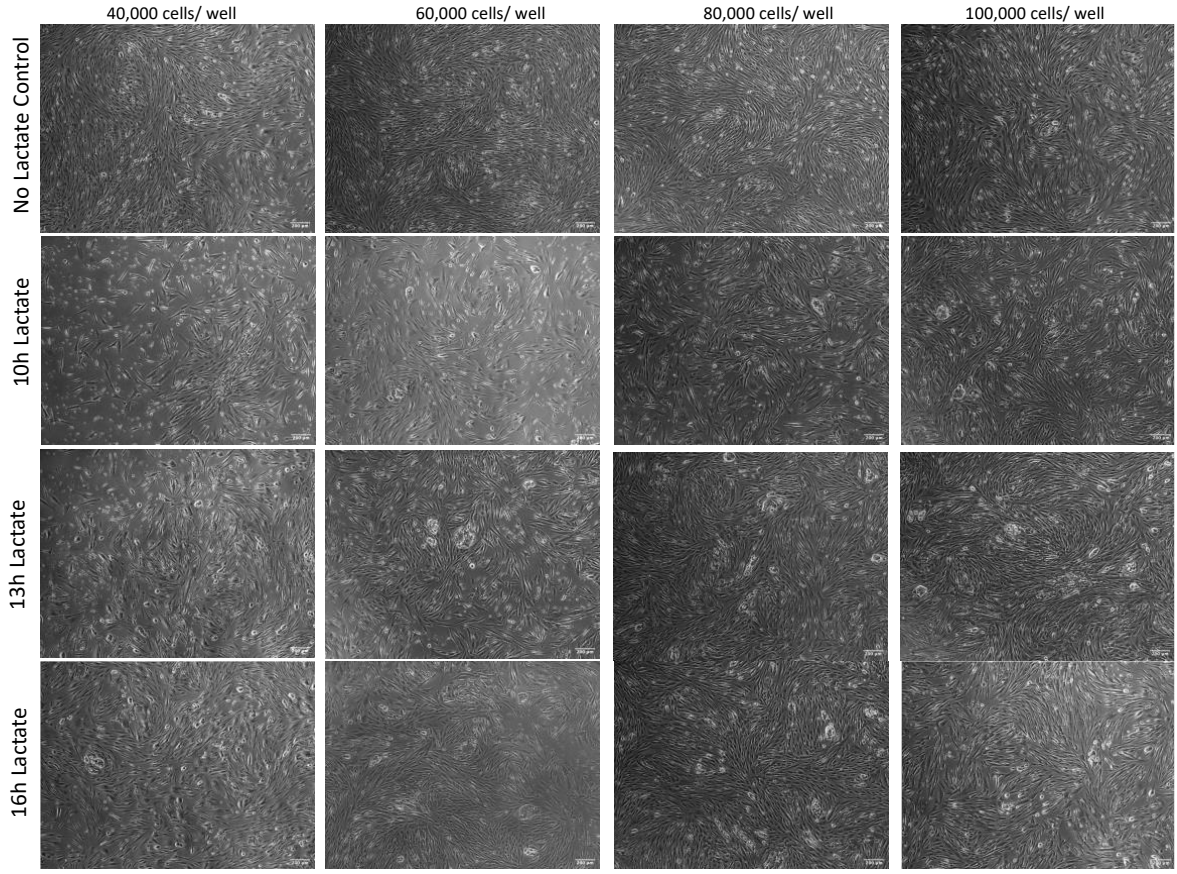

Figure 52: Images of reprogrammed cells with different lactate treatment lengths, taken on Day 14 at 5X magnification.

5.4 Conclusion

The cell density of 60,000 cells/well was previously chosen from Aim 1 as the optimal density for Stage 2 when shaking is part of the process. In this experiment, the cell densities of 80,000 cells/well and 100,000 cells/well formed the greatest number of colonies across all treatment lengths. However, at 60,000 cells/well, the 13h treatment also had comparable

results. It also showed no impact on cell viability at Day 7 counts. Due to this, the 13h treatment at a cell density of 60,000 cells/well was selected for further analysis in Aim 3.

Chapter 6 Aim 3 - Small-Scale Dynamic Culture Reprogramming with Addition of Lactate

6.1 Overview

In Aim 1 and 2, the best conditions of shaking, lactate treatment and cell density were established. The objective of this aim was to combine the previous results and evaluate the overall effect of lactate and shaking on colony formation and cell growth. The optimal conditions for this aim included a 13h lactate treatment, shaking in Stage 2 and a cell density of 60,000 cells/well in Stage 2. Analysis was done through a glucose and lactate assay on media samples, flow cytometry on the last day cells and fluorescent imaging of the cells on the last day followed by colony counts.

6.2 Introduction

The widespread use of hiPSC based therapies and disease models is dependent on the production of homogenous populations of large cell quantities. The standardization of protocols for expansion and differentiation is underway, but methods of reprogramming greatly diverge and often cause variability, particularly when integration into the genome is involved [28]. Non-integrating approaches, such as Sendai virus reprogramming, are available and have GMP potential but face challenges with low reprogramming efficiency, time needed, and labour required.

Research in metabolism has established a connection between the metabolic shift from OXPHOS to glycolysis and the cell's capability for reprogramming; cells which exhibit greater glycolytic capacity, have a higher reprogramming efficiency [75][77]. Previous work has also

showed that lactate treatment can prime cells for glycolysis thereby increasing the reprogramming efficiency [5]. Although lactate treatment during reprogramming may address challenges with reprogramming efficiency, there is still a need for better process monitoring and control, to reduce variability. Control of environmental parameters like pH, dissolved oxygen and agitation is possible with a bioreactor system, which has also been shown to influence pluripotency [7][33]. Due to the low output quantity of reprogrammed cells and the high associated cost, the feasibility and effect of combining lactate treatment and a bioreactor system needs to first be established at a small-scale. The proposed approach was to use lactate pre-treatment in a small-scale dynamic system where fluid movement is induced through shaking. This was done by combining the optimized conditions found from the previous aims.

6.3 Results and Discussion

Previous findings have showed that optimal conditions include a 13h lactate treatment, shaking in Stage 2 and a cell density of 60,000 cells/well in Stage 2. These conditions were combined to evaluate the effect on colony formation with the experiment set-up being found in Figure 53.

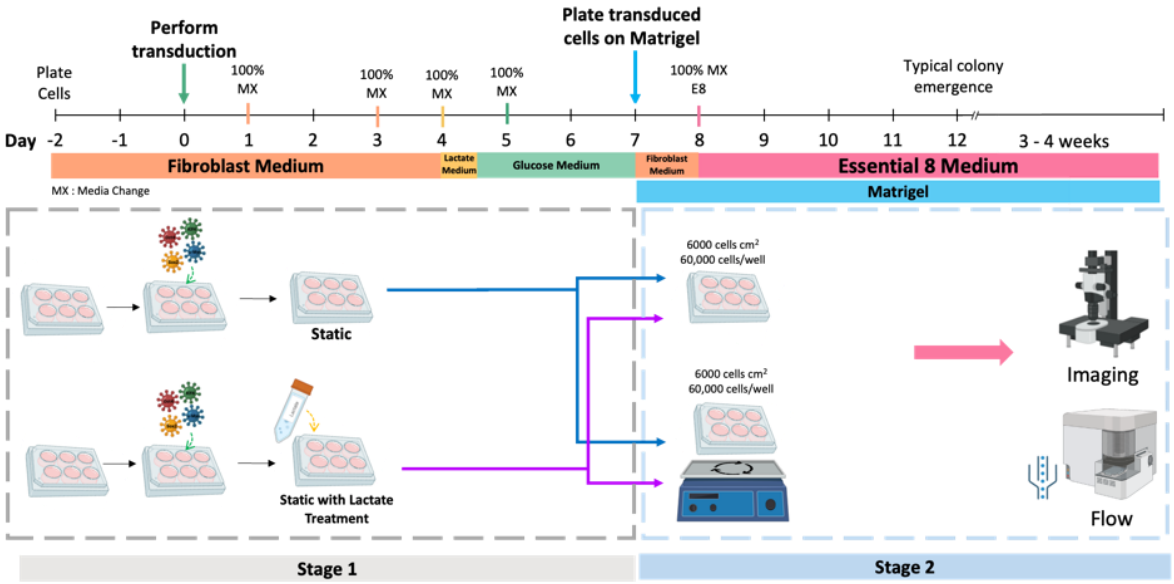

Figure 53: Examining colony formation after optimal conditions of 13h lactate treatment, Stage 2 shaking and 60,000 cells/well are used. Figure was created with BioRender.com.

The described experiment was performed twice to establish reproducibility. From herein the experiments will be referred to as Experiment 1 and Experiment 2. New reagents were needed for Experiment 2 including a new lot of FBS (ATCC, 30-2020) (Lot #: 80707225) and a new lot of the CytoTune™-iPS 2.0 kit (Invitrogen, A16517) (Lot No. L2190075).

Significant differences in cell growth were observed between Experiment 1 and Experiment 2. This was most likely due to the repeated freeze / thaw of the initial reprogramming kit used in Experiment 1 which impacted the transduction stage. Repeated freeze / thaw should be avoided as it decreases the viral titers and will affect the reprogramming process.

6.3.1 Day 7 and last day counts

Cell counts were done on Day 7 before passaging the cells and on the last day of the experiment, which was Day 23 for Experiment 1 and Day 24 for Experiment 2.

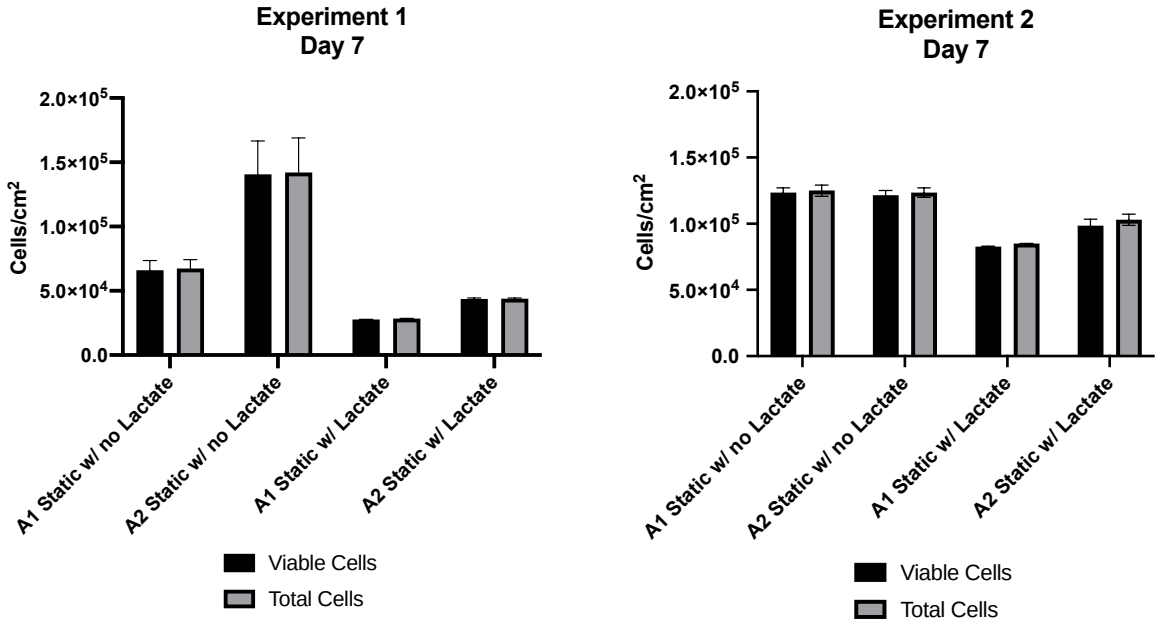

Figure 54: Day 7 counts of Experiment 1 and Experiment 2

Day 7 counts of Experiment 1 were found to be unusual in their significant differences between the wells of Static no Lactate conditions. As these wells were the same condition and

seeded with cells following the same protocol, the cell counts should be very similar such as those seen in Experiment 2. Again, it is hypothesized that the abnormality in counts is due to the reduced titer of the reprogramming kit.

For Experiment 2, the Day 7 counts showed a slight decrease in cell count of the lactate treated cells. As was previously discussed in Aim 2, cells treated with lactate may have a drop in cell counts due to toxicity of the increased ROS levels. Although this was not seen in the earlier conducted experiment, this has been reported in literature [5].

Despite the high level of variability during different batches of the reprogramming process, Day 7 counts may be an important indicator and predictor of future results. Significant differences in cell counts of the same condition, such as seen in Experiment 1, can indicate unequal exposure and uptake of reprogramming factors which may be due to a decrease in viral titers of the reprogramming kit. This does not necessarily mean that the reprogramming process will be unsuccessful as the wells are combined during passaging, but it does suggest that more variability is to be expected.

Figure 55 shows cell counts on the last day of each experiment. Although Experiment 1 had low counts on Day 7, it overall had higher cell counts and viability compared to the last day of Experiment 2. One possible explanation for this, specifically within the shaken conditions, is the loss of cells due to lifting and detachment. Over the course of Stage 2, many cells within the shaken conditions of both experiments would lift off and be washed out during daily media changes. It can be speculated, that the faster growing cells of Experiment 2, reached the detachment stage earlier therefore resulting in more cell loss over time. Additionally, if it is assumed that Experiment 1 had a reduced virus titer due to the repeated freeze /thaw, it can be hypothesized that these cells would grow more numerous albeit with a lower number of reprogrammed cells.

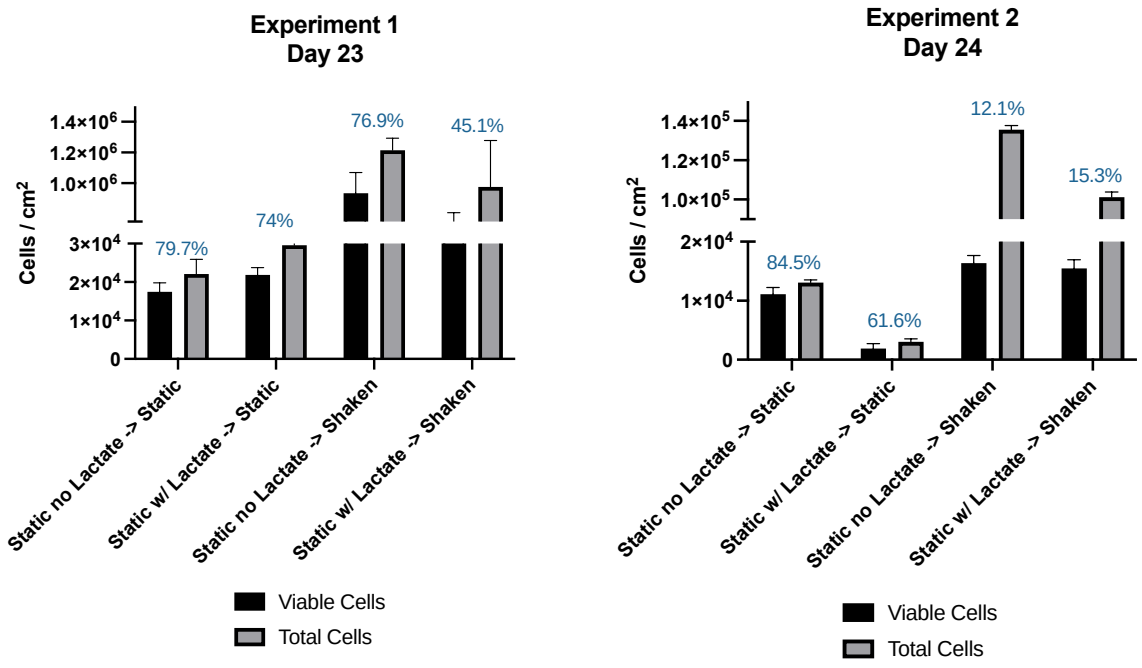

Figure 55: Cells counts performed on the last day of each experiment using a Nuclecounter. The last day for Experiment 1 was Day 23 and for Experiment 2, Day 24.

An interesting observation for the harvesting of Experiment 2 cells on Day 24, was the stickiness and difficulty of detachment of cells in the shaken conditions. The cells possessed strong cell-cell interactions, and although they were likely not viable, they remained on the plate through attachment to those around them. It was extremely difficult to remove the cells off the plate even with the help of a cell scraper tool (VWR, 10062-908). The difficulty of cell detachment and use of a manual tool to do so, could be the reason for low cell viability in the shaken conditions. Additionally, cells in the shaken condition were clumped together to the point of resembling a solid tissue when being lifted off the plate. The implications of this will be further discussed in the Image Analysis and Flow Cytometry sections below.

6.3.2 Image Analysis

Images of Experiment 1 are found in Figure 56 and images of Experiment 2 are found in Figure 57. In the Shaken with Lactate conditions of Experiment 1 and 2, as well as the

Shaken no Lactate condition of Experiment 2, the cell morphology is much different than that of fibroblasts or hiPSC colonies. These cells do not look healthy and although some have formed clumps, it is difficult to tell if these are in fact hiPSC type colonies. The formed cells are more string-like and less compact. It is hypothesized that this morphology may be due to the stress the cells are experiencing. The reprogramming process already causes the cells to be more fragile and the dynamic environment coupled with lactate treatment may be too much.

The alternative hypothesis, which was previously discussed, is an epithelial – mesenchymal transition (EMT) of the cells. The cell morphology within both Shaken conditions is no longer tight and compact which is characteristic of epithelial cells. In contrast, the cells are spreading out and potentially transitioning to a mesenchymal state as they detach from the surface [10]. Therefore, it is possible that the dynamic environment or the stress it induced, triggered EMT and caused the cell detachment and migration. To determine if these changes are occurring due to EMT, the expression of the genes E-cadherin and Snail can be examined. During EMT, there is a downregulation of E-cadherin, which plays a role in intracellular adhesion and an upregulation of Snail which represses transcription of E-cadherin and other epithelial markers [10]. EMT is a process that is typically seen during embryogenesis, inflammation, wound healing and cancer progression so its occurrence within this stage of reprogramming is not expected [99].

Addition future work should examine pick passaging of cells within the Stage 2 Shaken conditions into a static environment. This will help determine if the viability of these cells can be improved post-shaking and if hiPSC colony morphology can be recovered. The number of positively stained AP live colonies can also be assessed and compared to control.

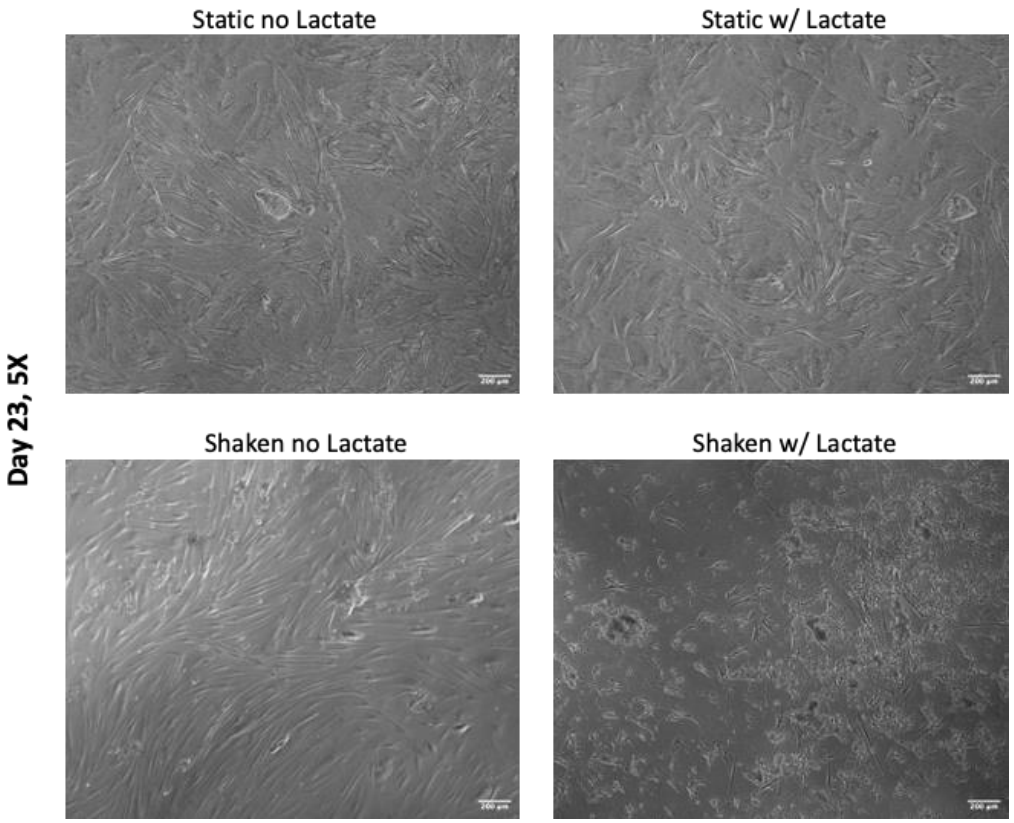

Figure 56: Experiment 1, Day 23 images at 5X magnification.

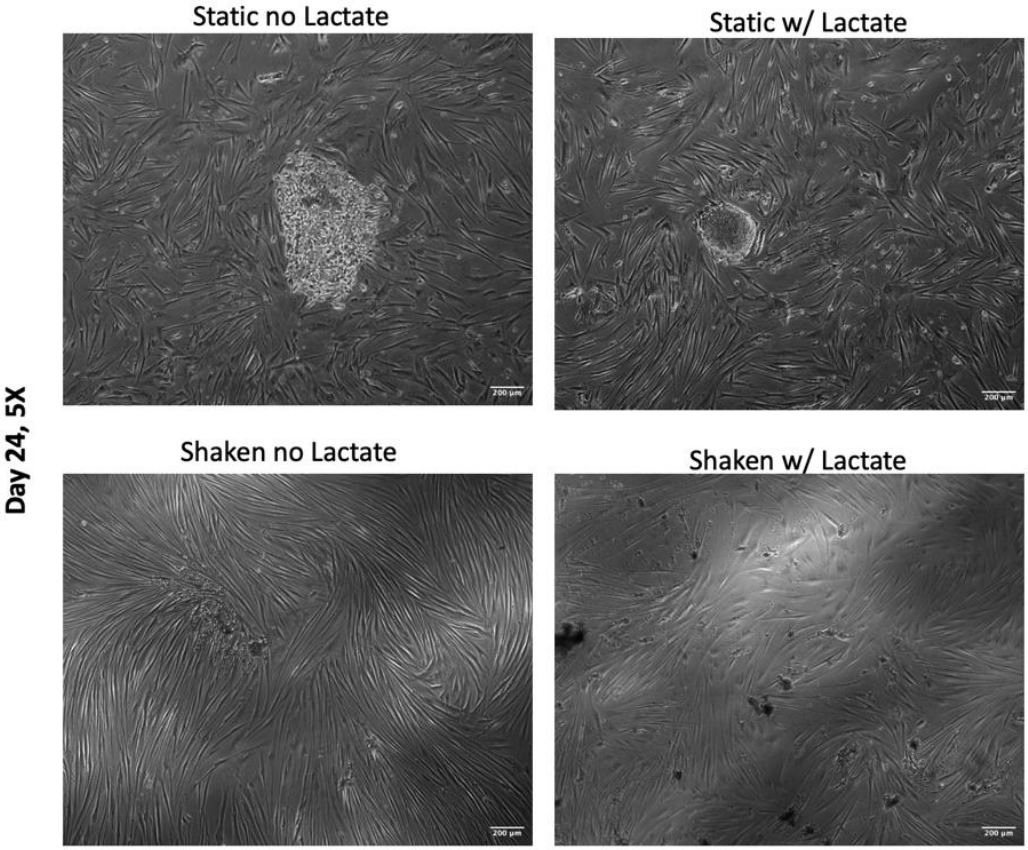

Figure 57: Experiment 2, Day 24 images at 5X magnification.

In both experiments, the Shaken Lactate condition resulted in many cells lifting which again may be due to the stressful environment. In general, Experiment 2 conditions have more signs of colony formation with distinct colonies seen in the Static no Lactate and Static with Lactate conditions. Colonies in the Static no Lactate condition of Experiment 2 appear more distinct and tightly packed thereby more closely resembling typical hiPSC colony morphology [94]. It should also be noted, that some of the colonies in the Static no Lactate condition of Experiment 2 began forming black centres. It is very likely that these are sites of necrosis due to cells in the middle not receiving enough nutrients and suggest that these colonies are overdue for pick passaging.

The non-standard appearance of hiPSC like colonies within the shaken conditions continued to present a challenge when counting colonies of the whole well even with Tra-1-60 and Nanog staining. In Figure 58, clumps of tissue can be seen positively stained for Nanog. The stained sections appear to be floating on top of the surface as opposed to being attached making it difficult to quantify the number of reprogrammed colonies. It is interesting that these cells express pluripotent markers despite not forming classic hiPSC colonies and not being attached.

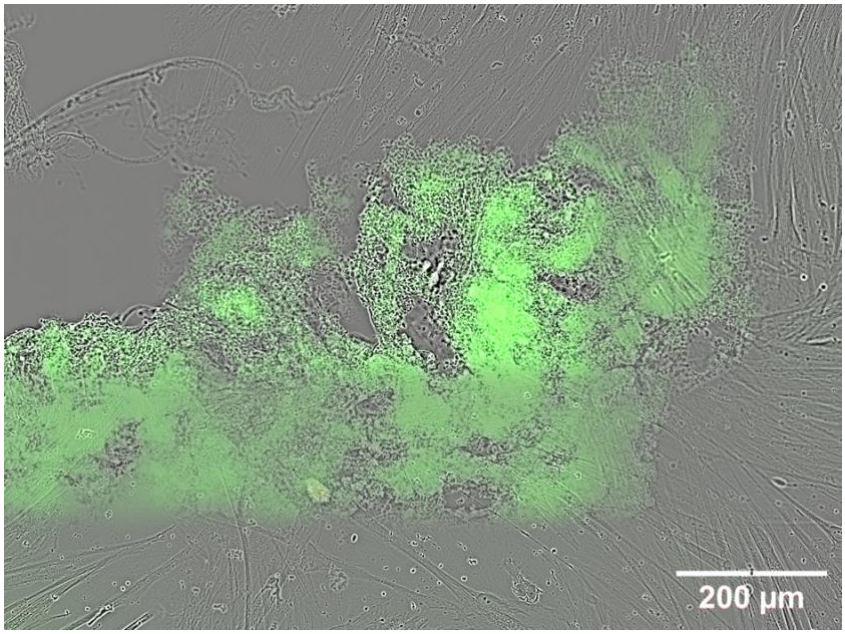

Figure 58: Nanog staining of shaken no lactate condition.

Comparison of Manual vs Automatic Colony Counting

Due to the many advantages of automatic colony counting, the feasibility of the automatic approach was tested and compared to manual counting. Figure 59 summarizes the colony numbers obtained from both approaches for the overall number of colonies, colonies expressing Nanog and colonies expressing Tra-1-60.

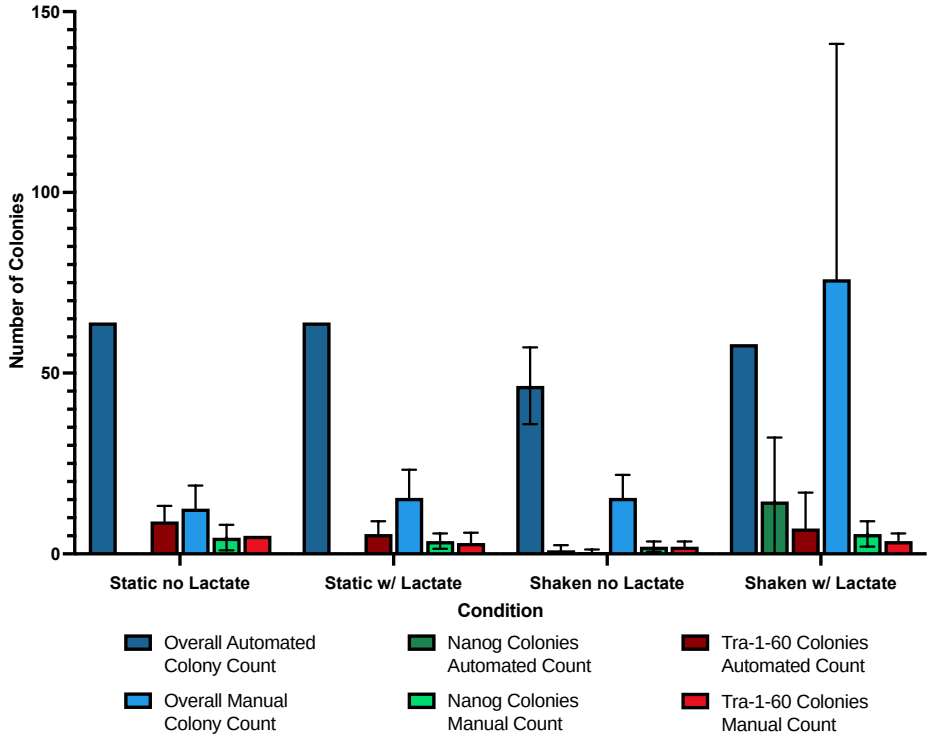

Figure 59: Colony counts comparing an automated to manual approach for overall colonies, Nanog+ colonies and Tra-1-60+ colonies.

Based on the overall results, it can be said that the automated approach typically picks up more colonies than are present. To reduce this deviation, only counted colonies above a certain range were used however this did not improve the results. Less difference in colony numbers is seen between the fluorescently selected colonies of Nanog and Tra-1-60 however the differences are still significant suggesting that the automatic approach cannot be used to draw conclusions. Therefore, the automatic approach from the CELLCYTE X should not be used for counts and other automatic counting software may be explored.

For the purposes of experiments discussed in this section, only manually counted colonies, with distinct edges and above 1000 μm^2 in size will be considered. Summary of the counted colonies can be found in Figure 60.

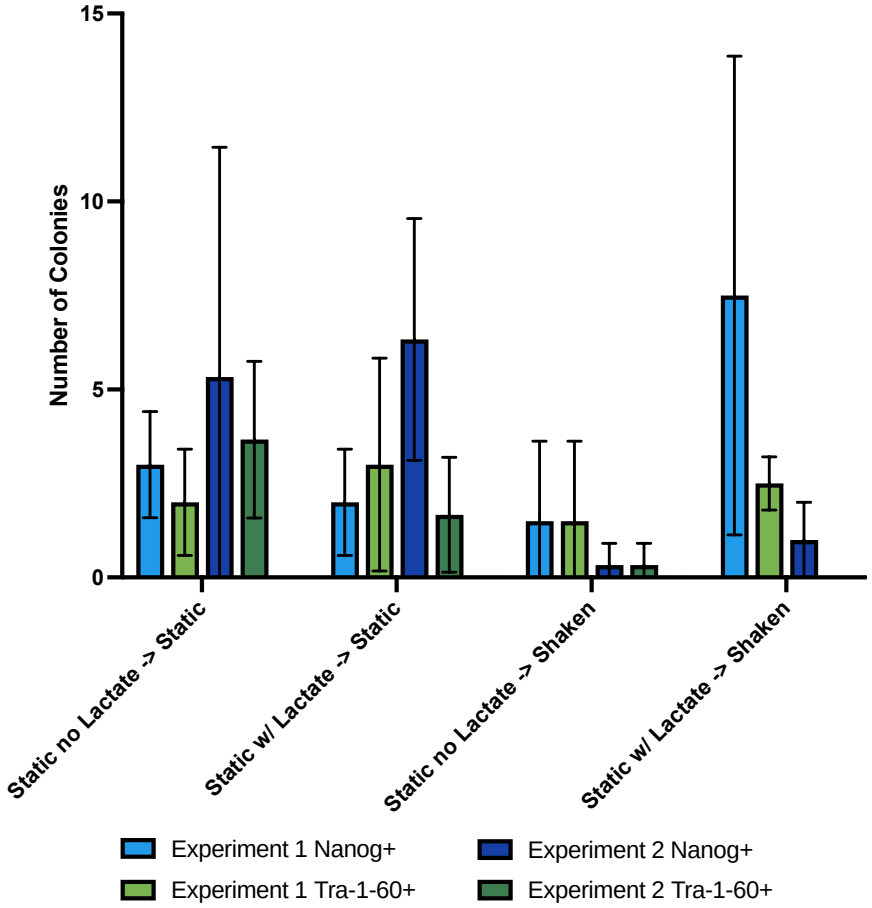

Figure 60: Summary of counted colonies expressing Nanog and Tra-1-60 in Experiment 1 and Experiment 2. Colonies were only counted if they had distinct hiPSC appearance and were larger than 1000 μm^2.

The sample size used for colony counts was 2 wells for Experiment 1 and 3 wells for Experiment 2. From the large standard of error, it can be concluded that there is significant variability in the number of colonies within the same condition. This variability makes it difficult to draw significant conclusions from the data.

6.3.3 Flow Cytometry

Cells were prepared for analysis with flow cytometry on the last day of each experiment, Day 23 for Experiment 1 and Day 24 for Experiment 2. The percentages of cells expressing each marker is summarized in Figure 61. These results show that a high percentage of cells expressed Tra-1-60 which has been seen in the previous data and is consistent with literature findings that suggest Tra-1-60 is an early marker of pluripotency [49][52]. In Experiment 2, Static w/ Lactate -> Shaken condition had the highest expression of Tra-1-60 followed by the other Shaken condition, Static no Lactate -> Shaken. As was previously discussed, these two conditions were the most difficult to harvest due to the strong attachment of cells to each other. It can be speculated that a correlation between high expression of Tra – 1- 60 and strong cell-cell interactions may exist. The hight expression of Tra-1-60 has been observed several times in Shaking conditions with lifted cells, suggesting a correlation between Tra-1-60 and EMT / MET although no literature validating this has been found. Additionally, these two conditions had a relatively high expression of Nanog despite lack of hiPSC colony formation and low expression of the other markers. For example, the Static w/Lactate -> Shaken condition had a high expression of both Tra-1-60 and Nanog, the highest among all the conditions despite the poor expression of SSEA4 and Tra-1-8. Nanog is a marker that is typically expressed during later stages of reprogramming, and it would be expected that other markers, which are expressed earlier, would be better expressed at this point.

From Experiment 1, the Static no Lactate -> Shaken condition had the highest expression of Tra-1-60 and Tra-1-81 while also being relatively high in SSEA4. This is followed by the Static w/Lactate -> Static condition. In Experiment 2, the Static w/Lactate -> Static condition and Static no Lactate -> Static condition were the top performers.

Experiment 1 results showed a minimal expression of Nanog across all conditions which is a stark contrast to Experiment 2, in which all conditions expressed at least over 25%

Nanog. Overall, most of the markers in Experiment 1 were less expressed compared to Experiment 2. This again can be explained by the reduced virus titer used in Experiment 1. It was previously discussed and postulated that Experiment 1 may have significantly more cells although they are not pluripotent. The flow cytometry results provide additional evidence for this as a significantly lower percentage of cells in Experiment 1 expressed pluripotency markers.

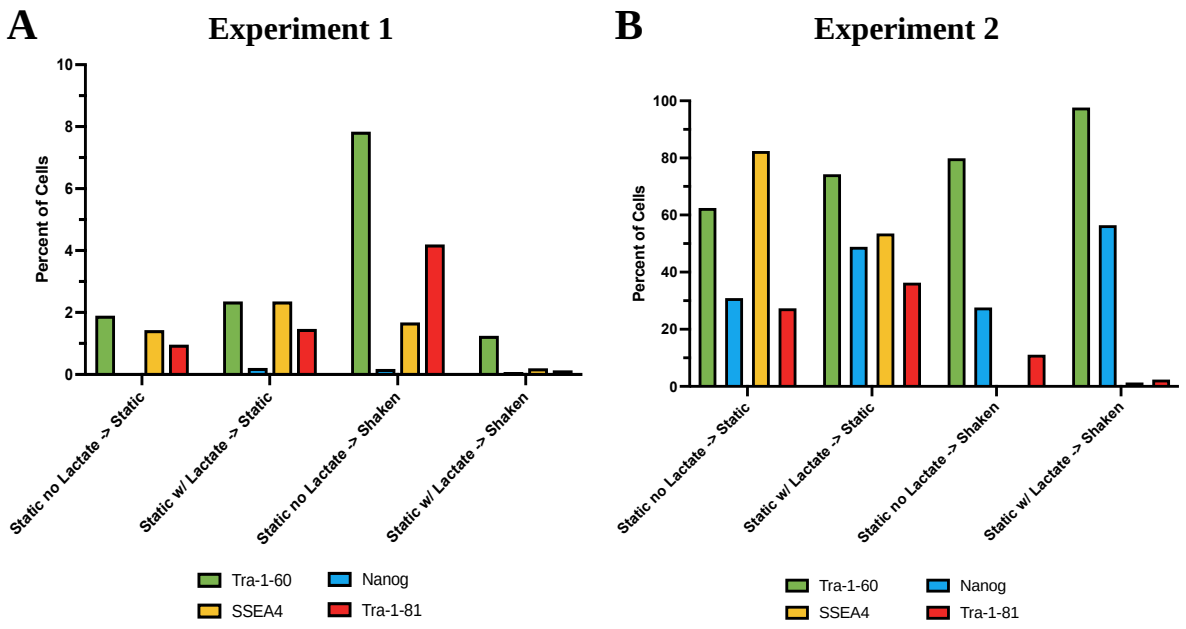

Figure 61: Expression of pluripotent markers using flow cytometry (A) Experiment 1 Day 23 (B) Experiment 2 Day 24.

Additional data can be obtained from a comparison between expression of CD44, a fibroblast marker, and the tandem expression of Tra-1-60 and Nanog as shown in Figure 62. The dual expression of these pluripotent markers increases the possibility of partially reprogrammed cells maturing into hiPSCs. Data from the two experiments shows that simultaneous expression of Tra-1-60 and Nanog is less than 1% in Experiment 1 despite a lower expression of CD44. This leads to the conclusion that the fibroblast expression is reduced but the cells are not yet expressing pluripotent markers and are in a partially reprogrammed stage. It is more difficult to form a conclusion regarding the second experiment, in which there

is a higher expression of Nanog and Tra-1-60 but also a high expression of CD44. This again can indicate an intermediate reprogramming stage.

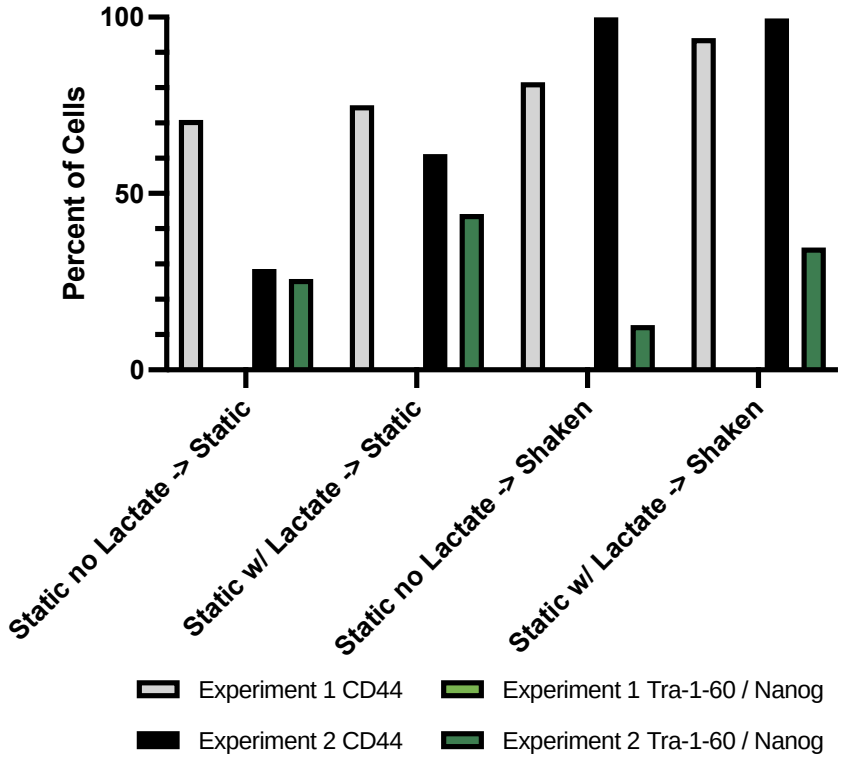

Figure 62: Comparison of CD44 and Tra-1-60 + Nanog expression in Experiment 1 and Experiment 2.

6.3.4 Lactate and Glucose Assay

To gain insight into the metabolic activity of cells in the different conditions, a lactate and glucose assay was performed. Media samples on Day 7 and the last day of the experiment were used for the assay. The resulting concentrations were normalized using cell numbers. To compare the amount of lactate produced to the glucose consumed, flux was determined. During glycolysis, 2 lactate molecules are produced per 1 glucose. This results in a flux of 2 and indicates that ratios closer to 2 are more glycolytic.

For Day 7, Experiment 1 and Experiment 2 results are found in Figure 63. Experiment 1 had a greater flux, this appears to be due to increased concentration of lactate compared to

Experiment 2. For Experiment 1, the lactate and glucose concentrations were the highest within the lactate treated conditions however there was no statistical difference in flux ratios. For Experiment 2, the flux ratio was overall lower than Experiment 1 but with no statistical differences between the wells. This data suggests that the lactate treatment did not impact cell metabolism within each experiment which does not align with past literature findings [5]. However, as the media containing 20mM of lactate was made new each time, the concentration of 20mM should be validated. At this time, it is hypothesized that the lactate concentration was below 20mM which was not sufficient for altering metabolism.

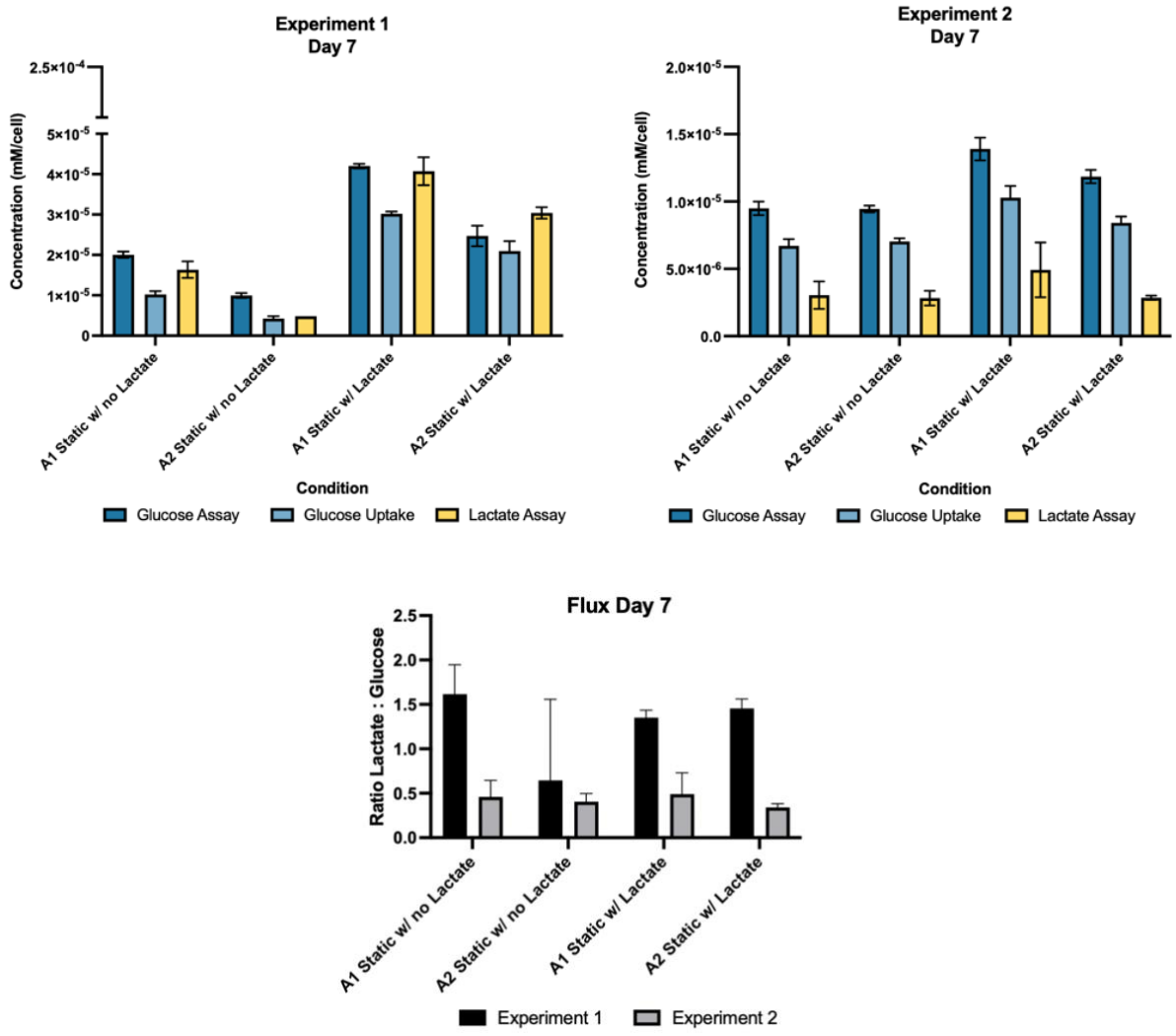

Figure 63: Results of the lactate and glucose assay for Experiment 1 and Experiment 2 on Day 7. Flux was used as a comparison of the amount of lactate produced to the glucose consumed.

For the last day, Experiment 1 and Experiment 2 results can be found in Figure 64.

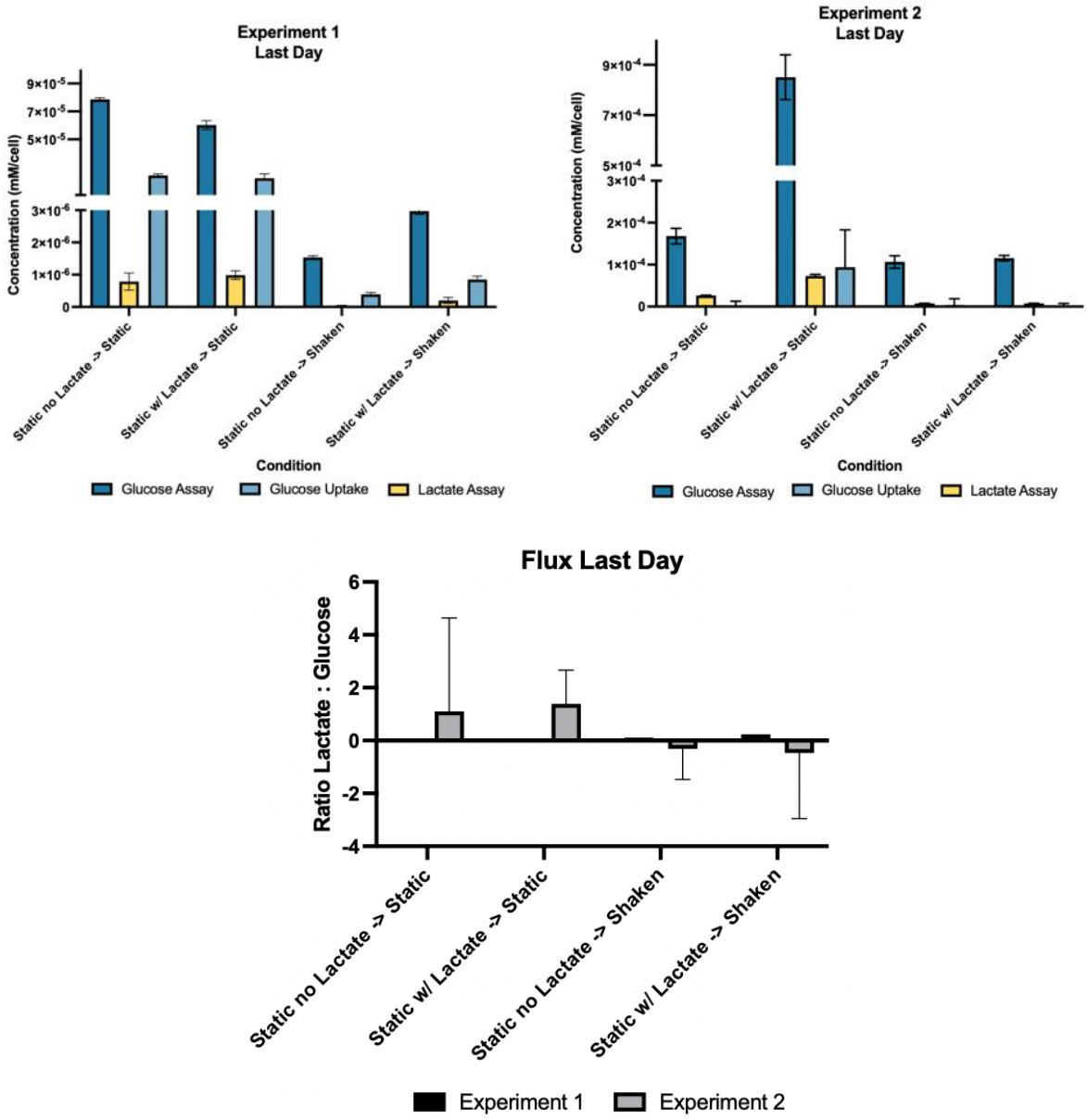

Figure 64: Results of the lactate and glucose assay for the last day of experiment.

From both Experiment 1 and 2, the amount of lactate in the media was reduced compared to the availability and uptake of glucose on Day 7. This was most evidently seen in the flux: for Experiment 1, the flux was around 0 for all conditions while the flux for Experiment 2 was very variant and dipped into the negative. The negative flux was a result of negative glucose uptake which means there was more glucose in the media sample than the media is formulated as. The media used was commercially manufactured therefore it is unlikely

to contain a higher glucose concentration than stated. A more probable explanation is the inaccuracy of the assay used to calculate the amount of glucose in the media samples.

Overall, the results of the metabolic assays raise some concerns, especially regarding the last day data. Experiment 2 data showed a large standard deviation and did not match the results described in the literature. As hiPSCs predominantly rely on glycolysis [72][100], a positive metabolic flux near 2 was expected. As previously hypothesized, the lactate treated wells should also have exhibited a greater flux compared to the no lactate conditions due to the increased capacity for glycolysis. Additional metabolic analysis with a larger number of replicates should be completed to validate these results and reduce the observed standard deviation.

6.4 Conclusion

In this Aim, the previously determined best conditions of shaking, length of lactate treatment and cell density were combined to evaluate the effect on colony formation and cell growth. The experiment was done twice to establish reproducibility although significant differences were observed, most likely due to Experiment 1 using a reprogramming kit that was previously freeze/thawed. The performance of the conditions was largely evaluated using flow cytometry due to the large standard deviation and low statistical significance of the image analysis.

As Experiment 1 cells were likely exposed to a reduced virus titer, it is hypothesized that cells experienced less cytotoxicity thereby having a greater fold expansion albeit with a lower number of reprogrammed cells. This was supported by flow cytometry results which showed a smaller percentage of cells expressing pluripotent markers compared to Experiment 2. Despite this, the Static no Lactate -> Shaken and Static w/Lactate -> Static conditions were the top performing based on the flow results of Experiment 1. The condition with previously determined optimal parameters, Static w/ Lactate -> Shaken, resulted in low cell viability and

minimal colony formation despite some expression of pluripotent markers. The poor performance of this condition was seen in both experiments. The Static no Lactate -> Static condition, which is the control, was also consistent between the two experiments and had the highest cell viability. Static w/Lactate -> Static condition and Static no Lactate -> Static condition were the best for Experiment 2.

In addition to this, the lactate and glucose assay showed a flux of near 0 for Experiment 1 - Day 23, which means very little lactate was produced compared to the glucose consumed. This indicates that little glycolytic activity was occurring within the well although this may be due to the high population of fibroblast cells still present. It is recommended that hiPSC - like colonies are passaged and metabolic analysis of those cultures is completed to provide a better comparison of metabolism.

For Experiment 2 on Day 24, flux ranged from -1 to 1. The negative flux suggests more glucose was present in the media sample than in the media used. This most likely suggests an issue with the glucose assay. Conditions of Static no Lactate -> Static and Static with Lactate -> Static showed a flow of 1 albeit with a large standard deviation. Although this result better aligns with literature data on hiPSC metabolism, the experiment should be reproduced to establish statistical power and reduce the standard deviation.

Chapter 7 Conclusions and Recommendations

7.1 Conclusions

Conclusions of optimal cell density for Stage 2 of reprogramming and the optimal time for using a dynamic system were determined in Aim 1. A dynamic system was created using a shaker to induce fluid motion and found to provide the best result in Stage 2 of reprogramming with the optimal seeding density being 60,000 cells/well. These findings aligned with previous

literature data regarding a positive impact of a dynamic environment on cell reprogramming through control of over-confluency [6].

Aim 1 also included feasibility testing of aggregate pre-formation following cell passaging on Day 7. Initial findings suggest the potential of reprogrammed cells to form aggregates and continue growing following static recovery. The recovered cells were also stained positive with AP live stain. Future work should examine if the expansion of reprogrammed pre-formed aggregates is possible in a 10 mL bioreactor. Additionally, these reprogrammed cells should be expanded in static after aggregate formation and undergo flow analysis to evaluate their pluripotent marker expression.

The objective of Aim 2 was to evaluate different lengths of time for the lactate treatment in Stage 1 as well as validate the effect of cell densities within Stage 2. The 13h treatment at a cell density of 60,000 cells/well was determined to be the best option with comparable cell growth to conditions of higher cell density. It was found that the 10h treatment was not long enough to impact colony formation. Treatment lengths of 10h, 13h, and 16h were chosen to prevent significant cell death as was seen in the 24h treatment condition from the literature [5], but the upper limit of time exposure is yet to be established. In the case of this study, the shortest length of treatment influencing colony formation was used but perhaps the longest treatment that does not cause significant cell death needs to be explored, to generate sufficient ROS levels.

Based on information obtained from literature and as well as the experimental results of Aim 1 and Aim 2, it was anticipated that the Static w/Lactate -> Shaken condition would produce the most hiPSC-like colonies in the shortest time. Despite the high expression of Nanog and Tra-1-60, this condition had poor cell viability and failed to create healthy colonies in both conducted experiments. The same was observed in the Static no Lactate -> Shaken condition, which had significant differences in results between Aim 2 and Aim 3. The

unpredictable results indicate that a dynamic environment has a significant impact on cell and colony growth, but its mechanism is not fully understood. One can speculate that the long-term difference in the health of reprogrammed cells may be dependent on their initial attachment during Stage 2; cells that are able to attach and withstand fluid forces, are able to continue growing and are more likely to form colonies. If cells are unable to attach properly at the beginning of Stage 2, they will be under significant stress with resulting daughter cells demonstrating unhealthy morphology such as seen in shaken conditions of Experiment 2. To avoid these excessive levels of stress, the impact of shaking at different times of Stage 2 should be examined more closely which may lead to better insight into the mechanisms involved.

The hypothesis of this work stated: "Transient exposure of somatic cells (fibroblasts) to lactate in a dynamic system will increase iPSC colony formation and reduce reprogramming time, due to a shift in metabolism from oxidative phosphorylation (OXPHOS) to glycolysis and positive effect of dynamic culture". It appears that this hypothesis has not been completely satisfied. Over the course of this work, an increase in hiPSC colony formation and a reduction in reprogramming time was observed with transient lactate exposure and a dynamic system, however, not when the two conditions were combined. The simultaneous utilization of both approaches significantly impacted cell growth despite an increase in the positive expression of some pluripotent markers. Future work should focus on better optimization of the two approaches separately such as through evaluating lactate treatment lengths between 10h and 24h and using intermittent agitation during Stage 2.

7.2 Recommendations

7.2.1 Preventing Contamination

The majority of work outlined in this thesis was conducted in a 6-well plate, making it challenging to maintain a sterile and contamination-free environment over the course of 20+

days. Due to the susceptibility of 6-well plates to various impurities, it is vital to eliminate as many contaminants as possible from the lab environment. Steps that should be taken before the start of any major reprogramming experiments include thorough cleaning of the incubator, cleaning of the reagent water bath, and filtering of all reagents prior to use. Sterile and aseptic lab technique needs to be carefully followed to avoid contamination risks. Mold contamination is the most common with this type of experiment and it must be noted that plates showing signs of mold, should never be opened in the BSC due to the airborne risk of spreading and further contamination.

7.2.2 Limitations and Future Work

Time was a major limiting factor for this project as the reprogramming process is time and labour intensive. This is the main reason pick passaging was not performed and emerging colonies were not expanded further. Instead, this project focused on laying the groundwork and establishing protocols for future studies of lactate pre-treatment and the effect of a dynamic system on reprogramming. Future work should therefore consider the long-term effect of lactate pre-treatment and dynamic culture after pick passage and expansion.

As discussed previously, the poor viability of cells in conditions using a dynamic system for Stage 2 of reprogramming suggests that the environment is too harsh for cell growth. In future studies, it may be beneficial to evaluate different lengths of time at which the dynamic system is used (ie. intermittent shaking). A more positive effect may also be seen if shaking begins on Day 8 as opposed to Day 7, to allow cells to attach to the surface before dynamic forces are introduced. To further optimize the lactate treatment, lengths of time between 10h and 24h should be tested. This thesis focused on 13h treatment as it did not cause cytotoxicity while still having an effect on colony formation, but longer treatment exposure may provide better long-term results.

As a suggestion for increasing the reproducibility of lactate treatment during reprogramming, a commercially obtained aqueous solution of lactate is recommended to reduce sources of error in the lactate concentration used. The same recommendation is made for the glucose stock solution used in the glucose recovery media.

Additional suggestions for future work include focusing on the expansion of reprogrammed preformed aggregates in a 10 mL bioreactor. The preformed reprogrammed cells should also be recovered and expanded in static after aggregate formation to be used for flow analysis and evaluation of pluripotent marker expression. This analysis would also determine if aggregate preformation can be used as a way to purify the culture from fibroblast cells.

7.3 Contribution to Scientific Knowledge

hiPSCs provide a source for almost any cell type and tissue made from a patient's own cells, preventing tissue rejection, and allowing for a multitude of applications. The development of a large-scale bioprocess is necessary for meeting clinical demand and is dependent on the establishment of stable hiPSC lines and their expansion in 3D dynamic culture systems like bioreactors. The ability to reduce the time and labour associated with reprogramming using lactate treatment or a dynamic system is a major step towards the development of a streamlined bioprocess for manufacturing of hiPSCs. Additionally, the successful use of lactate would provide a simple way of increasing reprogramming efficiency and can easily be integrated into current commercial kits. Thus, by improving the quality and output of hiPSCs, the availability of patient-specific treatment, for all Canadians, is one step closer.

References

[1] K. Takahashi and S. Yamanaka, “Induction of pluripotent stem cells from mouse embryonic and adult fibroblast cultures by defined factors,” *Cell*, vol. 126, no. 4, pp. 663–676, Aug. 2006.

[2] M. S. Rao and N. Malik, “Assessing iPSC reprogramming methods for their suitability in translational medicine,” *J. Cell. Biochem.*, vol. 113, no. 10, pp. 3061–3068, Oct. 2012.

[3] F. González, S. Boué, and J. Carlos Izpisúa Belmonte, “Methods for making induced pluripotent stem cells: reprogramming à la carte,” *Nat. Publ. Gr.*, 2011.

[4] A. D. Panopoulos *et al.*, “The metabolome of induced pluripotent stem cells reveals metabolic changes occurring in somatic cell reprogramming,” *Nat. Publ. Gr.*, vol. 22, no. 1, pp. 168–177, 2011.

[5] A. M. Kozlov, A. Lone, D. H. Betts, and R. C. Cumming, “Lactate preconditioning promotes a HIF-1α-mediated metabolic shift from OXPHOS to glycolysis in normal human diploid fibroblasts,” *Sci. Rep.*, vol. 10, no. 1, Dec. 2020.

[6] J. Sia, R. Sun, J. Chu, and S. Li, “Dynamic culture improves cell reprogramming efficiency,” 2016.

[7] M. Shafa *et al.*, “Derivation of iPSCs in stirred suspension bioreactors,” *Nat. Methods*, vol. 9, no. 5, pp. 465–466, May 2012.

[8] A. Romito and G. Cobellis, “Pluripotent Stem Cells: Current Understanding and Future Directions,” 2016.

[9] H. J. Rippon and A. E. Bishop, “Embryonic stem cells,” *Cell Prolif.*, vol. 37, no. 1, pp. 23–34, Feb. 2004.

[10] R. Li *et al.*, “A mesenchymal-to-epithelial transition initiates and is required for the nuclear reprogramming of mouse fibroblasts,” *Cell Stem Cell*, vol. 7, no. 1, pp. 51–63, 2010.

[11] H. Sun *et al.*, “Metabolic switch and epithelial–mesenchymal transition cooperate to regulate pluripotency,” *EMBO J.*, vol. 39, no. 8, p. e102961, Apr. 2020.

[12] X. Li, D. Pei, and H. Zheng, “Transitions between epithelial and mesenchymal states during cell fate conversions,” *Protein Cell*, vol. 5, no. 8, p. 580, Aug. 2014.

[13] R. Kalluri and R. A. Weinberg, “Review series The basics of epithelial-mesenchymal transition,” *J. Clin. Invest.*, vol. 119, 2009.

[14] K. Takahashi *et al.*, “Induction of Pluripotent Stem Cells from Adult Human Fibroblasts by Defined Factors,” *Cell*, vol. 131, no. 5, pp. 861–872, Nov. 2007.

[15] M. Wernig *et al.*, “In vitro reprogramming of fibroblasts into a pluripotent ES-cell-like state,” *Nat. 2007 4487151*, vol. 448, no. 7151, pp. 318–324, Jun. 2007.

[16] J. Yu *et al.*, “Induced pluripotent stem cell lines derived from human somatic cells,” *Science (80-.).*, vol. 318, no. 5858, pp. 1917–1920, Dec. 2007.

[17] M. Ohnuki and K. Takahashi, “Present and future challenges of induced pluripotent stem cells.”

[18] D. Lukovic *et al.*, “hiPSC Disease Modeling of Rare Hereditary Cerebellar Ataxias: Opportunities and Future Challenges,” *Neuroscientist*, vol. 23, no. 5, pp. 554–566, Oct. 2017.

[19] A. Sharma, S. Sances, M. J. Workman, and C. N. Svendsen, “Multi-lineage Human iPSC-Derived Platforms for Disease Modeling and Drug Discovery,” *Cell Stem Cell*, vol. 26, no. 3, pp. 309–329, Mar. 2020.

[20] Y. Avior, I. Sagi, and N. Benvenisty, “Pluripotent stem cells in disease modelling and drug discovery,” *Nat. Rev. Mol. Cell Biol. 2016 173*, vol. 17, no. 3, pp. 170–182, Jan. 2016.

[21] M. Stadtfeld and K. Hochedlinger, “Induced pluripotency: history, mechanisms, and applications,” *Genes Dev.*, vol. 24, no. 20, p. 2239, Oct. 2010.

[22] M. X. Doss and A. Sachinidis, “Current Challenges of iPSC-Based Disease Modeling and Therapeutic Implications,” *Cells 2019, Vol. 8, Page 403*, vol. 8, no. 5, p. 403, Apr. 2019.

[23] K. M. Giacomini, R. M. Krauss, D. M. Roden, M. Eichelbaum, M. R. Hayden, and Y. Nakamura, “When good drugs go bad,” *Nat. 2007 4467139*, vol. 446, no. 7139, pp. 975–977, Apr. 2007.

[24] A. Yamashita, Y. Tamamura, M. Morioka, P. Karagiannis, N. Shima, and N. Tsumaki, “Considerations in hiPSC-derived cartilage for articular cartilage repair,” *Inflamm. Regen.*, vol. 38, no. 1, pp. 1–7, Oct. 2018.

[25] B. Cristina Martins Fernandes Paes *et al.*, “Ten years of iPSC: clinical potential and advances in vitro hematopoietic differentiation.”

[26] B. A. Baghbaderani *et al.*, “cGMP-Manufactured Human Induced Pluripotent Stem Cells Are Available for Pre-clinical and Clinical Applications,” *Stem Cell Reports*, vol. 5, no. 4, p. 647, Oct. 2015.

[27] G. L. Boulting *et al.*, “A functionally characterized test set of human induced pluripotent stem cells,” *Nat. Biotechnol.*, vol. 29, no. 3, p. 279, Mar. 2011.

[28] F. Soldner and R. Jaenisch, “iPSC disease modeling,” *Science (80-.).*, vol. 338, no. 6111, pp. 1155–1156, Nov. 2012.

[29] B. S. Borys *et al.*, “Overcoming bioprocess bottlenecks in the large-scale expansion of high-quality hiPSC aggregates in vertical-wheel stirred suspension bioreactors,” *Stem Cell Res. Ther.*, vol. 12, no. 1, pp. 1–19, Dec. 2021.

[30] N. Cuesta-Gomez *et al.*, “Suspension culture improves iPSC expansion and pluripotency phenotype,” *Stem Cell Res. Ther. 2023 141*, vol. 14, no. 1, pp. 1–24, Jun. 2023.

[31] “Bioprocess Definition & Meaning - Merriam-Webster.” [Online]. Available: https://www.merriam-webster.com/dictionary/bioprocess#h1. [Accessed: 30-Jul-2023].

[32] M. Serra, C. Brito, C. Udia Correia, and P. M. Alves, “Process engineering of human pluripotent stem cells for clinical application.”

[33] L. Rohani *et al.*, “Stirred suspension bioreactors maintain naïve pluripotency of human pluripotent stem cells,” *Commun. Biol. 2020 31*, vol. 3, no. 1, pp. 1–22, Sep. 2020.

[34] S. Derakhti, S. H. Safiabadi-Tali, G. Amoabediny, and M. Sheikhpour, “Attachment and detachment strategies in microcarrier-based cell culture technology: A comprehensive review,” *Mater. Sci. Eng. C*, vol. 103, Oct. 2019.

[35] H. Tavassoli, S. N. Alhosseini, A. Tay, P. P. Y. Chan, S. K. Weng Oh, and M. E. Warkiani, “Large-scale production of stem cells utilizing microcarriers: A biomaterials engineering perspective from academic research to commercialized products,” *Biomaterials*, vol. 181, pp. 333–346, Oct. 2018.

[36] A. T. L. Lam, V. Ho, S. Vassilev, S. Reuveny, and S. K. W. Oh, “An allied reprogramming, selection, expansion and differentiation platform for creating hiPSC on microcarriers,” *Cell Prolif.*, vol. 55, no. 8, pp. 1–11, 2022.

[37] A. T. L. Lam, A. K. L. Chen, S. Q. P. Ting, S. Reuveny, and S. K. W. Oh, “Integrated processes for expansion and differentiation of human pluripotent stem cells in

suspended microcarriers cultures," *Biochem. Biophys. Res. Commun.*, vol. 473, no. 3, pp. 764–768, 2016.

[38] A. Chen, S. Ting, J. Seow, S. Reuveny, and S. Oh, "Considerations in designing systems for large scale production of human cardiomyocytes from pluripotent stem cells," *Stem Cell Res. Ther.*, vol. 5, no. 1, Jan. 2014.

[39] M. Lecina, S. Ting, A. Choo, S. Reuveny, and S. Oh, "Scalable platform for human embryonic stem cell differentiation to cardiomyocytes in suspended microcarrier cultures," *Tissue Eng. - Part C Methods*, vol. 16, no. 6, pp. 1609–1619, Dec. 2010.

[40] C. A. V. Rodrigues, T. G. Fernandes, M. M. Diogo, C. L. da Silva, and J. M. S. Cabral, "Stem cell cultivation in bioreactors," *Biotechnol. Adv.*, vol. 29, no. 6, pp. 815–829, Nov. 2011.

[41] D. E. S. Nogueira *et al.*, "Strategies for the expansion of human induced pluripotent stem cells as aggregates in single-use Vertical-Wheel™ bioreactors," *J. Biol. Eng.*, vol. 13, no. 1, pp. 1–14, Sep. 2019.

[42] C. A. Rodrigues *et al.*, "Scalable culture of human induced pluripotent cells on microcarriers under xeno-free conditions using single-use vertical-wheel™ bioreactors," 2018.

[43] B. S. Borys *et al.*, "Optimized serial expansion of human induced pluripotent stem cells using low-density inoculation to generate clinically relevant quantities in vertical-wheel bioreactors," 2020.

[44] B. S. Borys *et al.*, "Using computational fluid dynamics (CFD) modeling to understand murine embryonic stem cell aggregate size and pluripotency distributions in stirred suspension bioreactors," *J. Biotechnol.*, vol. 304, pp. 16–27, Oct. 2019.

[45] T. Dang *et al.*, "Computational fluid dynamic characterization of vertical-wheel

bioreactors used for effective scale-up of human induced pluripotent stem cell aggregate culture," *Can. J. Chem. Eng.*, vol. 99, no. 11, pp. 2536–2553, Nov. 2021.

[46] R. Olmer *et al.*, "Suspension Culture of Human Pluripotent Stem Cells in Controlled, Stirred Bioreactors," *Tissue Eng. Part C. Methods*, vol. 18, no. 10, p. 772, Oct. 2012.

[47] H. Singh, P. Mok, T. Balakrishnan, S. N. B. Rahmat, and R. Zweigerdt, "Up-scaling single cell-inoculated suspension culture of human embryonic stem cells," *Stem Cell Res.*, vol. 4, no. 3, pp. 165–179, May 2010.

[48] A. Yilmaz and N. Benvenisty, "Defining Human Pluripotency," *Cell Stem Cell*, vol. 25, no. 1, pp. 9–22, Jul. 2019.

[49] Y. Buganim, D. A. Faddah, and R. Jaenisch, "Mechanisms and models of somatic cell reprogramming," 2013.

[50] R. H. Quintanilla, J. S. T. Asprer, C. Vaz, V. Tanavde, and U. Lakshmipathy, "CD44 Is a Negative Cell Surface Marker for Pluripotent Stem Cell Identification during Human Fibroblast Reprogramming," *PLoS One*, vol. 9, no. 1, p. e85419, Jan. 2014.

[51] B. Papp and K. Plath, "Epigenetics of Reprogramming to Induced Pluripotency," *Cell*, vol. 152, no. 6, pp. 1324–1343, Mar. 2013.

[52] E. M. Chan *et al.*, "Live cell imaging distinguishes bona fide human iPS cells from partially reprogrammed cells.," *Nat. Biotechnol.*, vol. 27, no. 11, pp. 1033–1037, Oct. 2009.

[53] K. M. McKinnon, "Flow Cytometry: An Overview," *Curr. Protoc. Immunol.*, vol. 120, p. 5.1.1, Feb. 2018.

[54] T. Ma, M. Xie, T. Laurent, and S. Ding, "Progress in the reprogramming of somatic cells," *Circ. Res.*, vol. 112, no. 3, p. 562, Feb. 2013.

[55] I. Kogut *et al.*, “High-efficiency RNA-based reprogramming of human primary fibroblasts.”

[56] V. Poletti and F. Mavilio, “Interactions between Retroviruses and the Host Cell Genome,” *Mol. Ther. - Methods Clin. Dev.*, vol. 8, pp. 31–41, Mar. 2018.

[57] N. Malik and M. S. Rao, “A Review of the Methods for Human iPSC Derivation.”

[58] A. Al Abbar, S. Ching Ngai, N. Nograles, S. Yusuf Alhaji, and S. Abdullah, “Induced Pluripotent Stem Cells: Reprogramming Platforms and Applications in Cell Replacement Therapy.”

[59] K. Hu, “Vectorology and Factor Delivery in Induced Pluripotent Stem Cell Reprogramming.”

[60] M. Stadtfeld, M. Nagaya, J. Utikal, G. Weir, and K. Hochedlinger, “Induced pluripotent stem cells generated without viral integration,” *Science (80-.).*, vol. 322, no. 5903, pp. 945–949, Nov. 2008.

[61] K. Okita, M. Nakagawa, H. Hyenjong, T. Ichisaka, and S. Yamanaka, “Generation of mouse induced pluripotent stem cells without viral vectors,” *Science (80-.).*, vol. 322, no. 5903, pp. 949–953, Nov. 2008.

[62] L. Warren *et al.*, “Highly Efficient Reprogramming to Pluripotency and Directed Differentiation of Human Cells with Synthetic Modified mRNA,” *Cell Stem Cell*, vol. 7, no. 5, pp. 618–630, Nov. 2010.

[63] L. Warren and C. Lin, “mRNA-Based Genetic Reprogramming,” 2019.

[64] H. Zhou *et al.*, “Generation of Induced Pluripotent Stem Cells Using Recombinant Proteins.”

[65] J. Seok Bang *et al.*, “Optimization of episomal reprogramming for generation of

human induced pluripotent stem cells from fibroblasts," 2018.

[66] A. Yen, L. Wang, C. Yuen, and Y. Loh, "Episomal Induced Pluripotent Stem Cells: Functional and Potential Therapeutic Applications."

[67] A. M. Drozd, M. P. Walczak, S. Piaskowski, E. Stoczynska-Fidelus, P. Rieske, and D. P. Grzela, "Generation of human iPSCs from cells of fibroblastic and epithelial origin by means of the oriP/EBNA-1 episomal reprogramming system," *Stem Cell Res. Ther.*, vol. 6, no. 1, pp. 1–17, Jun. 2015.

[68] N. Fusaki, H. Ban, A. Nishiyama, K. Saeki, and M. Hasegawa, "Efficient induction of transgene-free human pluripotent stem cells using a vector based on Sendai virus, an RNA virus that does not integrate into the host genome," *Proc. Jpn. Acad. Ser. B. Phys. Biol. Sci.*, vol. 85, no. 8, pp. 348–362, Oct. 2009.

[69] H.-O. Li *et al.*, "A Cytoplasmic RNA Vector Derived from Nontransmissible Sendai Virus with Efficient Gene Transfer and Expression," *J. Virol.*, vol. 74, no. 14, pp. 6564–6569, Jul. 2000.

[70] H. Ban *et al.*, "Efficient generation of transgene-free human induced pluripotent stem cells (iPSCs) by temperature-sensitive Sendai virus vectors," *Proc. Natl. Acad. Sci. U. S. A.*, vol. 108, no. 34, pp. 14234–14239, Aug. 2011.

[71] R. J. Deberardinis and C. B. Thompson, "Cellular metabolism and disease: what do metabolic outliers teach us?," *Cell*, vol. 148, no. 6, pp. 1132–1144, Mar. 2012.

[72] J. Spyrou, D. K. Gardner, and A. J. Harvey, "Metabolism Is a Key Regulator of Induced Pluripotent Stem Cell Reprogramming," *Stem Cells Int.*, vol. 2019, 2019.

[73] C. D. L. Folmes, H. Ma, S. Mitalipov, and A. Terzic, "Mitochondria in Pluripotent Stem Cells: Stemness Regulators and Disease Targets."

[74] M. G. V. Heiden, L. C. Cantley, and C. B. Thompson, “Understanding the warburg effect: The metabolic requirements of cell proliferation,” *Science (80-.).*, vol. 324, no. 5930, pp. 1029–1033, May 2009.

[75] C. D. L. Folmes, P. P. Dzeja, T. J. Nelson, and A. Terzic, “Metabolic Plasticity in Stem Cell Homeostasis and Differentiation,” *Cell Stem Cell*, vol. 11, no. 5, pp. 596–606, 2012.

[76] X. Xu, S. Duan, F. Yi, A. Ocampo, G. H. Liu, and J. C. Izpisua Belmonte, “Mitochondrial Regulation in Pluripotent Stem Cells,” *Cell Metab.*, vol. 18, no. 3, pp. 325–332, Sep. 2013.

[77] C. D. L. Folmes *et al.*, “Somatic oxidative bioenergetics transitions into pluripotency-dependent glycolysis to facilitate nuclear reprogramming,” *Cell Metab.*, vol. 14, no. 2, p. 264, Aug. 2011.

[78] S. Yang and G. Lian, “ROS and diseases: role in metabolism and energy supply,” *Mol. Cell. Biochem.*, vol. 467, no. 1, p. 1, Apr. 2020.

[79] G. Zhou, S. Meng, Y. Li, Y. T. Ghebre, and J. P. Cooke, “Optimal ROS Signaling Is Critical for Nuclear Reprogramming,” *Cell Rep.*, vol. 15, no. 5, pp. 919–925, May 2016.

[80] E. V. Skvortsova, I. B. Nazarov, A. N. Tomilin, and S. A. Sinenko, “Dual Mode of Mitochondrial ROS Action during Reprogramming to Pluripotency,” *Int. J. Mol. Sci.*, vol. 23, no. 18, Sep. 2022.

[81] M. G. Vander Heiden, “Targeting cancer metabolism: a therapeutic window opens,” *Nat. Rev. Drug Discov. 2011 109*, vol. 10, no. 9, pp. 671–684, Aug. 2011.

[82] M. V. Liberti and J. W. Locasale, “The Warburg Effect: How Does it Benefit Cancer Cells?,” *Trends Biochem. Sci.*, vol. 41, no. 3, pp. 211–218, Mar. 2016.

[83] M. Lee and J.-H. Yoon, “Metabolic interplay between glycolysis and mitochondrial oxidation: The reverse Warburg effect and its therapeutic implication,” *World J Biol Chem*, vol. 6, no. 3, pp. 148–161, 2015.

[84] L. Liang *et al.*, “‘Reverse Warburg effect’ of cancer-associated fibroblasts (Review),” *Int. J. Oncol.*, vol. 60, no. 6, Jun. 2022.

[85] N. J. Lanning *et al.*, “A Mitochondrial RNAi Screen Defines Cellular Bioenergetic Determinants and Identifies an Adenylate Kinase as a Key Regulator of ATP Levels,” *Cell Rep.*, vol. 7, no. 3, pp. 907–917, 2014.

[86] M. R. Hildebrandt *et al.*, “Precision Health Resource of Control iPSC Lines for Versatile Multilineage Differentiation,” *Stem Cell Reports*, vol. 13, no. 6, p. 1126, Dec. 2019.

[87] M. Arora, “Cell Culture Media: A Review,” *Mater. Methods*, vol. 3, Mar. 2013.

[88] M. Feoktistova, P. Geserick, and M. Leverkus, “Crystal Violet Assay for Determining Viability of Cultured Cells,” *Cold Spring Harb. Protoc.*, vol. 2016, no. 4, p. pdb.prot087379, Apr. 2016.

[89] K. A. Patel *et al.*, “Validation of automated fluorescent-based technology for measuring total nucleated cell viability of hematopoietic progenitor cell products,” *Transfusion*, vol. 62, no. 4, pp. 848–856, Apr. 2022.

[90] D. Shah, M. Naciri, P. Clee, and M. Al-Rubeai, “NucleoCounter - An efficient technique for the determination of cell number and viability in animal cell culture processes,” *Cytotechnology*, vol. 51, no. 1, pp. 39–44, May 2006.

[91] U. Singh, R. H. Quintanilla, S. Grecian, K. R. Gee, M. S. Rao, and U. Lakshmipathy, “Novel Live Alkaline Phosphatase Substrate for Identification of Pluripotent Stem Cells,” 2012.

[92] R. Abujarour, B. Valamehr, M. Robinson, B. Rezner, F. Vranceanu, and P. Flynn, "Optimized surface markers for the prospective isolation of high-quality hiPSCs using flow cytometry selection," *Sci. Rep.*, vol. 3, 2013.

[93] S. Preibisch, S. Saalfeld, and P. Tomancak, "Globally optimal stitching of tiled 3D microscopic image acquisitions," *Bioinformatics*, vol. 25, no. 11, p. 1463, Jun. 2009.

[94] T. Rivera, Y. Zhao, Y. Ni, and J. Wang, "Human-Induced Pluripotent Stem Cell Culture Methods Under cGMP Conditions," *Curr. Protoc. Stem Cell Biol.*, vol. 54, no. 1, Sep. 2020.

[95] A. Kahn-Krell *et al.*, "Bioreactor Suspension Culture: Differentiation and Production of Cardiomyocyte Spheroids From Human Induced Pluripotent Stem Cells," *Front. Bioeng. Biotechnol.*, vol. 9, p. 674260, Jun. 2021.

[96] R. Zweigerdt, R. Olmer, H. Singh, A. Haverich, and U. Martin, "Scalable expansion of human pluripotent stem cells in suspension culture," *Nat. Protoc.*, vol. 6, no. 5, pp. 689–700, Apr. 2011.

[97] R. Zweigerdt, "Large scale production of stem cells and their derivatives," *Adv. Biochem. Eng. Biotechnol.*, vol. 114, pp. 201–235, 2009.

[98] R. J. Krawetz, X. Li, and D. E. Rancourt, "Human embryonic stem cells: caught between a ROCK inhibitor and a hard place," *BioEssays*, vol. 31, no. 3, pp. 336–343, Mar. 2009.

[99] T. Chen, Y. You, H. Jiang, and Z. Z. Wang, "Epithelial-mesenchymal transition (EMT): A biological process in the development, stem cell differentiation and tumorigenesis," *J. Cell. Physiol.*, vol. 232, no. 12, p. 3261, Dec. 2017.

[100] C. D. Folmes, T. J. Nelson, and A. Terzic, "Energy metabolism in nuclear reprogramming," *Biomark. Med.*, vol. 5, no. 6, pp. 715–729, 2011.